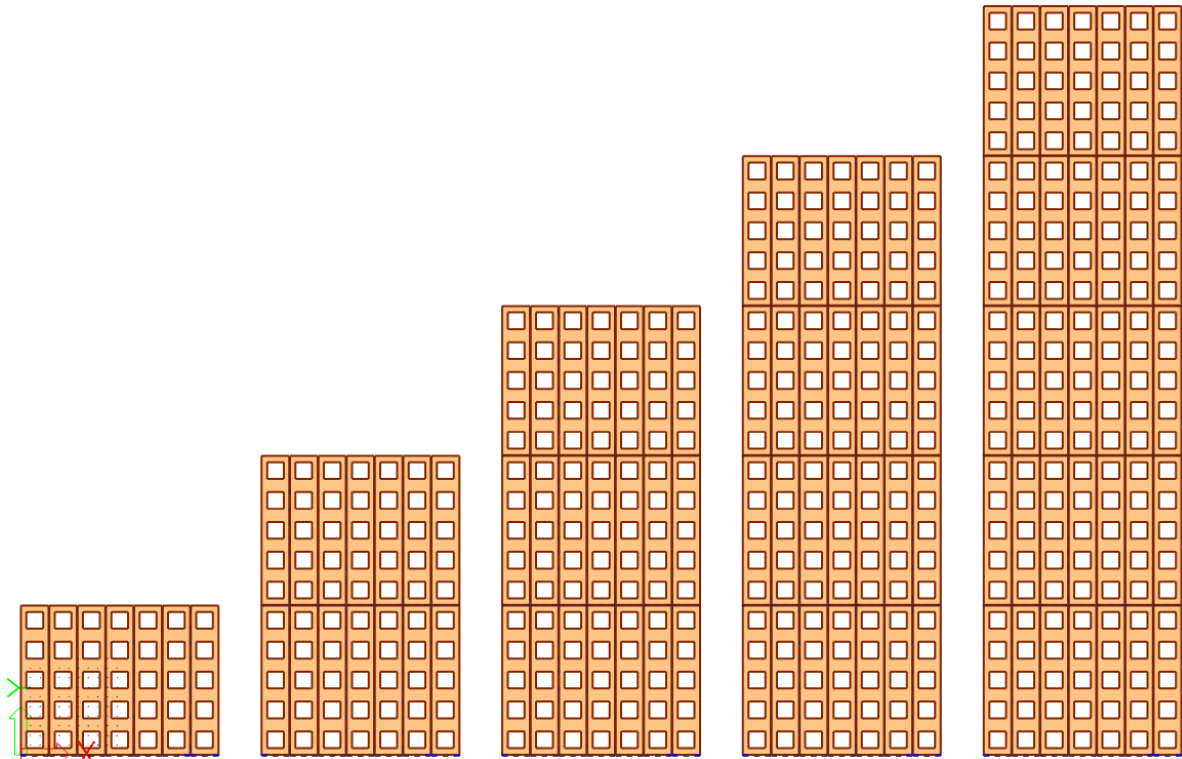


# Structural analysis of CLT walls in façades of a multistory building



Pim Mol

February 2023

# Structural analysis of CLT walls in façades of a multistory building

by

Pim Mol

to obtain the degree of Master of Science  
at the Delft University of Technology,  
to be defended on Wednesday February 1<sup>st</sup>, 2023

Student Number:	4724054	
Project duration:	September 2020 – Februari 2023	
Thesis committee:	Prof. Dr. Ir. J. W. G. van de Kuilen	TU Delft chairman
	Dr. Ir. G. J. P. Ravenshorst	TU Delft
	Ir. H. Alkisaei	TU Delft
	Ir. J. Lauppe	Lüning
	Ir. T. Vermeend Msc	UCA
	Ir. M. Spijksma Msc	UCA

An electronic version of this thesis is available at <http://repository.tudelft.nl/>.

**URBAN  
CLIMATE  
ARCHITECTS**



# Summary

This thesis report provides an analysis of the structural behavior of façades made of CLT panels with openings. These openings will have a significant influence on the transfer of forces in the panels, as well as the stiffness of the façade. The connections required to transfer the forces between the panels are designed. Deformations of the connections introduce additional deformation of the façade itself. The components that influence the force transfer and deformation of the façade have been identified in this research. Their contributions have been investigated. The theoretical calculations have been compared to computer results. The resulting conclusions aid designers in an early design phase regarding the feasibility of a CLT façade structure.

The main focus of the research has been on the mechanical fastener connections that are required for the CLT façades. The research question is stated as:

*“What is the influence of mechanical fastener connections on the strength and stiffness of CLT façades that function as the main stability system?”*

The research started with the goal to find the limitations of CLT façades for multi-story timber buildings. In order to find these limitations, a complete understanding of the structural behavior of the façade was required. Since connections were found to be of great influence the research focused on this topic.

The structural behavior of the façade was defined as the top deformation of the structure and the force transfer and resulting stresses in the panels. The dynamic response of the structure has not been analyzed. Seven components were identified that influence the stiffness and force transfer in the structure.

- Bending of the façade *bending stiffness adjusted for openings*
- Shear of the façade *shear stiffness adjusted for openings*
- Bending of lintels *derived to calculate top deformation*
- Bending of piers *calculated using the method of Schelling*
- Sliding of connections *shear key connections on the horizontal edges of the panels*
- Rocking of connections *elongation of hold-down connections*
- Additional bending deformation of connections *calculated using the method of Schelling*

Computer models were used to verify the overall behavior of the façade as found with the theory. The computer model did not verify each individual component.

Peak shear forces in the CLT panels near the corners of openings determine the required panel thickness. When these shear forces are reduced (for example by applying a concrete core in the structure) the required panel thickness can be reduced.

Top deformations of a façade with a width of 20 meter limit the maximum height to 45 to 55 meter, depending on the connection stiffness.

The main contributor to the top deformation is the connection stiffness of the connections between the vertical edges of the CLT panels. These influence the collaboration between the panels, hence significantly affect the bending stiffness and corresponding bending forces in the panels.

The lintels of the façade panels highly influence the load distribution in the façade. There is no accurate method to calculate this influence on the load distribution.

# Acknowledgements

This report is the final step in order to finish my masters Building Engineering at the Delft University of Technology. It marks the end of my time as a student, and is the beginning of a new chapter.

First of all I would like to express my gratitude to my graduation committee; Jan-Willem van de Kuilen, Geert Ravenshorst, Hoessein Alkisaie, Joost Lauppe, Meindert Spijksma and Tim Vermeend. I thank you all for guiding me in what can be considered one of the most peculiar times to embark on a masters thesis. The Covid pandemic has been a difficult time for everybody, and I am grateful for your efforts to guide me to the best of your capabilities. Thanks to your feedback and critical questions during our meetings I have developed myself in the field of timber engineering that will help me in my career as a structural engineer.

I would like to thank my parents, who have supported me unconditionally. I am grateful for the freedom I have been given to do things my own way.

To my friends, who have frequently asked the question “When are you going to finish that thesis of yours?”. It has finally been answered.

And finally to Jalisa, for her loving support despite all of my quirks.

*P. Mol*

*Breda, January 2023*

# Content

<b>1</b>	<b>Introduction .....</b>	<b>7</b>
1.1	Background .....	7
1.2	Problem description.....	7
1.3	Goals and Objectives.....	7
1.4	Main research question.....	8
1.5	Sub-questions and methodology.....	8
1.6	Methodology .....	10
1.7	Definitions .....	12
1.8	Limitations.....	13
<b>2</b>	<b>Background information.....</b>	<b>14</b>
2.1	CLT panels .....	14
2.2	CLT connections .....	16
2.3	Resistance of a single bolt .....	20
2.4	Multiple shear plane steel-to-timber connections.....	20
2.5	CLT façades .....	24
<b>3</b>	<b>Boundary conditions for the design .....</b>	<b>28</b>
3.1	Floor plan .....	28
3.2	Loads on the structure .....	31
3.3	Façade panels .....	34
3.4	Façade properties.....	34
<b>4</b>	<b>Structural design of CLT façades .....</b>	<b>35</b>
4.1	Overview of the structural mechanics of CLT façades loaded in-plane.....	36
4.2	Forces on the structure .....	40
4.3	Required CLT panels.....	43
4.4	Top deflection.....	44
4.5	Forces on the connections .....	45
<b>5</b>	<b>Connection design.....</b>	<b>47</b>
5.1	Overview of the connections .....	47
5.2	Design of the connections .....	49
5.3	Resistance of the applied connections .....	52
5.4	Design stiffnesses of the connections.....	54
5.5	Multi-linear load-displacement curves .....	56
<b>6</b>	<b>Computer model.....</b>	<b>61</b>
6.1	Setup of the structural model.....	62
6.2	Modelling of the additional elements .....	66

6.3	Calculations .....	69
6.4	Model workflow .....	71
<b>7</b>	<b>Results.....</b>	<b>72</b>
7.1	Results for models without fastener stiffness .....	73
7.2	Results for models with fastener stiffness .....	74
7.3	Results compared .....	75
7.4	Results of models with additional elements .....	84
7.5	Results compared .....	89
<b>8</b>	<b>Discussion.....</b>	<b>96</b>
<b>9</b>	<b>Conclusions and recommendations.....</b>	<b>98</b>
9.1	Conclusions .....	98
9.2	Recommendations .....	102
<b>10</b>	<b>Sources.....</b>	<b>104</b>
10.1	Sources chapter 1.....	104
10.2	Sources chapter 2.....	104
10.3	Sources chapter 3.....	105
10.4	Sources chapter 4.....	105
10.5	Sources chapter 5.....	105
10.6	Sources chapter 6.....	105

# 1 Introduction

## 1.1 Background

Timber is becoming a more popular structural material every year. More and more attention is paid to sustainability aspects in the built environment, hence the shift towards timber products. This goes hand in hand with developments in the field of timber engineering. Glued laminated structures have been used for over a century, but CLT in the built environment is a relatively new product. An increasing amount of buildings are built with timber products and the height of these buildings increases as well. As new boundaries are challenged, new problems have to be solved as well.

## 1.2 Problem description

In several mid-rise CLT structures the stability system is provided by cores or walls (in CLT or concrete). Walls can be located internally as apartment dividing walls, or in the façade. Walls in the façade require openings for windows and doors to allow access to balconies. This in turn reduces the strength and stiffness of the wall panels in the façade. The internal walls however limit the flexibility of the floor plan in the design phase as well as in a future transformation.

## 1.3 Goals and Objectives

In order to built structures of CLT panels with a high level of flexibility, research will be done on the structural behavior of a façade structure made of CLT panels with openings. The structural behavior of CLT panels is already quite well understood based on research and realized projects, hence the focus of this research is on the connections required to construct the façade structure.

The aim of this thesis is to find out how connections may influence the strength and stiffness of CLT façades that function as the main stability system and what the limiting factors are of such a structure. In order to reach this goal, first a thorough understanding of the structural behavior of a CLT structure is required. Then the connections have to be defined in terms of their load-displacement behavior. Finally a computer software can be used to calculate several models in which design parameters are researched. The study results lead to an insight into important parameters for designing a CLT façade structure.

A case study by Urban Climate Architects (UCA) is used to design such a CLT façade structure. Dimensions have been based on the floor plan as proposed by UCA. This design was then slightly altered to suit the structural requirements.

Corresponding objectives are to:

1. determine an analytical calculation method based on current theory on CLT structures with openings and the influence of connection stiffness on the structural behavior.
2. define the non-linear load-displacement behavior of connections.
3. use a computer software to make structural models and compute the structural behavior.

## 1.4 Main research question

One of the challenges related to timber products, in this case CLT, is the connection between the elements. For timber structures connections have always been important to be considered in an early design stage. For an increasing height of a timber structure with a given floorplan, this becomes even more relevant as forces increase. This thesis focusses on the connections between CLT panels and how they influence the structural behavior of a stability system made of CLT structure. The research question has been formulated as:

*“What is the influence of mechanical fastener connections on the strength and stiffness of CLT façades that function as the main stability system?”*

## 1.5 Sub-questions and methodology

In order to answer the main research question, several sub-questions related to this research question have been formulated with the objectives in mind. Each chapter goes into one sub-question.

Chapter 2      background information

*“What is the current state of research on the resistance and stiffness of CLT structures with openings and connections?”*

To answer this question, a literature study has been performed on three topics being CLT panels, connections in CLT and the structural mechanics of CLT panels with openings.

Chapter 3      boundary conditions

*“What are the boundary conditions to take into account?”*

This chapter explains the design of the floor plan as proposed by UC Architects as well as the resulting consequences that this has on the starting points for the research.

Chapter 4      structural design of CLT façades

*“How to design a façade with CLT panels?”*

Having presented the current theories on CLT structures with openings and the influence of connections on the structure, the calculations for the forces in the panels and connections are made and presented in this chapter. Based on the acting forces the required thickness of the CLT panels is defined. Knowing the required panel thickness for safety requirements a first indication of the top deflection is calculated.

## Chapter 5 Connection design

*“What are the required connections for the CLT façade structure to resist the forces acting on them?”*

The forces in the connections as calculated in the previous chapter are used to design suitable connections. Based on these designs a non-linear load-displacement curve is defined. These are used in the computer program to get a realistic model of the façade structure.

## Chapter 6 Computer model

*“How to model the CLT façade structure?”*

An overview is given of the input that is used for the computer model, together with an overview of the computer model itself. The validation of the model is presented in the appendices.

## Chapter 7 Results of the computer model

*“What are the forces in the CLT panels according to the computer models?”*  
*“What is the top deflection of the CLT façade according to the computer models?”*

Two questions are answered in this chapter, both related to the computer results. The chapter itself only presents the outcome of the computer calculations.

Results are presented for CLT façades with and without the connection stiffness modelled and additional stability elements included in the model.

## Chapter 8 Conclusions

*“What do the results indicate for the design of the CLT façade?”*

The results have been calculated in the previous chapter and now the implications of these results are interpreted.

## Chapter 9 Recommendations

Recommendations are made for further study on this topic.

## 1.6 Methodology

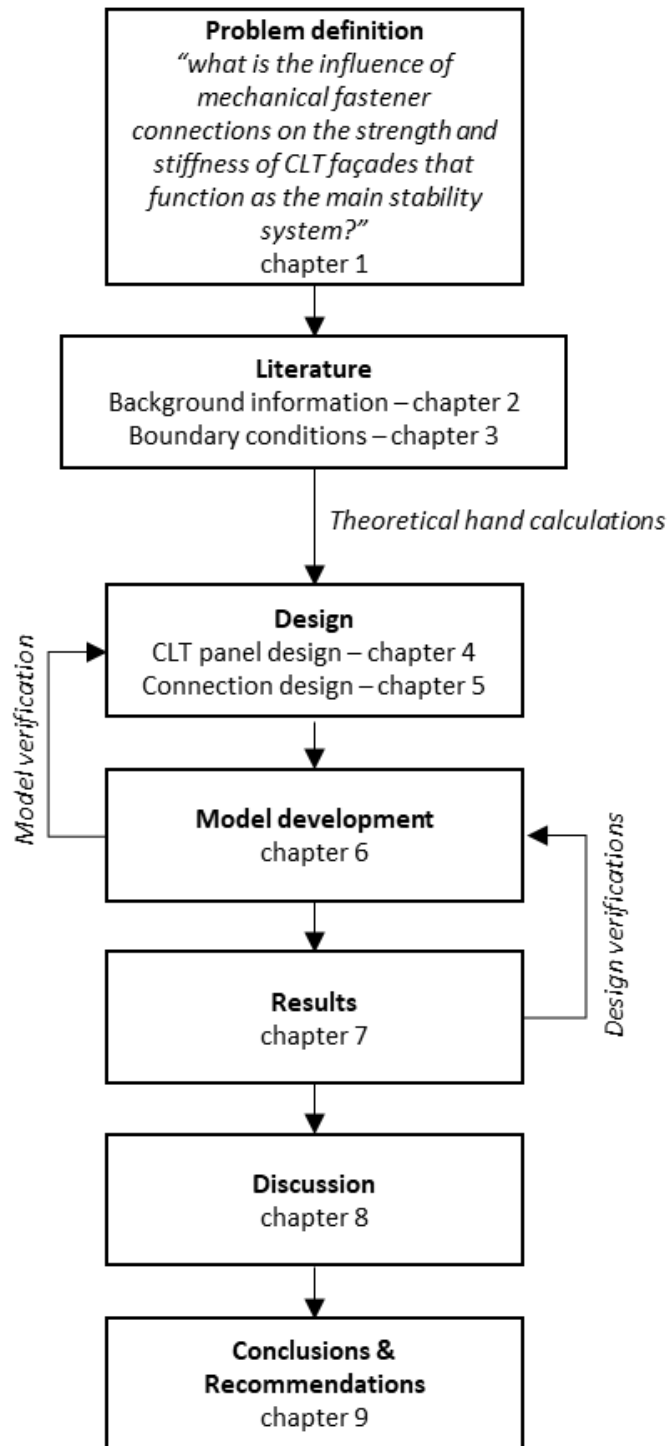


Figure 1, methodology scheme

### 1.6.1 Workflow of the model

The model has been used to perform structural calculations. But in order to have the required panel and connection properties theoretical calculations have been used to get a first indication.

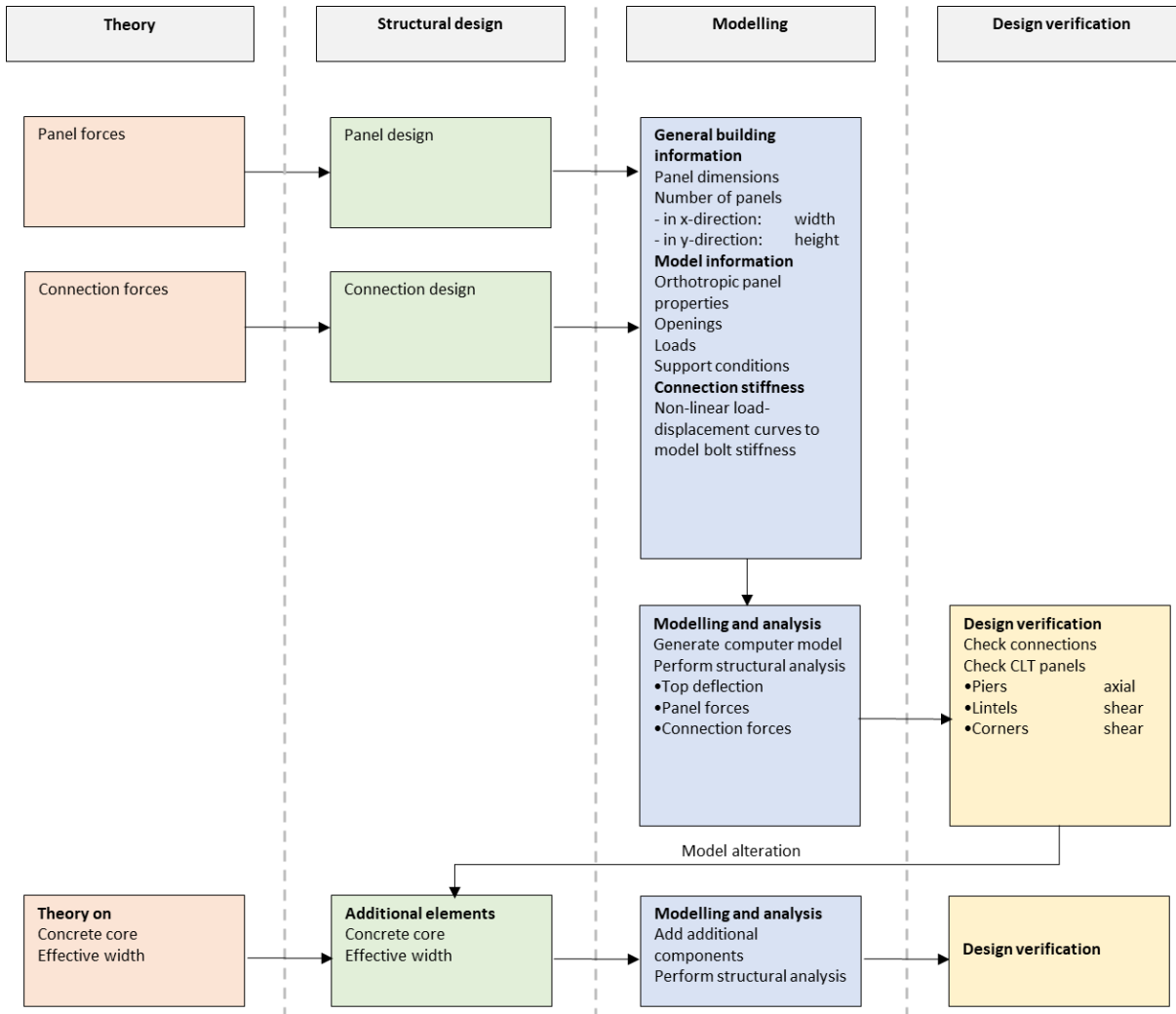


Figure 2, workflow of the model

## 1.7 Definitions

Terms that are frequently used throughout this thesis are defined below.

### *Structural behavior*

The structural behavior of the CLT façade is referring to the behavior of the façade regarding its resistance to loads, the distribution of forces and deformation.

### *CLT façade*

The CLT façade is considered to be the whole façade made of CLT panels with openings and the connections as well. It does not include any beneficial contribution of the transversal walls.

### *Theoretical hand calculations*

Theoretical calculations that have been performed in the initial design phase of the CLT panel thickness and the connections. Most of these calculations have been performed by hand due to their simplicity. Microsoft Excel or Maple has been used for some of the theoretical calculations.

### *Hold-down connections*

The connections at the bottom of the CLT panels that prevent uplift resistance against the overturning moment

### *Shear key connections*

The connections at the horizontal and vertical CLT panel edges that transfer forces from one panel to the next by means of shear forces.

## 1.8 Limitations

In order to answer the main research question only a handful of factors can be researched. This means that there are some limitations on the research itself:

- Dimensions of the façade are considered to be a given value, based on the floor plan.
- Openings in the façade are rectangular, with a fixed percentage for openings.
- Influence of the foundation stiffness is not considered in this research.
- Eurocode 5 (version 2012) does not refer to CLT, but is an important source for this thesis.
  - A new Eurocode 5 (draft 2022) was made available during this thesis.
- Only mechanical connections are considered for the research, where bolts have been used for the initial design of the connections.

## 2 Background information

Literature has been studied related to three topics. Firstly the properties of CLT have been studied. Both the properties of the base material and the orthotropic plate behavior will be elaborated on. Secondly the connections are researched. The type of connections and the strength and stiffness calculations will be introduced. The actual design of the connections will be explained in chapter 5. Thirdly the theory for deflection of CLT wall assemblies will be explained. Four ways in which connections influence the stiffness of the structure are discussed. All this information combined will answer the first sub-question:

*“What is the current the resistance and stiffness of CLT structures with openings and connections?”*

### 2.1 CLT panels

Cross-laminated timber (CLT) is a product that is increasingly used in the built environment. This chapter will go into the material briefly. A quick introduction of the material will be provided. Then the properties of the used CLT panels will be given with validation of these properties. First the base material will be introduced and then the cross-sectional values will be elaborated.

#### 2.1.1 Cross-Laminated Timber

Cross-laminated timber was developed in the early 1990's. A lot of research has been done since. The elements are made of crosswise laminated wooden boards. Because of this feature it is different from glulam and more suitable for panel elements like walls and floors.



*Figure 3, CLT panel [ masstimberservices.com, 2021 ]*

The CLT panels are made in a factory. The grade of the timber used is C24. However, due to the fact that the individual boards are loaded primarily in tension, many research papers also indicate the strength grade as a value for tensile strength of the timber boards. Timber graded C24 is similar to timber T14 graded for tension. Openings can be made in the panels, but will increase routing time, which in turn results in higher costs and longer production times. If more openings are necessary, smaller rectangular panels are possible with lintels in between. For this thesis, large openings are applied in the panels to create window openings that allow for daylight entry.

Elements can be made up to certain dimensions, which differ from different manufacturers. Maximum dimensions for CLT panels are 3,50 by 17,8 meter for products made by Derix. Transport of these larger panels will become a critical point of attention. For normal transport, panels cannot be larger than 3,00 by 15,6 meter.

### 2.1.2 CLT properties

Spruce C24 is normally used for structural timber beams. But the actual behavior of CLT panels is more related to the tensile strength of the base material. Hence the fact that the material parameters for CLT panels are sometimes described by this tensile strength. This is also the case in the research done by Brandner et al. (2016). Formulas were presented to calculate strength parameters depending on the tension strength of the longitudinal boards ( $f_{t,0,l,k}$ ). The table below shows these equations. It also provides the design values for each material parameter. These have been calculated based on a  $k_{mod}$  value of 0,9 and a  $\gamma_{M,CLT}$  of 1,25.

Table 1, design values for CLT panels

	Material parameters for	Equation	Design value	Unit
$f_{m,0,d}$	Bending strength out of plane	$3,2 * f_{t,0,l,k}^{0,8}$	19,0	N/mm <sup>2</sup>
$f_{t,0,d}$	Tensile strength parallel	$1,2 * f_{t,0,l,k}$	11,5	N/mm <sup>2</sup>
$f_{c,0,d}$	Compressive strength parallel	$f_{c,0,k} = f_{m,0,k}$	19,0	N/mm <sup>2</sup>
$f_{v,d}$	Shear strength of net-area	5,50	3,96	N/mm <sup>2</sup>
$f_{v,t,d}$	Shear strength of glued area	2,50	1,80	N/mm <sup>2</sup>
$f_{r,d}$	Rolling shear strength	0,80	0,58	N/mm <sup>2</sup>
$E_{0,mean}$	Modulus of elasticity	$1,05 * E_{0,l,mean}$	11.600	N/mm <sup>2</sup>
$G_{s,mean}$	Shear modulus	450	450	N/mm <sup>2</sup>
$\rho_k$	Characteristic density	$\rho_k = 1,1 \rho_{k,l}$	385	kg/m <sup>3</sup>
$\rho_m$	Mean density	$\rho_m = \rho_{m,l}$	420	kg/m <sup>3</sup>

### 2.1.3 Orthotropic plate

A CLT panel can be considered as an orthotropic plate. This is shown in Figure 4. The x-direction is the strong direction as the fibers of most boards are in that direction, giving it a higher axial resistance. The forces acting on the panels are given by  $n_x$ ,  $n_y$  and  $n_{xy}$  [kN/m]. The stresses  $\sigma_{90,d}$  and  $\sigma_{0,d}$  [N/mm<sup>2</sup>] are indicated in the image as well.

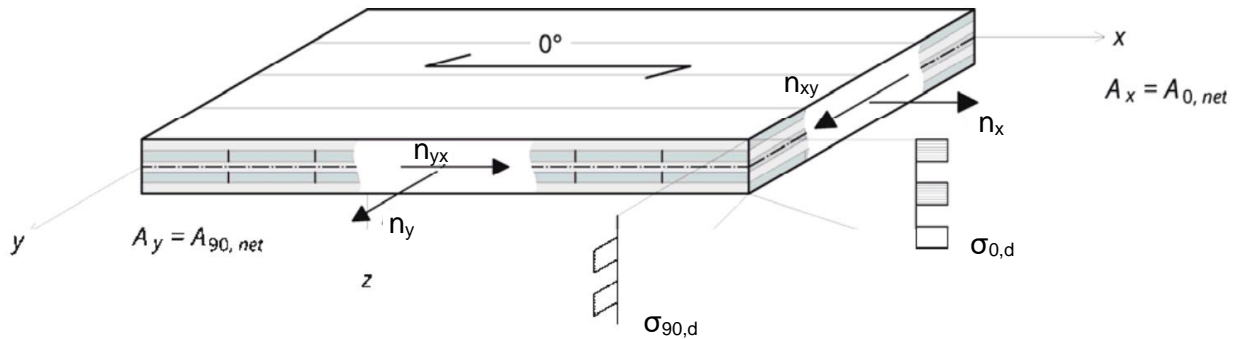


Figure 4, orthotropic CLT plate [adjusted from Proholz, Cross-Laminated Timber Structural Design, 2014]

The orthotropic properties of CLT panels have been calculated in appendix A2.6. Plate mechanics uses the Poisson's ratio  $\nu$  to account for deformation perpendicular to the direction of loading. There is no relation between load in one direction and stiffness in the perpendicular direction. So for CLT this  $\nu$  value is to be taken as 0.

## 2.2 CLT connections

Connections are required to construct a façade of multiple CLT panels. This in turn reduces the overall stiffness of the structure when compared to a similar façade without connections. This chapter gives an overview of the strength and stiffness properties of dowelled fasteners in CLT.

There are several stages between initial loading and final failure of a fastener:

- 1) Slip
- 2) Linear elastic stiffness
- 3) Plastic stiffness
- 4) Plateau stage - yielding
- 5) failure

When a specimen is tested an initial load is applied that will cause the fastener to move, embedding it in the timber. Once the fastener is fully embedded, a linear elastic stiffness is found. For connections with multiple fasteners however, not all fasteners are contributing at the same time. So the actual stiffness of the fastener will not immediately be reached once initial slip has occurred, nor will it be a linear elastic stiffness.

Yielding of the fastener may occur depending on the type and geometry of the connection. After yielding a plastic stiffness can occur until the maximum load is reached (in case of ductile connections). Finally the connection will fail. In ductile connections this is after significant deformation. Brittle connections may fail suddenly, even without any yielding of the fastener. Ductile failure behavior of the connection is preferable. The load-displacement curves for multiple type of joints are given in Figure 5.

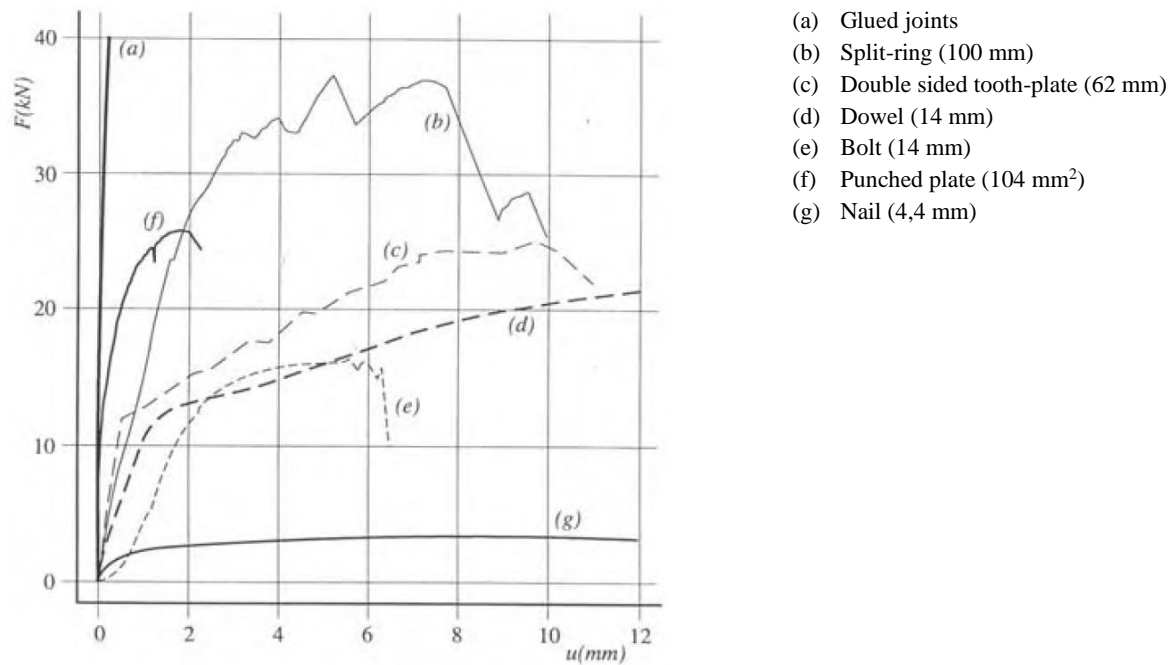


Figure 5, load-displacement curves for multiple type of joints [STEP 1, Timber engineering]

### 2.2.1 Testing of connections

Timber connections are tested according to CEN-EN 26891. Based on the test results several parameters can be found (Figure 6). The stiffness of a connection in serviceability limit state is defined as  $k_{ser}$  and an equation to calculate this value is presented in Eurocode 5. In testing, this value is defined as the slope of the curve between 10% and 40% of the estimated force  $F_{est}$ . Once 40% of the estimated force is reached, the connection is unloaded until 10% of  $F_{est}$  and then fully loaded until failure. This approach allows to observe the elastic stiffness  $K_e$ . Which is defined by Reynolds et al. (2022) as the unload-reload stiffness. A zero-stiffness region is measured between the zero load intersection of the unload-reload line. This zero-stiffness region is larger than the initial slip by default as it consists of the initial hole clearance and the plastic deformation of the timber around the hole edge. Similarly, the elastic stiffness  $K_e$  is larger than the SLS stiffness  $K_{ser}$  by default.

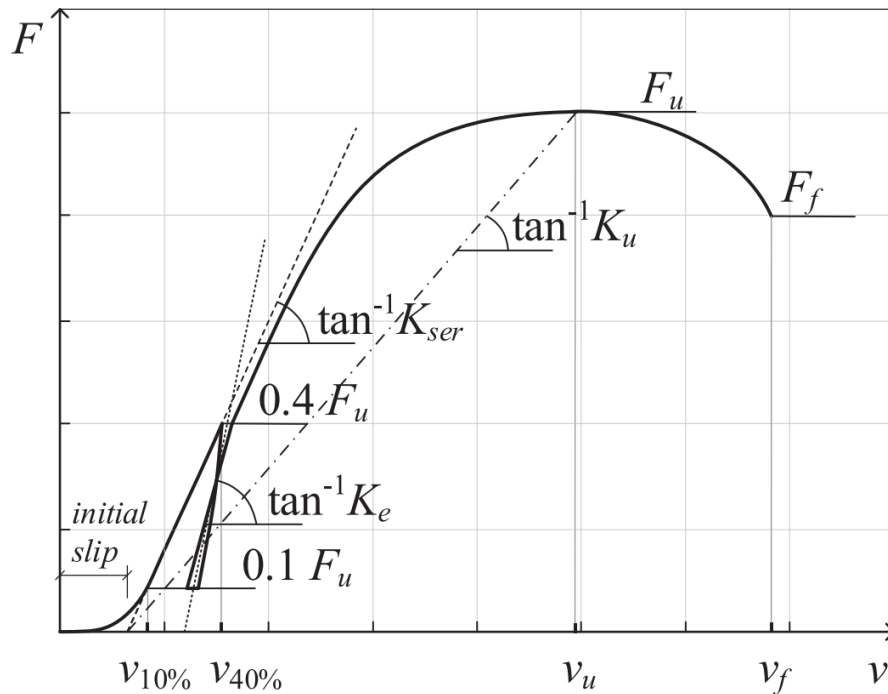


Figure 6, definitions of different slip-moduli for the non-linear load-deformation curve of a connection (Jockwer, Caprio and Jorissen; 2021)

Appendix A2.7 contains the test results of multiple researches on timber-to-steel dowelled fasteners. The load-deformation curves show a similar trajectory as the figure above. Some discrepancies are found as not all curves entail the initial slip part of the curve.

### 2.2.2 Initial slip

The first initial slip in a connection that is observed is less than the hole clearance for multi-fastener connections. However, under unloading-reloading conditions plastic deformation of the timber around the fastener will occur. Hence the behavior will more closely resembles the description given by Reynolds et al. (2022). Eurocode 5 specifies slip indirectly in the requirements for detailing. The hole clearance in timber is at most 1,0 mm larger than the bolt diameter. For steel plates the hole clearance is at most 2 mm or 0,1d larger than the bolt diameter (largest of the two). Plastic deformation of the timber was found to be 0,15 mm on average for several timber species, increasing the zero-stiffness region.

### 2.2.3 Elastic stiffness

The elastic stiffness of a fastener is given in Eurocode 5 by equation (1) for SLS calculations and equation (2) for ULS calculations. The stiffness equation is an equation based on a regression analysis of many test results on timber-to-timber joints using softwood (Sandhaas and van der Kuilen, 2017). Test results of timber connections show large scatter as well. This makes that the current equations cannot accurately predict the results found in experiments, as there are more parameters that influence this stiffness. Furthermore, there is only a weak correlation present between the density and dowel diameter and the stiffness (Sandhaas, 2012).

$$k_{sls} = k_{ser} = \frac{\rho_m^{1,5} * d}{23} \quad (1)$$

Eurocode 5 also states that the stiffness  $k_{ser}$  may be doubled for steel-to-timber connections.

Connections loaded in ULS have a lower stiffness than the same connection loaded in SLS.

$$k_{uls} = \frac{2}{3} k_{ser} \quad (2)$$

### 2.2.4 Effective number of bolts in timber (related to stiffness)

According to Jorissen (1998) the stiffness of a group of bolts in a timber to timber connection is not the sum of the individual stiffnesses. An effective stiffness of 30% is proposed for connections with multiple rows of fasteners.

Sandhaas and Van de Kuilen (2017) observed that the stiffness of grouped high strength steel dowels in a steel to timber connection had a reduced stiffness when compared to the stiffness of a single bolt. Hence an effective number  $n_{ef}$  was proposed to enhance the prediction quality. This value was found to be 0,48 for 12 mm dowels and 0,68 for 24 mm dowels (with 1, 3 or 5 fasteners per connection). There was no hole clearance in the timber, but the steel plates had a 2 mm tolerance. It is also questioned whether  $k_{ser}$  is an appropriate predictor for stiffness joints. Influences of manufacturing and assembling are included in the stiffness behavior.

Reynolds et al. (2022) researched the effective number of dowels for stiffness and slip in multi-dowel timber connections with slotted-in steel plates. They concluded that for softwood, in theory, the effective number of dowels reduces most when going from one to two rows of dowels as the stresses in the timber increase the most (due to accumulation) leading to premature failure as a result of splitting. Connections with four and five rows of dowels both showed an effective number of 0,60. This effective number was calculated for the unload-reload stiffness  $K_e$ .

Test results showed that the effective number of dowels in reality is lower than the theoretical results. The observed effective number of dowels was found to be closer to 0,50 for five rows of dowels.

One larger connection with seven rows and five rows of dowels with three slotted-in steel plates was tested. Test results indicated an effective number of dowels of 0,20 where an effective number of dowels of 0,61 was expected based on computer simulations. This suggests that “additional processes are restricting the number of dowels contributing to the connection stiffness” (Reynolds et al, 2022).

In conclusion it can be said that the stiffness of a multi-fastener connection under unloading-reloading conditions is best described by a zero stiffness region (or initial slip) and an elastic stiffness  $K_e$  rather than the serviceability stiffness  $k_{ser}$ . According to Sandhaas and van der Kuilen (2017) it “can be questioned whether  $k_{ser}$  is an appropriate predictor for the stiffness of joints as it includes influences of manufacturing and assembling”.

#### 2.2.5 Deformation at failure

The deformation at failure is found based on the results from Jorissen. (1998). The average failure of the connections was 10 mm, similar to the results by Sandhaas (2012) for single fastener . However, for multi-fastener connections, the maximum deformation is reduced due to brittle failure.

## 2.3 Resistance of a single bolt

The resistance of a connection depends on the type of fastener. The type of joint is considered to be a steel-to-timber connection with bolts. Calculations in Eurocode 5 are according to the European Yield Theory by Johansen (1949). Design resistance can be found by multiplying the governing characteristic resistance with the  $k_{mod}$  factor and a  $\gamma_M$  factor. The correction factor  $\beta$  includes the different embedment strength. This factor is considered to be 1,0 as the embedment strength in CLT deviates less on the angle of the grain than standard timber, and the density of all members is considered to be equal. The resulting resistance  $F_{v,Rd}$  is the resistance per shear plane. The resistance of the fastener is the sum of the resistance per shear plane. The European Yield Theory for calculating the resistance of a single shear plane has been presented in Appendix A2.9.

### 2.3.1 Effective number of bolts in timber (related to strength)

Jorissen states in his PhD work that “the relative reduction in load carrying capacity per fastener is higher for a multiple fastener connection with two fasteners than for a multiple fastener connections with more fasteners in a row”. This is also found in test results. What contradicted the theoretical predictions was that a connection with nine fasteners showed a reduced load per fastener when compared to a connection with five fasteners. Stress accumulation and consequent perpendicular splitting of the timber is the main contributor to the reduced resistance per fastener. His research resulted in the equation that is currently presented in Eurocode 5 for the effective number of bolts.

## 2.4 Multiple shear plane steel-to-timber connections

Connections with multiple shear planes can be calculated as the sum of the minimum load-bearing capacities of all shear planes (timber engineering book v2). Eurocode 5 paragraph 8.1.3 describes two criteria for multiple shear planes. The first criteria states that the resistance of each shear plane should be determined by assessing each shear plane as if part of a three-member connection. The second criteria states that the failure of the shear planes should be either all ductile failure modes or all brittle failure modes. A combination of ductile and brittle failure modes is not allowed.

An example is given by Hartl, Leijten and Hilson (timber engineering book v2, E15) of a connection with five members (four shear planes). There is symmetry which makes that shear plane 1 equals shear plane 4. And shear plane 2 is the same as shear plane 3. Internal elements have a thickness  $t_1$  that is half the thickness of the member.

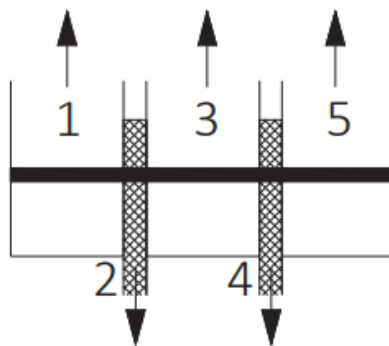
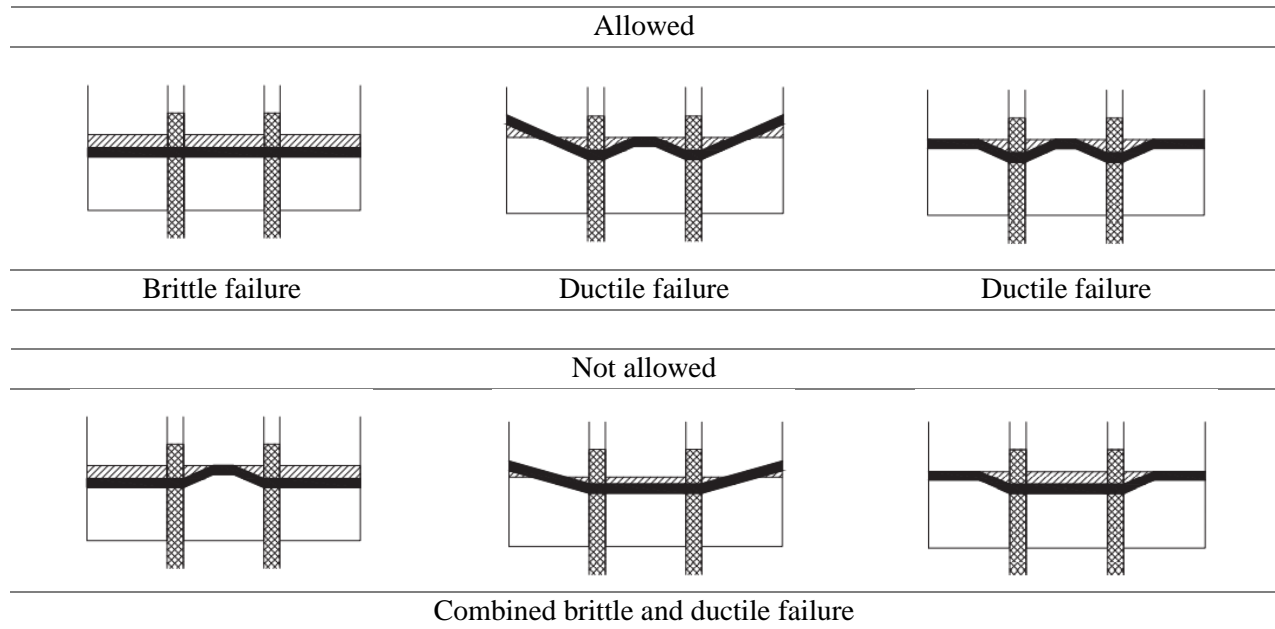


Figure 7, definitions of a fastener with four shear planes in a steel-to-timber connection (timber engineering book v2)

For the figure above several failure modes have been given. Not all of these failure modes are allowed according to the second criteria given in the Eurocode. Only three failure modes are allowed. Of these three modes, two have a complete ductile failure behavior and are therefore preferred.



#### 2.4.1 Rope effect $F_{ax,Rk}$

The rope effect is an additional resistance of the fastener due to axial forces that are generated due to deformation. The value of the rope effect and the contribution on the overall resistance depends on the type of fastener. For bolts with washers the rope effect can result in an additional resistance per shear plane of 25%.

The axial force in the bolt is generated by a washer. The following formula can be used to calculate the rope effect.

$$F_{ax,Rk} = \frac{\pi}{4} (D_{ext}^2 - D_{int}^2) * 3 * f_{c,90,k} \quad (3)$$

#### 2.4.2 Embedment strength $f_{h,k}$

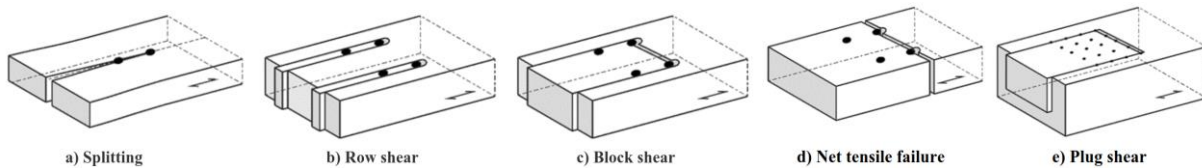
The embedment strength of CLT is given by the ETA for Derix panels (ETA-11/0189). This equation was presented by Uibel and Blass (2006).

$$f_{h,CLT,k} = \frac{32 * (1 - 0,01 * d)}{1,1 * \sin^2 \alpha + \cos^2 \alpha} \quad (4)$$

The angle of the grain has a 9% influence on the embedment strength of CLT. Compared to spruce timber (37% for  $k_c = 1,59$ ).

### 2.4.3 Block shear and plug shear failure

Block shear and plug shear failure for multiple shear planes are assumed to be not relevant for CLT panels. Appendix A2.10 however shows that there is a risk of brittle group shear failure for CLT depending on the interpretation of the new Eurocode 5 draft. Brown and Li (2020) and Azinovic et al. (2022) observed brittle failure in CLT for grouped fasteners. The new Eurocode 5 draft does not specify how to define brittle failure of multi-fastener connections, hence it is not included.



### 2.4.4 Minimum spacings and edge and end distances

In order to avoid splitting of timber, a minimum distance between fasteners is required. Several requirements have been defined depending on the location of the fastener, direction of the grain and direction of loading. The following figure is given in Eurocode 5 to clarify this.

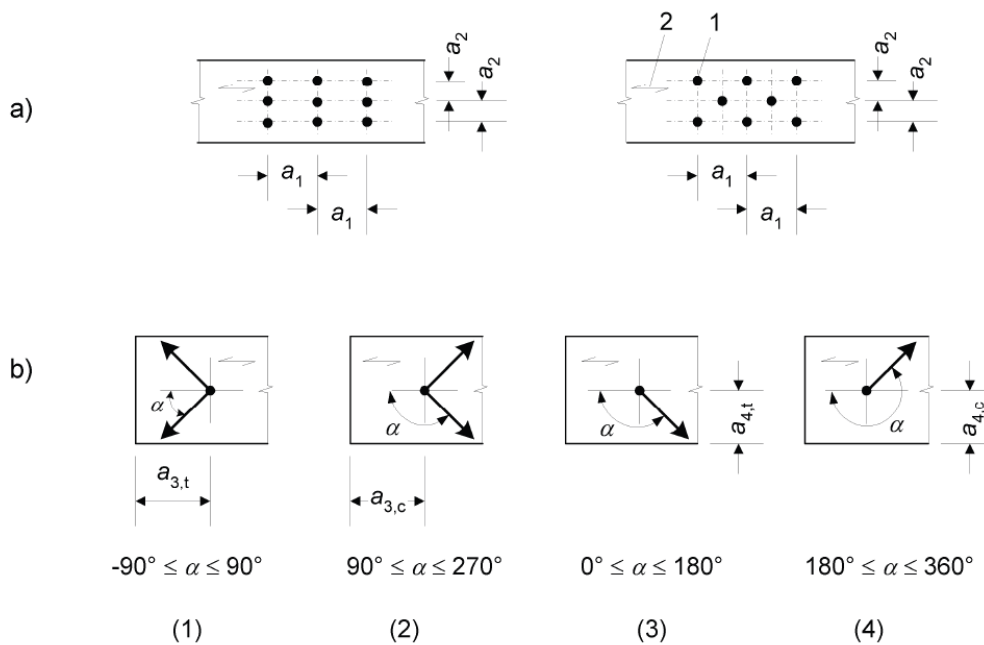


Figure 8, spacings and end and edge distances according to Eurocode 5

The current Eurocode only specifies distances for fasteners in timber. The ETA for Derix products provides the edge and end distances for CLT panels. The requirements for bolts are given in the table below.

Table 2, spacings and end and edge distance requirements

	Angle	Bolts in timber (EC5)	Bolts in CLT ETA Derix 2019
<b>a1</b>	$0^\circ \leq \alpha \leq 360^\circ$	$(4 +  \cos \alpha )d$	$3 + 2 \cos \alpha $ ; <i>min</i> $4d$
<b>a2</b>	$0^\circ \leq \alpha \leq 360^\circ$	$4d$	$4d$
<b>a3,t</b>	$-90^\circ \leq \alpha \leq 90^\circ$	$\max\{7d; 80 \text{ mm}\}$	$5d$
<b>a3,c</b>	$90^\circ \leq \alpha \leq 150^\circ$	$1 + 6 \sin \alpha d$	$4d$
	$150^\circ \leq \alpha \leq 210^\circ$	$\max(3,5d; 40 \text{ mm})$	
	$210^\circ \leq \alpha \leq 270^\circ$	$a_{3,t} \sin \alpha $	
<b>a4,t</b>	$0^\circ \leq \alpha \leq 180^\circ$	$\max\{(2 + 2 \cos \alpha )d; 3d\}$	$3d$
<b>a4,c</b>	$180^\circ \leq \alpha \leq 360^\circ$	$3d$	$3d$

This shows that the required spacing for fasteners in tension ( $a_{3,t}$  and  $a_{4,t}$ ) in CLT panels may be lower than in standard timber.

#### 2.4.5 Effective number of bolts (related to strength)

The effective number of bolts takes into account the influence of splitting of the timber in perpendicular direction to the grain. As this decreases the resistance of the connection. The European Technical Assessment (ETA-11/0189) for Derix CLT panels considers the effective number of bolts to be equal to the applied number of bolts, for fasteners with a diameter larger than 10 mm. In other words  $n_{ef} = n$ . This is expected to be caused by the fact that the lay-up of CLT reduces this splitting of timber, the effective number of bolts is similar to the applied number of bolts. So there is no reduction of the total resistance. This does not however justify for the accumulation of stresses that is known to occur.

## 2.5 CLT façades

Shear walls made of CLT are composed of multiple CLT panels that are connected to one another. The deflection of the wall is the result of four components. The first two are bending and shearing of the CLT panel. The second two components are sliding and rocking (or uplift) which is related to the connections. Connections on the vertical edges of the CLT panels also cause a reduction of the bending stiffness. This in turn increases the bending deformation of the façade.

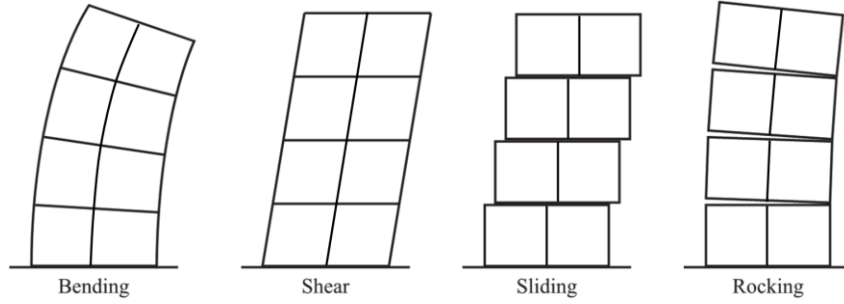


Figure 9, four components of a CLT shear wall deflection [adjusted from T. Znabei]

$$w = w_{bending} + w_{shear} + w_{sliding} + w_{rocking} \quad (5)$$

The in plane stiffness of the CLT façade can be represented as a series of springs. Each spring represents the stiffness of one deflection component. The façade stiffness is the equivalent stiffness of these four stiffnesses. A reciprocal formula is used to determine the equivalent stiffness.

$$k_{eq}^{-1} = k_{bending}^{-1} + k_{shear}^{-1} + k_{sliding}^{-1} + k_{rocking}^{-1} \quad (6)$$

Openings in the CLT panels will reduce the bending and shear stiffness of the façade and introduce additional components that contribute to the top deflection. The bending stiffness has to be calculated for the cross-section at the height of the openings. The shear stiffness has to be calculated for two cross-sections. One at the height of the openings, and one for the full width of the façade. The effective shear stiffness is then the weighted average of these two values.

### 2.5.1 Additional deformation due to openings

The two additional components are local deformations of the piers around the openings and deformation of the lintels. This is due to the fact that the façade starts to act as a portal frame. The horizontal elements (lintels) can undergo vertical deformation which in turn reduces the stiffness of the façade. The vertical elements (piers) can undergo horizontal deformation of which the sum is to be added to the top deflection of the façade.

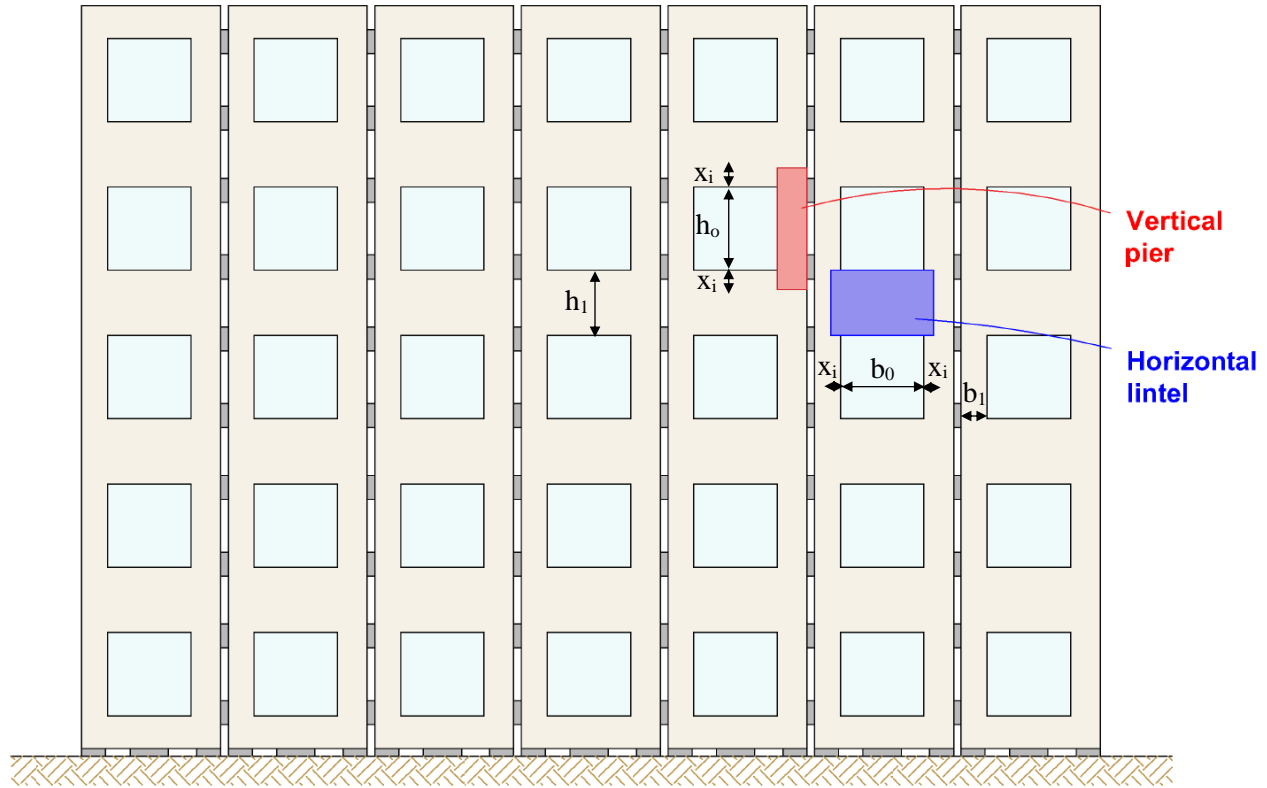


Figure 10, location of the piers and lintels in the façade structure

The effective length of the internal piers is described by Hsiao (2014). These principles will also be used for the case of CLT panels. The equation for the effective length of the pier is shown below.

$$h_{pier} = h_0 + \sum x_i \quad (7)$$

$$x_i = \frac{1}{4} b_1 < \frac{1}{2} h_1 \quad (8)$$

The deflection of the vertical piers and the horizontal lintels can then be calculated based on the basic forget-me-nots.



Bending moments

$$M = \frac{V l}{2}$$

Deflection

$$w = \frac{V l^3}{12 E I}$$

Figure 11, mechanical scheme of a beam with fixed ends on both sides of which one has a rolling condition [CTB2220 reader]

### 2.5.2 Deformation due to connections

Connections contribute to deformation of the structure in several ways; rocking deformation, sliding deformation and additional bending deformation due to a reduced bending stiffness (which will be referred to as additional bending deformation).

### 2.5.3 Rocking deformation

Rocking deformation is the result of elongation of the connections in tension and compression of the CLT panels due to compressive forces (Chen and Popovski, 2014). It is assumed that the panels rotate as rigid bodies and that at least half of the width of the façade is in compression. Chen and Popovski present equations based on equilibrium of the rigid body and can be solved using an iterative procedure.

The iterations are required since the tensile force ( $R_{t,hdI}$ ) in the connection is depending on the width of the compression zone  $L_c$ .

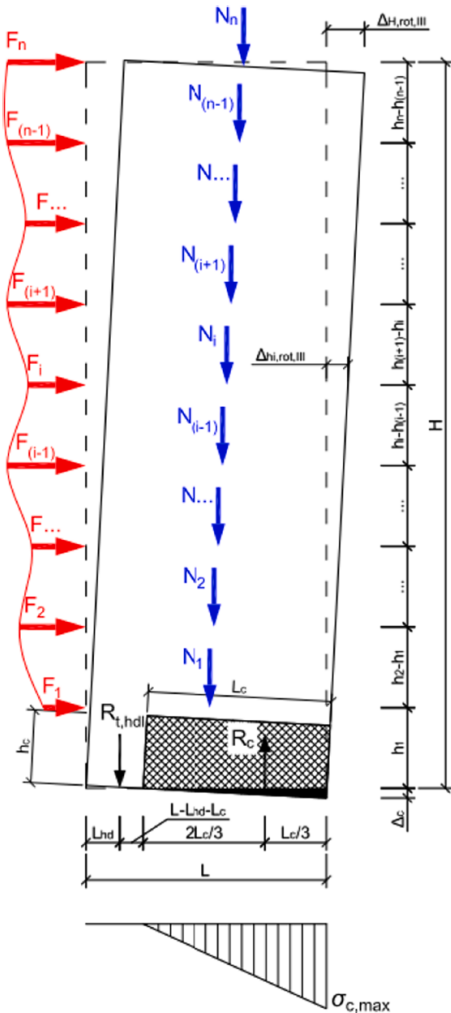


Figure 12, deflection due to rotation from Chen and Popovski, 2014

Where  $k$  is an indentation factor of 2,0 according to Chen and Popovski

$$R_c = \sum_{j=1}^n N_j + R_{t,hdI} \quad (9)$$

$$\sum_{j=1}^n F_j h_j = \left( \frac{L}{2} - \frac{L_c}{3} \right) \sum_{j=1}^n N_j + R_{t,hdI} \left( L - \frac{L_c}{3} \right) \quad (10)$$

$$R_c = \frac{1}{2} \sigma_{c,max} L_c t \quad (11)$$

$$\sigma_{c,max} = E_{eff} \frac{\Delta_c}{k L_c} \quad (12)$$

$$\tan(\theta_{rot}) = \frac{\Delta_c}{L_c} = \frac{R_{t,hdI}/k_{v,hd}}{L - L_c} \quad (13)$$

### 2.5.4 Sliding deformation

Sliding deformation is the result of deformation of the connections on the horizontal edges of the CLT panels. The total sliding deformation is the sum of the deformation of each layer. The following equation has been derived.

$$\frac{(q_{wind} - \mu_F * q_{weight}) * h * n}{2 * b * k_{con}} \quad (14)$$

Where,

- b is the width of the connections
- h is the height of the façade
- n is the number of sliding surfaces
- $k_{con}$  is the stiffness of the connection in horizontal direction

### 2.5.5 Additional bending deformation

Additional bending deformation is an additional deformation due to the fact that the bending stiffness of the façade is reduced. This deformation can be calculated with the method of Schelling

### 2.5.6 Method of Schelling

The method of Schelling is similar to the gamma-method, which is described in Eurocode 5. Both methods are used to calculate the bending stiffness and axial stresses in a built-up girder. A reduction factor  $\gamma$  is defined for each element due to deformations in the connections. The  $\gamma$ -value is the reduction of the bending stiffness contribution of the ‘Steiner part’ of that element due to slip of the connections. A derivation of the method of Schelling is presented in Appendix A2.1.

The method can be used to calculate the additional bending deformation of the façade structure by considering each CLT panel as one element and taking into account the connection stiffnesses on the vertical edges of the panels.

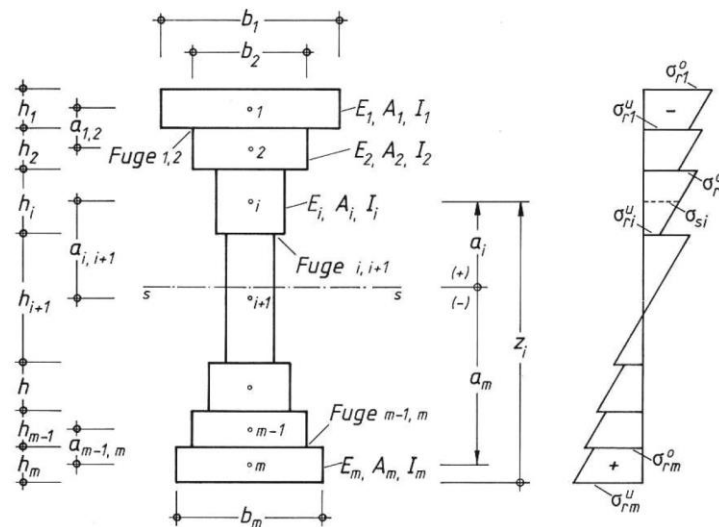


Figure 13, variables for the calculation of the gamma-values (Schelling, W. 1982)

### 3 Boundary conditions for the design

The boundary conditions defined in this chapter are the starting points for the research. The design by UC Architects is introduced. The provided floor plan is used to base dimensions on. CLT panels have been designed with openings in order to allow daylight to enter the building. Loads on the structure are calculated for the given floor plan as well as façade properties based on the panel design for the given structure.

#### 3.1 Floor plan

This thesis is based on a design by Urban Climate Architects. They have designed a tower of which the main load bearing structure is preferred to be in timber. Dimensions of the elements are based on the floor plan of the tower.

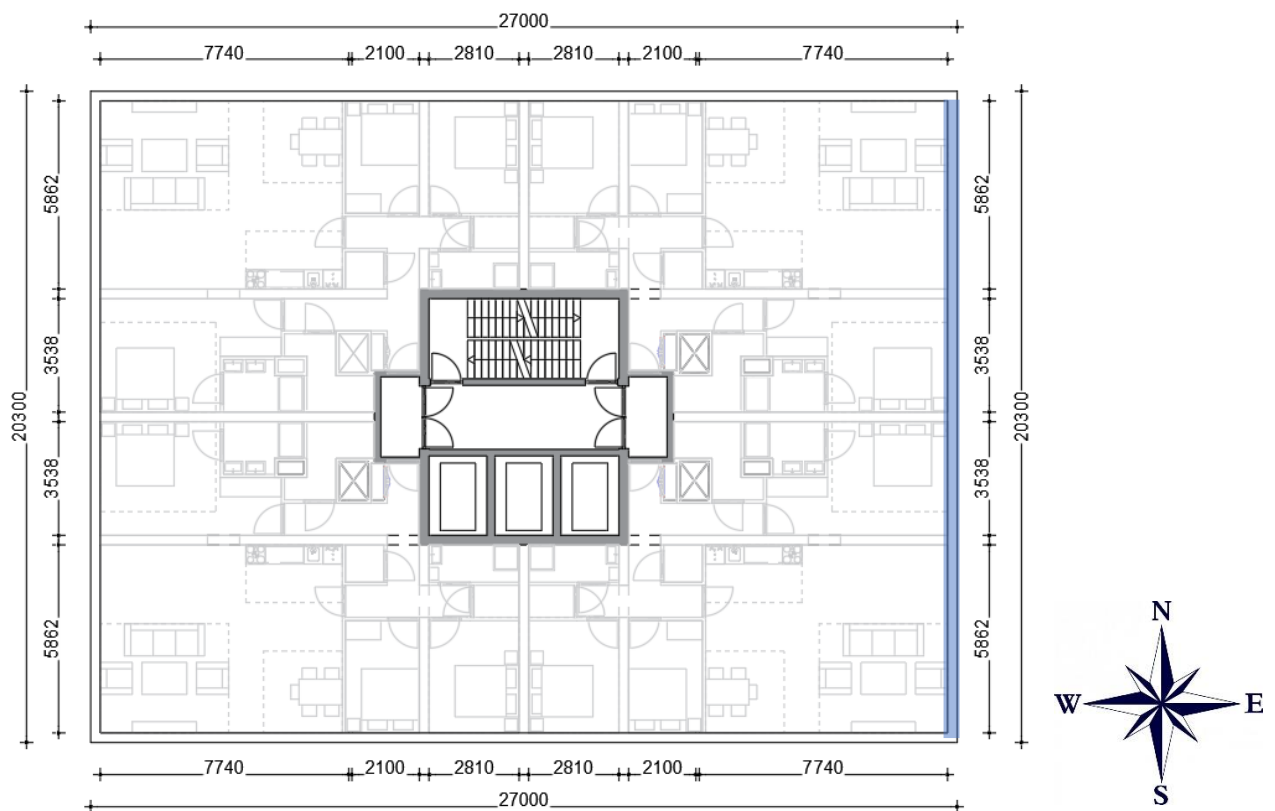


Figure 14, floor plan based on the design by UCA

The story height is 3,1 meter for each story. The east and west façade have a width of 20,3 meter. The north and south façade have a width of 27,0 meter. Research will be done on the east façade (in blue) as this façade receives most wind load, while having a lower bending stiffness due to the smaller width.

The CLT walls will be insulated on both sides in order to provide additional fire resistance to the structure on the inside, and thermal insulation on the outside. The floor is a hybrid CLT-concrete floor of which the concrete is assumed to be in situ, providing additional rigidity for the floor. In case this is not required, and the CLT plates suffice as the only structural element of the floor, the concrete can be replaced by gravel for demountability reasons. The mass of the gravel is required however in order to add weight to the structure.

The floor is positioned onto steel angles that are attached to the façade panel. The panels are then fixed in place by lag bolts. The insulated wall panels on the inside hide the steel angle afterwards and provide space for electrical sockets.

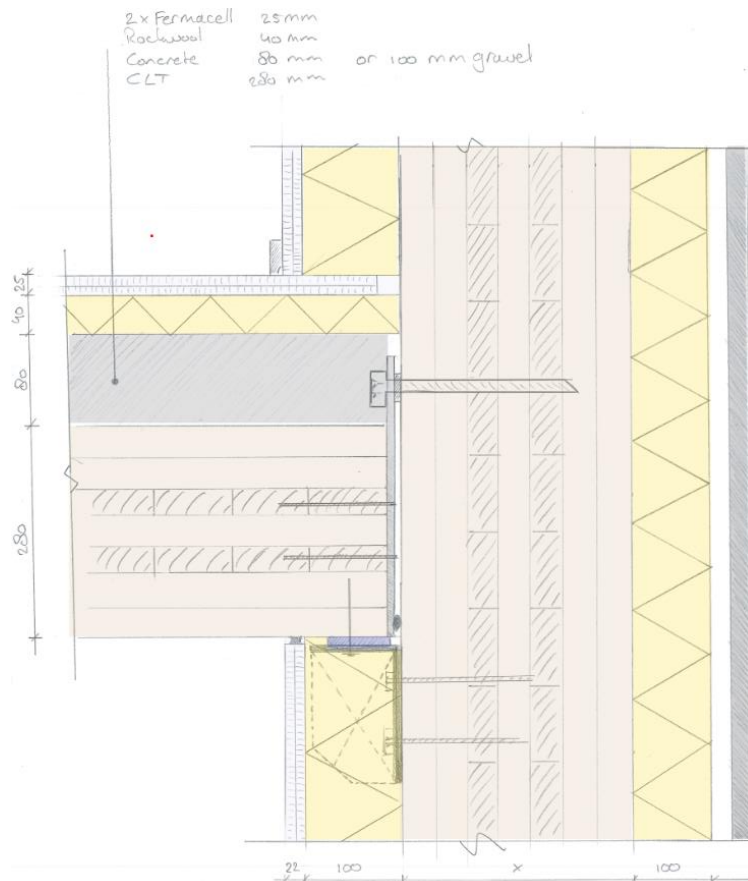


Figure 15, vertical detail of the CLT façade with a timber-concrete composite floor

### 3.1.1 Floor element layout

The floor transfers load to the façade and the core. The direction of the CLT panels has been shown in Figure 16. The size of the core has been increased in width in order to decrease the span of the floor. Beams are required to support the floor plates. These beams have been indicated with blue lines. Due to the timber-concrete composite action, the expected load distribution from the floor to the façade (shown in red) is not linear along the façade. Near the corners it is distributed over both façades, hence the trapezoidal shape of the load distribution.

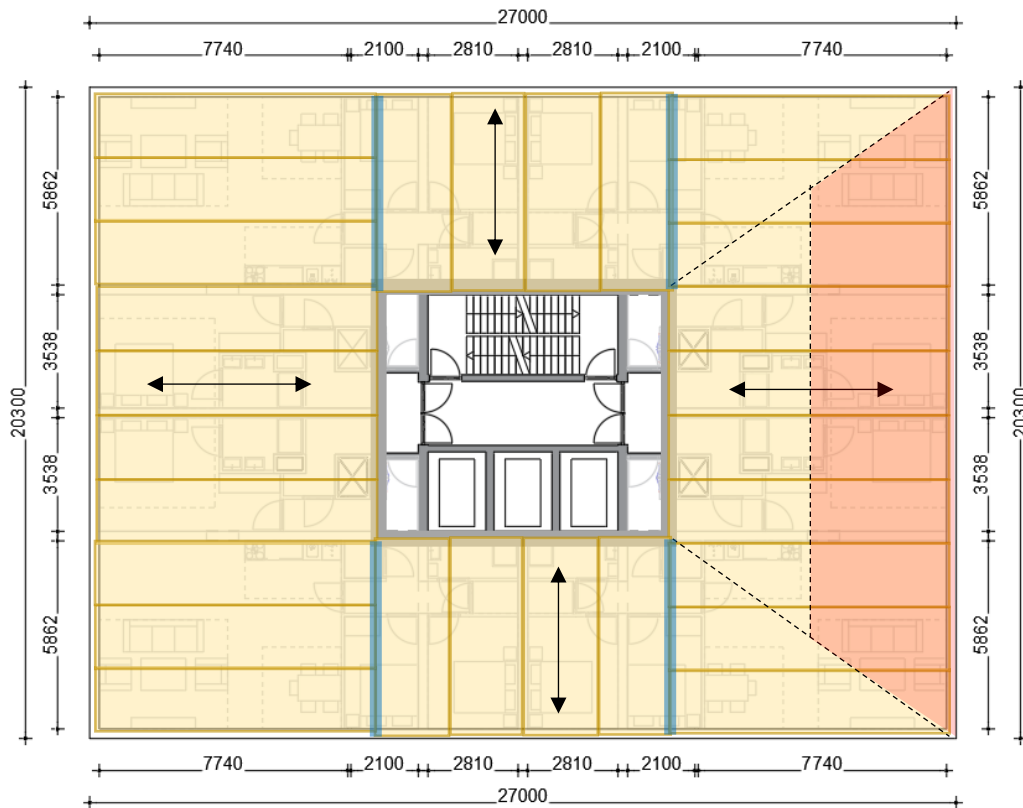


Figure 16, floor and panel layout

The floor in the figure above spans from the core to the façade. Figure 16 shows a larger core as indicated in Figure 14. This is due to the fact that 8 meter is a more realistic span for hybrid CLT-concrete floors.

## 3.2 Loads on the structure

The loads acting on the structure will be calculated for the given dimensions. First the load combinations will be explained. Then the prescribed loads that act on the façade and finally a comprehensive table of the loads will be presented.

### 3.2.1 Load combinations

Load combinations have been defined according to NEN-EN 1990. Consequence class CC2 is used to calculate the design values. This is also the case for the model with a height of 77,5 meter. According to the codes, structures that exceed a height of 70 meter have to be calculated in CC3. But in order to use the same computer model, without many deviations, it was decided to make an exception. The reference lifetime is 50 years, as is usual for most buildings.

Five load combinations are shown in the table below. The ultimate limit state combination has been split into two combinations. The first is the ‘ULS tension’ combination. This load case gives the maximum tension stresses in the façade as a result of wind forces. This considers permanent load as favorable, because it suppresses the tensile forces. The wind load is unfavorable, hence it is the governing variable load. The other variable loads are nullified, as is stated in appendix A1 (application on buildings) of EN1990. The ‘ULS compression’ combination considers all loads to be unfavorable, as all of the loads contribute to the maximum compression forces.

Table 3, combinations in CC2

Combination	Permanent		Wind	Variable
	Favorable	Unfavorable		
ULS max compression	1,20		1,50 $Q_{k,i}$	1,50 $\psi_{0,i} Q_{k,i}$
ULS max tension		0,90	1,50 $Q_{k,i}$	0,00 $\psi_{0,i} Q_{k,i}$
SLS characteristic	1,00		1,00 $Q_{k,i}$	1,00 $\psi_{0,i} Q_{k,i}$
SLS frequent	1,00		1,00 $Q_{k,i}$	1,00 $\psi_{1,i} Q_{k,i}$
SLS quasi-permanent	1,00		1,00 $Q_{k,i}$	1,00 $\psi_{2,i} Q_{k,i}$

The effect in ULS can be written as

$$E_d = \sum_{j \geq 1} \gamma_{G,j} G_{k,j} + \gamma_p P + \gamma_{Q,1} Q_{k,1} + \sum_{i > 1} \gamma_{Q,i} \psi_{0,i} Q_{k,i} \quad (15)$$

The effect in SLS can be written as

$$E_k = \sum_{j \geq 1} G_{k,j} + P + Q_{k,1} + \sum_{i > 1} \psi_{0,i} Q_{k,i} \quad (16)$$

### 3.2.2 Vertical loads

Loads have been calculated in appendix A3.1. The main loads acting on the façade are the live and dead loads of the floor, façade loads and wind loads. The floor loads are applied with a trapezoidal load-distribution. Façade loads have an equal distribution over the width of the façade.

Table 4, loads on the structure

Type of loading	Load per story	Remark
	<i>kN/m</i>	
$Q_{\text{floor,G}}$	14,82	For a floor span of 8 meter
$Q_{\text{floor,Q}}$	4,08	Including $\psi_0 = 0,4$ for all floors
$Q_{\text{façade}}$	2,54	Including 34% openings
$Q_{\text{CLT}}$	Variable	Depending on the type of panel
$Q_{\text{wind}}$	Variable	Depending on the height

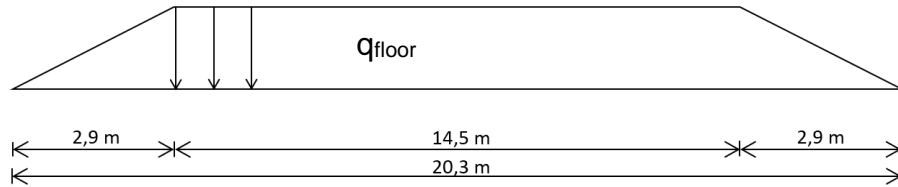


Figure 17, trapezoidal load-distribution on the east façade

### 3.2.3 Wind loads

The Dutch national annex of Eurocode 1991-1-4 on wind loads provides a table with wind loads depending on the building height. The height of the structure and the location will then give a maximum wind load. The location of the building is undefined. Zone II (in Dutch ‘Gebied II’) has been chosen as a reference, as this results in wind loads that are applicable to most of the Netherlands. It is assumed that there are no surrounding buildings. This makes that there is a higher wind load acting on the structure as would otherwise be the case.

Depending on the height of the building, the wind load on the structure is subdivided into strips. Each strip has the height of five stories, equal to that of the panel. The maximum wind pressure is taken from. (Figure 18).

The wind pressure on a structure  $w_e$  is calculated by multiplying the maximum wind load with a pressure coefficient. This pressure coefficient is in between 1,3 and 1,5. It is the sum of a value of 0,8 for wind pressure and a value of 0,5 to 0,7 for wind suction. The value for the wind suction depends on the height to depth ratio ( $h/d$ ). For  $h/d < 1$  the value  $C_{pe,s}$  is 0,5 and for  $h/d > 5$  the value  $C_{pe,s}$  is 0,7.

$$w_e = q_p(z) * C_{pe} \quad (17)$$

The maximum wind load at the top of each façade is calculated according to the values of the table below. According to 7.2.2. (4) of NEN-EN 1991-1-4: NB (national annex) the wind load may be multiplied by a factor 0,85 for lack of correlation between wind pressure and wind suction. The value for  $C_{pe}$  has been calculated for the maximum height of 77,5 meter and is applied for all other heights as well. Friction of wind on the considered façade wall is included by increasing the wind load by 5%.

The  $c_s c_d$  factor has been calculated in appendix A3.2 and was found to be 0,98 for a height of 77,5 meter. All values for  $c_s c_d$  have been chosen to be 1,00 for convenience.

The second order factor has not been included in the wind load, although it was found to have a contribution of 6,6% for the height of 77,5 meter (Appendix A3.4). Second order effects may be excluded if they are below 10% (NEN-EN 1992). However, given the fact that the foundation influence is not included, the calculated factor is an underestimation.

Table 5, characteristic wind loads

Height	$q_p(z)$ $kN/m^2$	$C_s C_d$	factor	$C_{pe}$	friction	b m	$w_e$ $kN/m$
77,5 meter	1,54	1,00	0,85	1,44	1,05	13,5	27,1
62,0 meter	1,45	1,00	0,85	1,40	1,05	13,5	24,7
46,5 meter	1,35	1,00	0,85	1,36	1,05	13,5	22,3
31,0 meter	1,21	1,00	0,85	1,33	1,05	13,5	19,6
15,5 meter	0,99	1,00	0,85	1,30	1,05	13,5	15,7

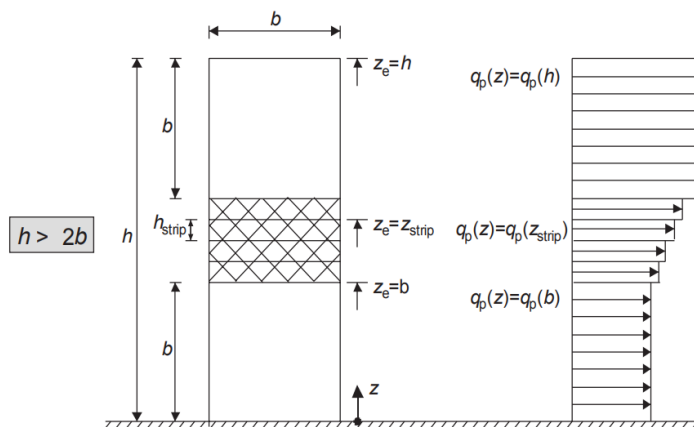
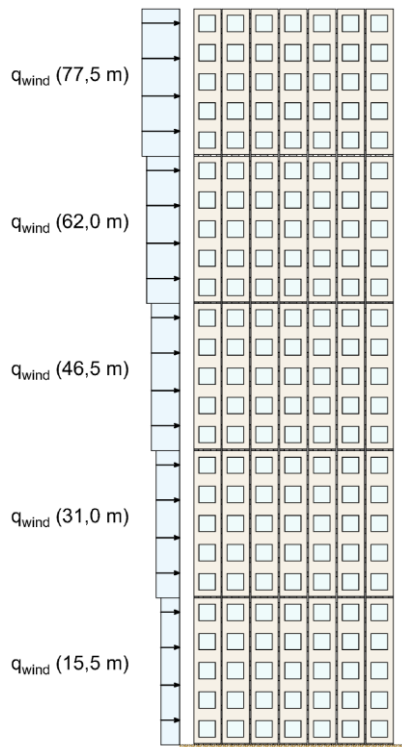


Figure 18, wind load on the façade

### 3.3 Façade panels

The façade panels are designed to use the maximum dimensions available on the market for the given design. That is why the panels are 2,9 by 15,5 meter. When positioned vertically they have the height of five stories of 3,1 meter. Seven panels next to each other make a total width of 20,3 meter, which is equal to the width of the east façade.

Openings in the CLT panels are required in order to allow for daylight entry. According to Dutch building codes 10% of the floor area needs to be used as the equivalent open area in the façade. Based on the floor plan in Figure 14 the required area per opening is 1,51 m<sup>2</sup>. However, this does not take into account several factors like shadows from balconies and window frames or floorplan design. To include these factors, the required open area is doubled. The required area of 3,02 m<sup>2</sup> implies that the dimensions of the opening, in case they are square, is 1,74 by 1,74 meter. This translate into a 34% contribution of the openings of the total façade area.

### 3.4 Façade properties

The in-plane façade stiffness under shear and bending has been calculated for the considered CLT panels. The shear stiffness is calculated with equation (18) where the width is the weighted average width over the height. This way the average shear stiffness of the façade is calculated including the influence of the openings. The shear stiffness for CLT panels is 450 N/mm<sup>2</sup> and the thickness of the whole panel may be used.

The bending stiffness of the façade is calculated at the height of the openings. Only the vertical piers contribute to the bending stiffness of the façade according to the parallel axis theorem. The bending stiffness is then calculated with equation (19).

$$GA_s = \frac{5}{6} * G * t * b \quad (18)$$

$$EI = E * \sum_{i=1}^n \frac{1}{12} * t_0 * b_{pier}^3 + A_{pier} * e_i^2 \quad (19)$$

The resulting façade stiffnesses have been summarized in Table 6.

Table 6, in-plane façade stiffnesses

Panel	t <sub>0</sub>	t <sub>90</sub>	t	GA <sub>s,avg</sub>	EI	W	∑EI <sub>p,min</sub>	∑EI <sub>p,max</sub>
	mm	mm	mm	kN	Nmm <sup>2</sup>	mm <sup>3</sup>	Nmm <sup>2</sup>	Nmm <sup>2</sup>
				x10 <sup>3</sup>	x10 <sup>15</sup>	x10 <sup>9</sup>	x10 <sup>15</sup>	x10 <sup>15</sup>
<b>LL-190/7s</b>	150	40	190	959	495	4,20	0,396	1,41
<b>LL-260/7s</b>	200	60	260	1312	660	5,60	0,528	1,89
<b>LL-300/9s</b>	240	60	300	1514	792	6,72	0,634	2,26
<b>LL-360/9s</b>	240	120	360	1817	792	6,72	0,634	2,26
<b>LL-400/11s</b>	280	120	400	2019	923	7,84	0,739	2,64

## 4 Structural design of CLT façades

This chapter is divided into five parts. First an overview of the deformation components is presented. These components define the force distribution and deformation of the façade. Results of the forces in the panels are presented in chapter 4.2.

Based on the forces that are acting on the structure the appropriate CLT panels are chosen. A first indication of the top deflection is given in chapter 4.4. Finally, the forces on the connections are presented based on similar equations. The connection design is presented in the subsequent chapter, given its importance in this research.

These parts altogether should answer the following question:

*“How to design a façade with CLT panels?”*

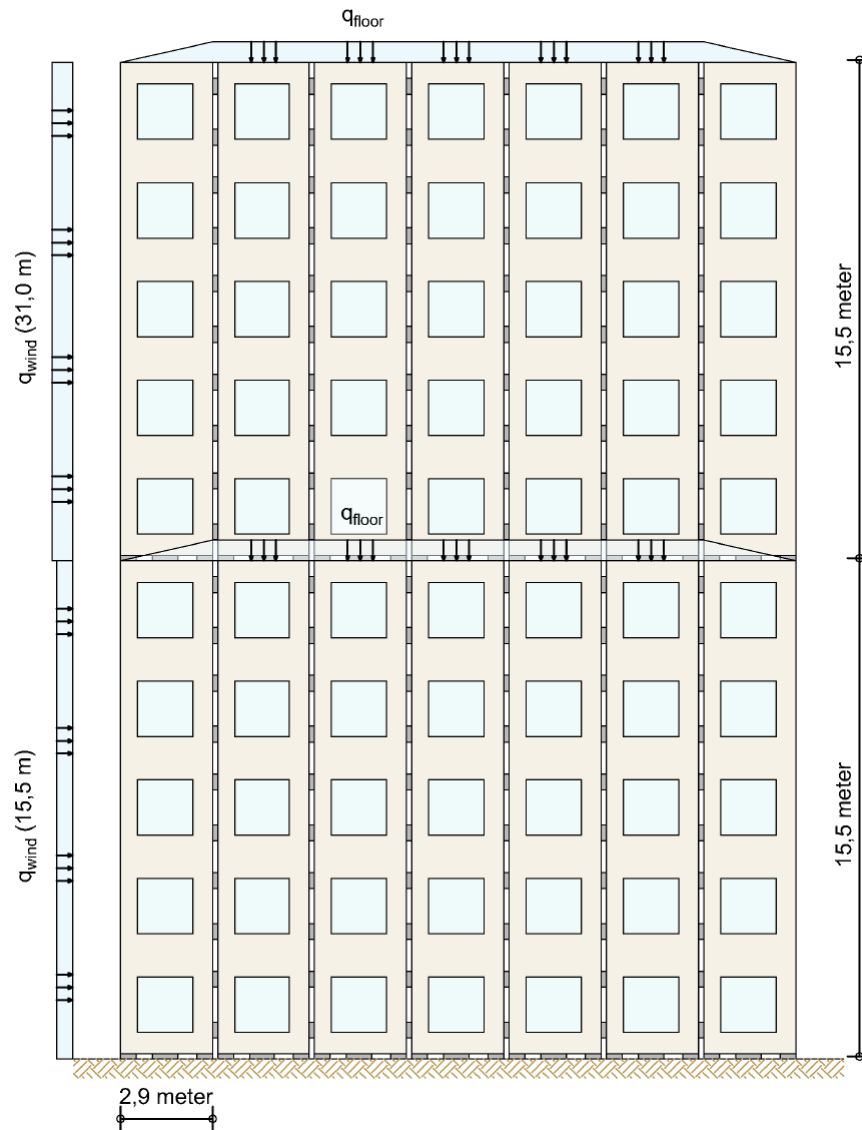


Figure 19, view of a façade with a height of 31,0 meter including loads and annotation

#### 4.1 Overview of the structural mechanics of CLT façades loaded in-plane

An overview of all deflection components is presented below. It shows the type of deflection that is expected, the equations to calculate the deflection (or the method to apply) and some additional remarks. The figures are also presented in larger scale in Appendix A4.1.

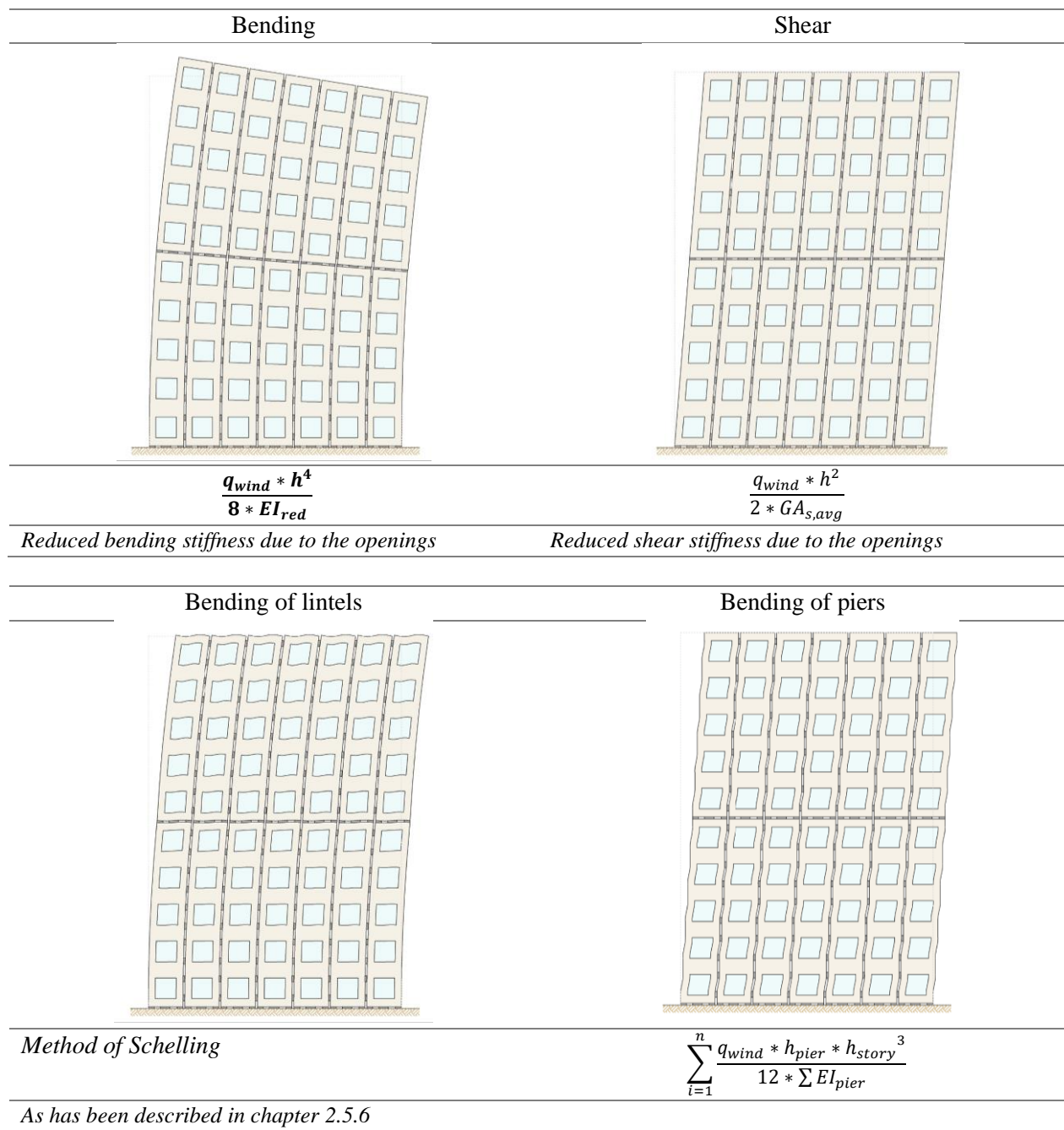


Figure 20, overview of deflection components of CLT panels with openings

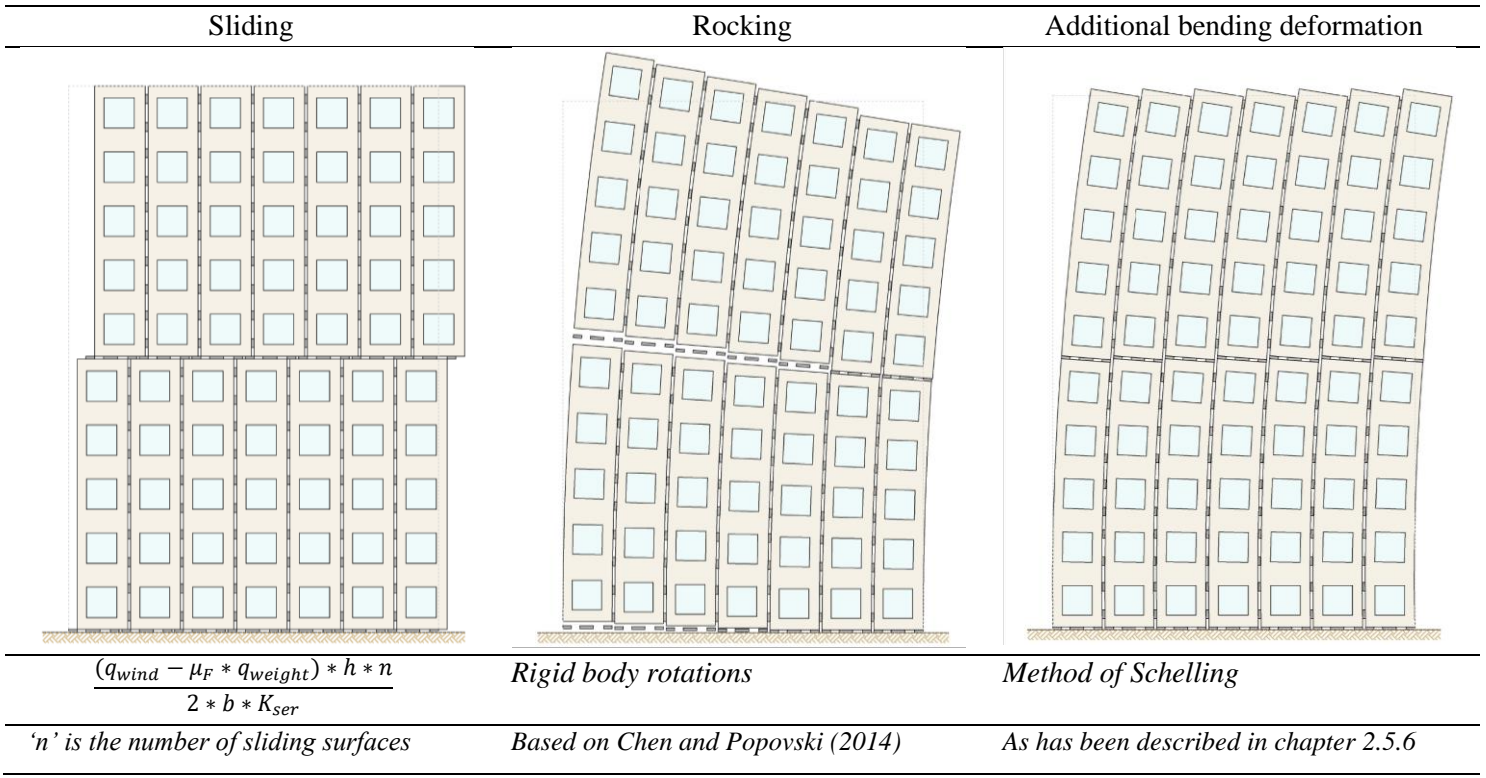


Figure 21, overview of deflection components due to deformation of the connections

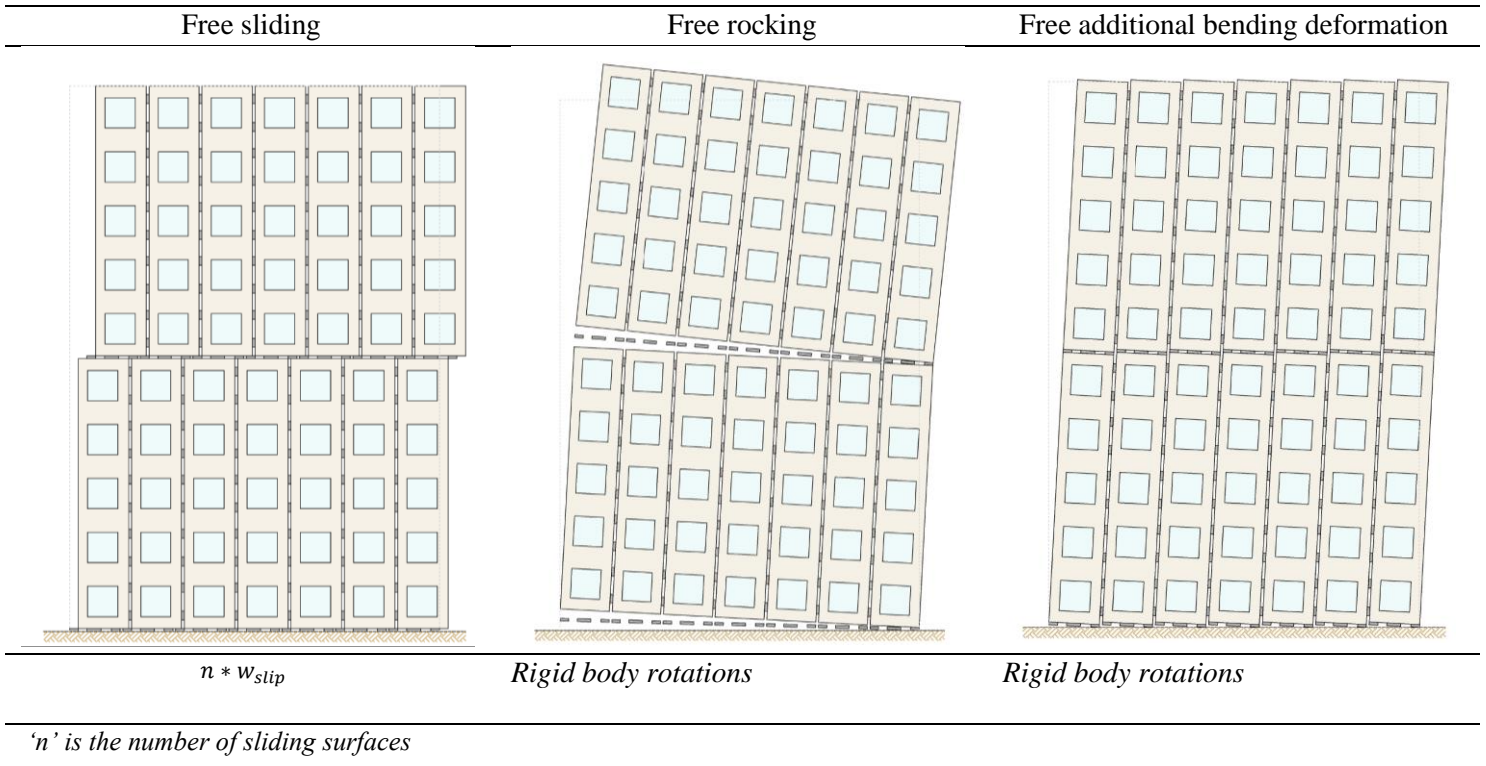


Figure 22, overview of deflection components due to free initial slip in the connections

#### 4.1.1 Bending of the panels

The bending deformation of panels is calculated using a basic equation for bending deflection of a cantilever beam with a reduced bending stiffness to account for openings.

$$w_{bending} = \frac{q_{wind} * h^4}{8 * EI_{red}} \quad (20)$$

#### 4.1.2 Shear of the panels

Shear deformation is calculated based on equation (21).

$$w_{shear} = \frac{q_{wind} * h^2}{2 * GA_{s,avg}} \quad (21)$$

Research has been done by Dujic et al. (2007) regarding the shear stiffness of fenestrated panels. For the presented panels with rectangular openings, the difference between the equations by Dujic et al. and the equation above was negligible (Appendix A4.2).

#### 4.1.3 Bending of piers

The bending of the vertical piers is included in the top deformation by calculating the horizontal force at each floor level and then adding the deformation of the piers at each level. The height of the pier is based on Hsiao (2014).

$$w_{bending,piers} = \sum_{i=1}^n \frac{q_{wind} * h_{pier} * h_{story}^3}{12 * \sum EI_{pier}} \quad (22)$$

#### 4.1.4 Bending of lintels

The bending of the horizontal lintels is included by considering the façade as vertical elements that are connected by the lintels. Deformation of the lintels leads to slip in between those vertical elements. This is analogous to a beam with several elements that is joined with connections. But in this case the stiffness is the resistance of the lintels to deformation as given by the mechanical scheme in Figure 11.

The additional bending deformation can be calculated using the method of Schelling.

#### 4.1.5 Rocking

Rocking is the rotation due to uplift of the hold-down connections of the façade panels that results in an additional deformation of the top. Depending on the connection stiffness and load on the structure, different cases of rocking can be defined. Chen and Popovski (2014) defined several cases of rocking. Two cases have been shown below. The first (left image) is in case the upper panels rotate around the outer edge. The second (right image) is in case the upper panel remains for the most part in direct contact with the panels below.

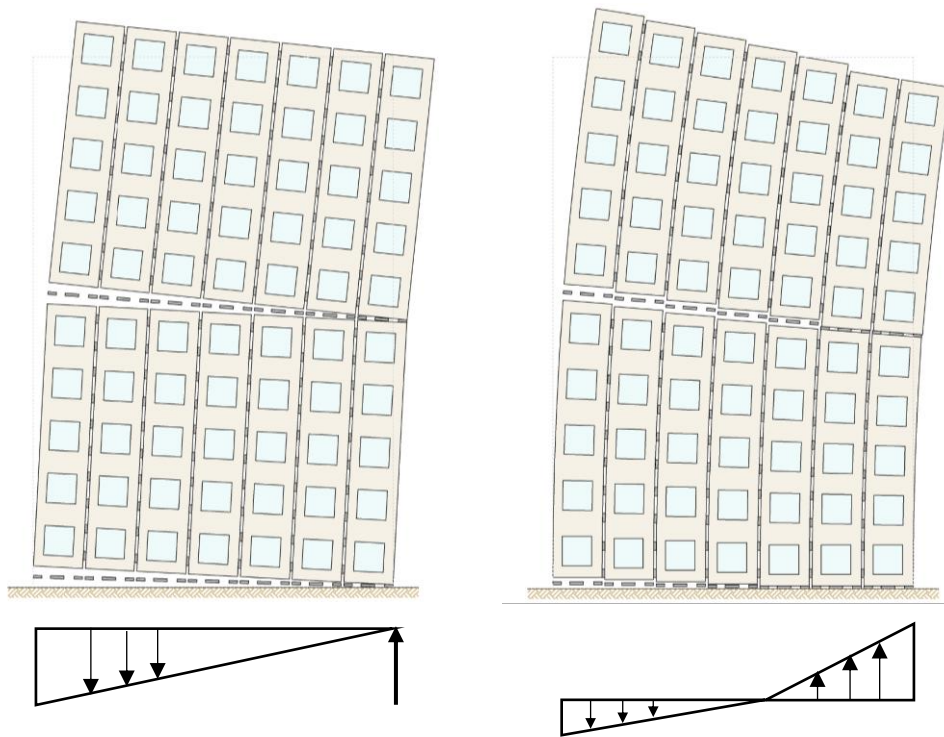


Figure 23, two cases of rocking deformation

Chapter 2.5.3 presented the equations for rocking deformation assuming rigid body rotations.

#### 4.1.6 Additional bending deformation

The method of Schelling is used to calculate the additional bending deformation of the façade as a result of deformations of the connections on the vertical edges of the panels. First the average gamma-value for the façade excluding the openings is calculated. This average gamma-value is the effective cooperation of the façade panels. Multiplying the average gamma-value with the bending stiffness of the façade including openings will then give the bending stiffness for the façade including openings.

## 4.2 Forces on the structure

Forces on the panels have been calculated according to linear-elastic theory. Axial forces are the result of bending moments from wind load and vertical load from dead load and live load whereas shear forces are the result of wind load on the façade only.

There are several forces acting on the façade panels and the connections:

- $n_{y,c}$  and  $n_{y,t}$  Axial forces on the façade panels and connections
- $n_{xy}$  Horizontal shear forces on the façade panels, highest values are found in the piers
- $n_{xy}$  Horizontal shear forces on the connections at the horizontal edges of the façade
- $n_{yx}$  Vertical shear forces on the connections at the vertical edges of the façade

Forces are given as a force per meter [kN/m], which is similar to a stress in the panel [ $\text{N}/\text{mm}^2$ ] multiplied by the thickness. This is a better representation than a stress as CLT panels have a different contributing thickness depending on the type and direction of the load.

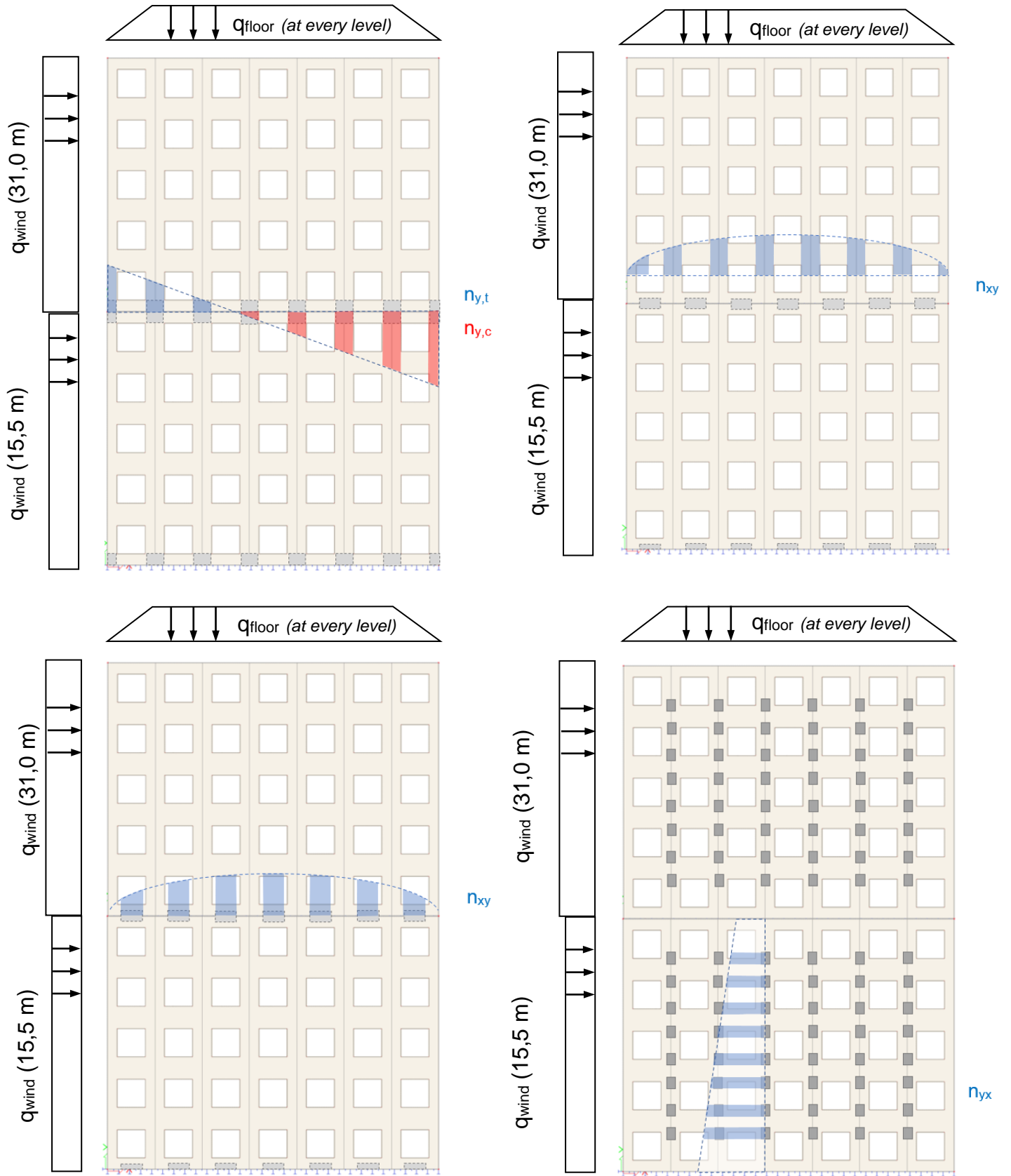


Figure 24, force distribution on the façade

#### 4.2.1 Axial forces on the structure

The axial forces on the structure are calculated with equation (23). It consists of three parts being the axial forces from bending moments from wind on the façade, vertical load from dead weight and axial forces from additional bending moments due to a local effects.

$$n_y = \frac{M_{Ed}}{W} \pm \frac{N_{Ed}}{A} \pm \frac{M_{Ed, pier}}{W_{pier}} \quad (23)$$

These forces do not take into account any influence that connections may have on the force transfer of the structure. This makes that there is a risk of underestimating the (axial) forces on the structure which in turn may result in failure of elements.

The bending moments on the piers depend on several factors which makes that it is difficult to predict their values with theoretical calculations. That is why they have not been included in further calculations. Connections are designed to have an overcapacity by designing them to have a maximum unity check of 0,70.

#### 4.2.2 Shear forces on the structure (horizontal edge)

The shear force on the structure can be calculated with equation (24). The total horizontal shear force is the sum of the wind force over the height of the structure above. This shear force is then distributed over the amount of elements. The resulting shear force is distributed in a parabolic shape. Hence the middle element will receive most shear force which is accounted for by a factor 3/2.

$$n_{xy} = \frac{3}{2} * \frac{\sum_{i=1}^n q_{wind,i} * h_i}{n_{con}} \quad (24)$$

#### 4.2.3 Shear forces on the structure (vertical edge)

The shear force on the vertical edges can be calculated with equation (26). The connections are loaded by a shear force as a result of the increment in bending moment  $\Delta M$  acting on the structure. This increment in bending moment is divided by the lever arm ( $2/3 b$ ) in order to find the resulting axial forces. These axial forces are the shear forces that have to be transferred by the shear connections on the vertical edge.

Per story there are two connections applied, meaning that the calculated shear force can be divided by two. Connections near the outer panels of the façade are loaded by a lower shear force similar to the parabolic distribution of shear forces for the connections on the horizontal edges of the panels. The same equations can be used for the shear force in the lintels.

$$\Delta M = \frac{1}{2} * q_{wind} * [h^2 - (h - h_{story})^2] \quad (25)$$

$$n_{yx} = \frac{\Delta M}{2/3 * b} \quad (26)$$

#### 4.2.4 Shear forces in the corners of openings

According to Pai, Lam and Haukaas (2016) the force transfer around openings in CLT shear walls shows the highest forces in the corners of the opening. Shear forces are 50% higher than in the piers or lintels.

#### 4.2.5 Calculated forces

The forces on the CLT panels are calculated with the presented equations from chapter 4.2. The shear force on the vertical edge of the façade  $V_{Ed,v}$  is calculated based on  $\Delta M$ , which is the increment of bending moment for one story height. This shear force is to be resisted by the horizontal lintel and the connections applied on the interface between the panels.

Table 7, forces on the structure

Model	$q_{w,k}$ kN/m	$V_{Ed,h}$ kN	$V_{Ed,v}$ kN	$M_{Ed}$ kNm	$\Delta M_d$ kNm	$n_{xy, pier}$ kN/m	$n_{yx, lintel}$ kN/m	$n_{xy, corner}$ kN/m	$n_{y,t}$ kN/m	$n_{y,c}$ kN/m
<b>15,5 meter</b>	15,7	365	84	2829	1132	67	63	101	0	519
<b>31,0 meter</b>	19,6	821	188	13.424	2544	152	141	228	149	1262
<b>46,5 meter</b>	22,3	1339	307	33.515	4152	247	231	371	669	2338
<b>62,0 meter</b>	24,7	1913	438	64.669	5932	353	329	530	1582	3807
<b>77,5 meter</b>	27,1	2544	583	108.617	7885	470	438	705	2952	5733

$V_{Ed,h}$	total shear force on the horizontal edge of the façade [kN]
$V_{Ed,v}$	total shear force to be transferred on the vertical edge of the façade for one story [kN]
$M_{Ed}$	total bending moment on the façade [kNm]
$\Delta M$	additional bending moment due to one story [kNm]
$n_y$	axial force per meter width of the pier [kN/m]
$n_{xy}$	shear force per meter width of the pier [kN/m]

#### 4.3 Required CLT panels

Based on the forces as calculated the required CLT panels have been selected. Unity checks have been performed in order to indicate the performance of the panel in tension, compression and shear. The panels that will be used for modelling are shown in black. Alternative panels are in grey.

Table 8, required CLT panels and corresponding unity checks

Model	Panel type	Unity checks			
		$n_{y,t}$	$n_{y,c}$	$n_{xy}$	$n_{xy, corner}$
<b>15,5 meter</b>	LL-190/7s	0,00	0,22	0,42	0,63
<b>31,0 meter</b>	LL-260/7s	0,06	0,36	0,64	0,96
<b>46,5 meter</b>	LL-300/9s	0,24	0,56	1,04	1,56
<b>46,5 meter</b>	LL-400/11s	0,21	0,47	0,52	0,78
<b>62,0 meter</b>	LL-360/9s	0,57	0,90	0,74	1,11
<b>62,0 meter</b>	LL-400/11s	0,49	0,76	0,74	1,11
<b>77,5 meter</b>	LL-400/11s	0,92	1,15	0,99	1,49

Theoretical results indicate that the shear resistance of CLT panels is governing for the models with a height of 15,5 meter, 31,0 meter and 46,5 meter. The models with a height of 62,0 meter and 77,5 meter have a high unity check for both compression forces and shear forces.

#### 4.4 Top deflection

Based on the required panels, the top deformation for each height has been calculated. The maximum allowed deformation of the top is calculated as  $H/500$ . Based on the results it is expected that a façade structure, without the additional contribution of transversal walls or core element, cannot surpass a height of 65 meters for the given floor plan. Additional deformation due to connection stiffnesses is not included. It also needs to be noted that the deformation of the foundation, and the interaction between the foundation and the structure is not included. The actual height that is feasible for these conditions will therefore be lower.

The bending stiffness of the piers depends on the collaboration between the two piers of the adjacent CLT panels. A rigid connection between two panels makes that there is a high collaboration. The bending stiffness of the piers is taken as the average of the minimum and maximum bending stiffness as defined in Table 6. The effective length of the pier was found to be 2420 mm and the effective length of the lintels was found to be 2320 mm.

The table below shows the results for the top deflections of the façade as calculated in appendix A4.4 and A4.6.

*Table 9, top deflections for the façade structure based on the chosen CLT panels*

<b>Model</b>	<b>q<sub>k</sub></b>	<b>panel</b>	<b>W<sub>bending</sub></b>	<b>W<sub>shear</sub></b>	<b>W<sub>pier</sub></b>	<b>W<sub>intel</sub></b>	<b>W<sub>tot</sub></b>	<b>W<sub>max</sub></b>	<b>Unity check</b>
	<i>kN/m</i>		<i>mm</i>	<i>mm</i>	<i>mm</i>	<i>mm</i>	<i>mm</i>	<i>mm</i>	
<b>15,5 meter</b>	15,7	LL-190/7s	0,23	1,97	0,95	1,77	4,92	31	0,16
<b>31,0 meter</b>	19,6	LL-260/7s	3,43	7,17	3,27	6,20	20,1	62	0,32
<b>46,5 meter</b>	22,3	LL-300/9s	16,5	15,9	6,76	16,0	55,1	93	0,59
<b>46,5 meter</b>	22,3	LL-400/11s	14,1	11,9	5,80	7,97	39,8	93	0,43
<b>62,0 meter</b>	24,7	LL-360/9s	57,6	26,1	13,1	15,5	112	124	0,91
<b>62,0 meter</b>	24,7	LL-400/11s	49,4	23,5	11,2	15,5	100	124	0,80
<b>77,5 meter</b>	27,1	LL-400/11s	132	40,3	19,1	26,1	218	155	1,41

## 4.5 Forces on the connections

The equations presented for axial and shear forces are also applicable for the forces acting on the connections. These forces are summarized in the table below. The shear forces on the horizontal and vertical edge have been calculated with different methods, but yield comparable results. Horizontal shear force is calculated according to chapter 4.2.2 and vertical shear force is calculated according to chapter 4.2.3.

Table 10, theoretical forces on the connections

<b>Model</b>	<b>q<sub>w,k</sub></b>	<b>Panel</b>	<b>n<sub>y,t</sub></b>	<b>n<sub>y,c</sub></b>	<b>n<sub>xy</sub></b>	<b>n<sub>yx</sub></b>	<b>N<sub>y,t</sub></b>	<b>N<sub>y,c</sub></b>	<b>V<sub>xy</sub></b>	<b>V<sub>yx</sub></b>	<b>e</b>	<b>M<sub>Ed</sub></b>
	<i>kN/m</i>	<i>type</i>	<i>kN/m</i>	<i>kN/m</i>	<i>kN/m</i>	<i>kN/m</i>	<i>kN</i>	<i>kN</i>	<i>kN</i>	<i>kN</i>	<i>m</i>	<i>kNm</i>
<b>15,5 m</b>	15,7	LL-190/7s	0	519	67	72,4	0	301	78	42	0,12	3
<b>31,0 m</b>	19,6	LL-260/7s	149	1262	152	162	87	732	176	94	0,12	6
<b>46,5 m</b>	22,3	LL-400/11s	669	2338	247	265	388	1356	287	153	0,12	9
<b>62,0 m</b>	24,7	LL-400/11s	1582	3807	353	378	918	2208	410	219	0,24	26
<b>77,5 m</b>	27,1	LL-400/11s	2952	5733	470	503	1712	3325	545	291	0,24	35

n <sub>y,c</sub> ; n <sub>y,t</sub>	axial force (tension and compression) per meter width on the connection	[kN/m]
n <sub>xy</sub> ; n <sub>yx</sub>	shear force per meter width on the connection (horizontal and vertical edge of the panel)	[kN/m]
N <sub>y,t</sub>	tension force in the connection	[kN]
N <sub>y,c</sub>	compression force in the connection	[kN]
V <sub>xy</sub> ; V <sub>yx</sub>	shear force in the connection (horizontal resp. vertical edge of the panel)	[kN]
M <sub>Ed</sub>	bending moment in the shear connection on the vertical edge	[kNm]

The axial force is calculated as the axial force per meter multiplied by the width of the connection.

$$N_i = n_i * b_i \quad (27)$$

Where,

b<sub>i</sub> is the width of the considered connection

#### 4.5.1 Additional bending moment due to eccentricities

The shear force in the connection on the vertical edges of the CLT panels acts in the center of the bolt group. This results in an eccentricity in the connection that leads to an additional bending moment that has to be resisted. The bending moment is calculated as the shear force multiplied by half the eccentricity. The acting bending moment then has to be resisted by the bolts in the connection. Each bolt has a different contribution to this resistance, based on the distance to the center of rotation.

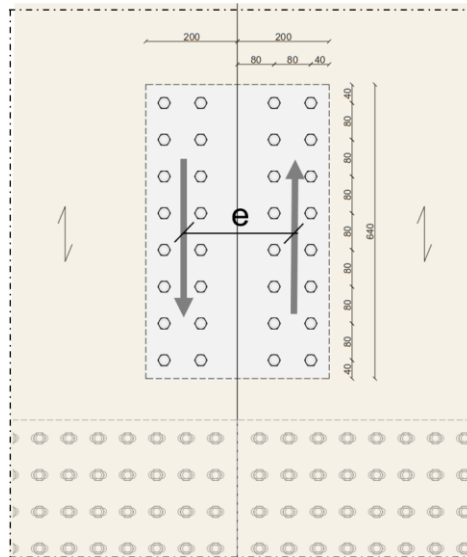


Figure 25, shear force on the connection on the vertical edges of two CLT panels

$$M_{Ed} = V_{Ed} * \frac{e}{2} \quad (28)$$

The additional bending moments are to be added to the shear forces on the bolts according to appendix A4.7

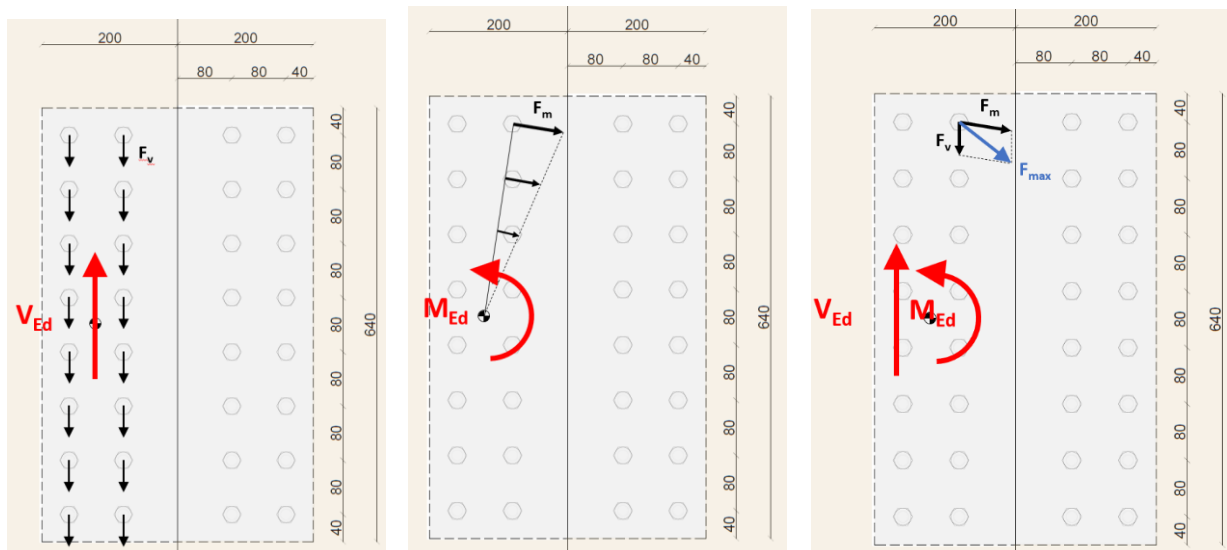


Figure 26, forces on the shear connection on the vertical edges of the panels

## 5 Connection design

This chapter presents the designed connections. Three types of connections have been designed being hold-down connections, shear connections on the horizontal edges of the panels and shear connections on the vertical edges of the panels. There is also a difference in connections between the foundation and the CLT panels, and connections between two CLT panels.

First an overview of the connections will be presented. Then the designs of the connections will be elaborated on. Relevant information from literature will be used for the actual connection design. The structural behavior of the connections is then interpreted in terms of non-linear load-displacement curves. These curves will be used in the computer models in order to find a more accurate structural behavior of the façade.

### 5.1 Overview of the connections

Figure 27 shows the location of the connections. Appendix A5.1 provides the same images on larger scale.

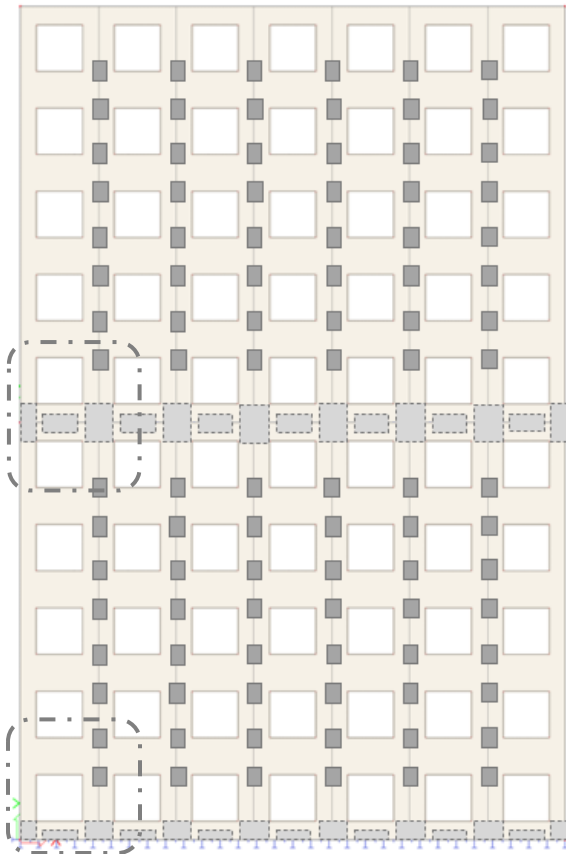
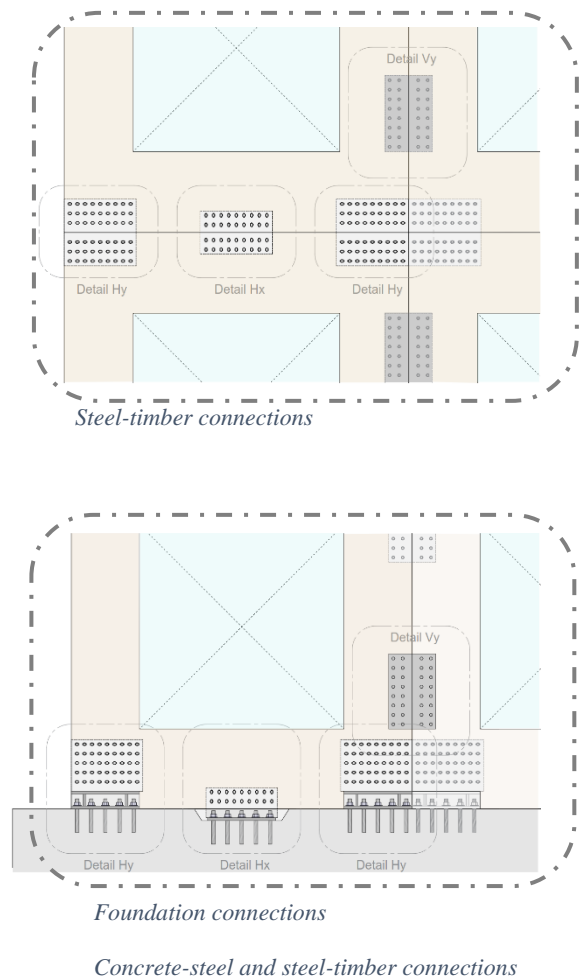


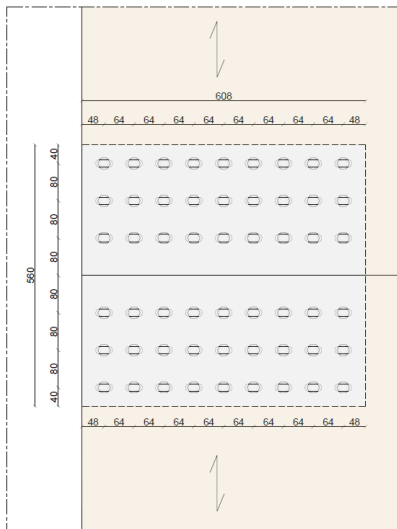
Figure 27, location of the connections in a CLT façade structure.



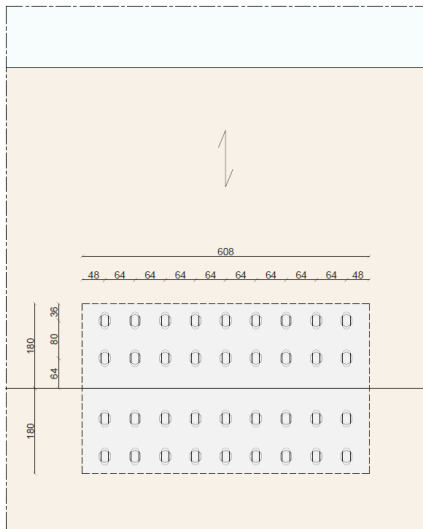
There are five different connections used in the façade, all of which are bolted connections. At the horizontal edges there are two type of connections that differ depending on the location (at the foundation or between CLT panels). These are hold-down connections and shear key connections. At the vertical edges there is another shear key connection applied.

- Hold-down connection between two CLT panels
  - Shear key connection between two CLT panels
  - Shear key connection between two CLT panels
  - Hold-down connection between CLT panel and foundation
  - Shear key connection between CLT panel and foundation
- on the horizontal edges  
on the horizontal edges  
on the vertical edges  
on the horizontal edges  
on the horizontal edges

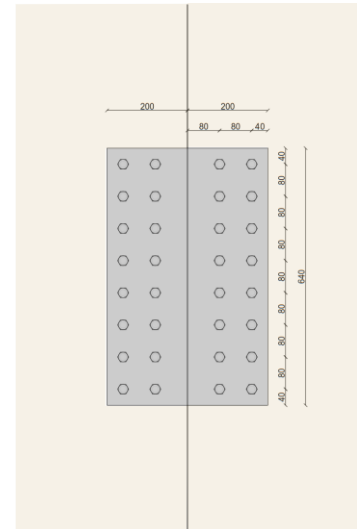
Hold-down double internal plate



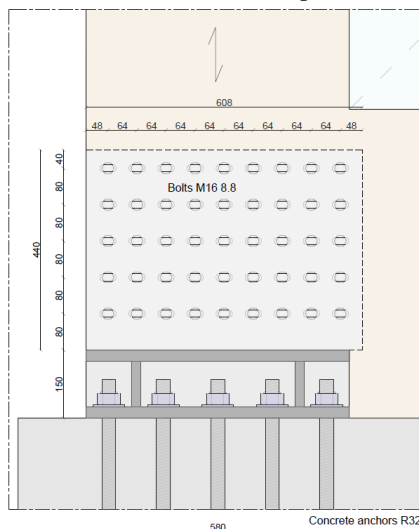
Shear key double internal plate



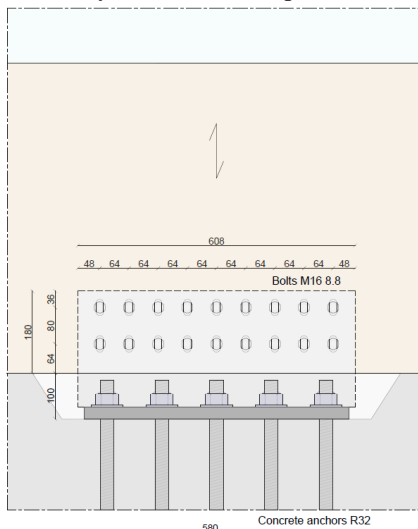
Shear key double external plate



Hold-down double internal plate



Shear key double internal plate



Shear key double external plate

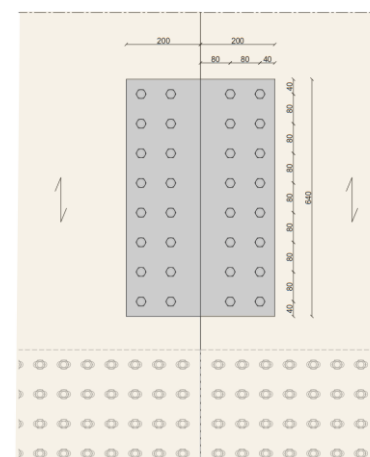


Figure 28, connections used for the façade structure (height of 77,5 meter)

## 5.2 Design of the connections

The design of the connections is based on the type of connection (hold-down or shear key) and force acting on the connection. This in turn is related to the resistance of a single bolt, and the minimum spacing required between bolts.

### 5.2.1 Starting points

The width of the hold-down connections is similar to the width of the piers in the CLT panel. This allows axial forces to transfer in a straight line to the foundation. These connections are designed as internal steel plates that then will be bolted once positioned on site.

Bolts M16 8.8 will be used for the calculations.

### 5.2.2 Flow chart

In order to design the connections and model their properties in the computer program, the following steps will be taken.

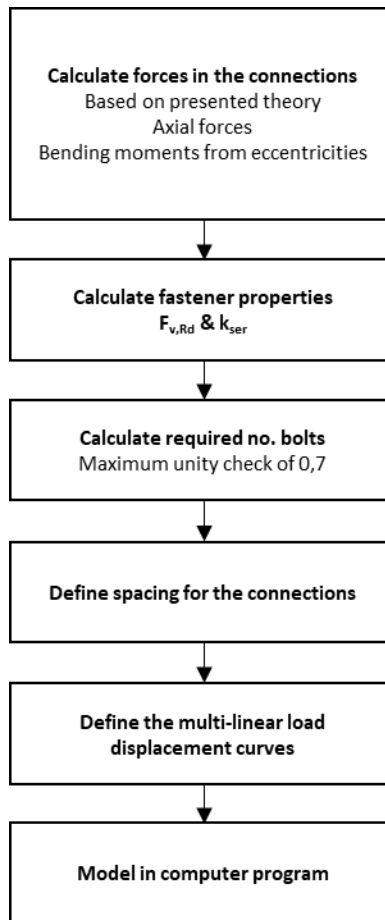


Figure 29, flow chart connection design

### 5.2.3 Embedment strength of CLT

The embedment strength of CLT depends for only 9% on the angle of the load related to the grain of the main boards. Given the fact that the load does not necessarily act in a 0° or 90° angle relative to the grain it is decided to use the lowest value of the embedment strength for all CLT connections ( $f_{h,CLT,k} = 24,1$  N/mm<sup>2</sup>).

### 5.2.4 Design resistance of bolts

The resistance of M16 bolts has been calculated for several type of connections in appendix A5.3. Using smaller bolts (M12) would lead to a larger number of connections, making the connection more labor intensive. Using larger bolts (M20) does not result in stronger connections, as the spacing in between the fasteners is also increased. Furthermore, the failure of larger diameter bolts tends to be more brittle, which is to be avoided.

In order to increase the load carrying capacity per bolt, connections with multiple steel plates have been examined. Three options were found. Which are single internal steel plates, double internal steel plates and double external steel plates. The connections with two internal steel plates have been designed such that the stresses in the timber (as a result of the resistance per shear plane) is equal in all parts.

$$\sigma_{in} = \sigma_{out} \quad (29)$$

$$\sigma_i = \frac{F_{v,Rd,i}}{t_i * d_i} \quad (30)$$

Sidenote in this approach is that the thickness  $t_i$  is that of the whole CLT member irrespective of the direction of the grain. This is due to the fact that the embedment stress is defined for each CLT member irrespective of the direction of the grain as well. Even though the net area, that is the area that is effectively resisting the load, is dependent on the direction of the grain.

The effective cross section of the CLT at the location of the connection is lower than that of the panel itself. The cross section is reduced on both sides by 20 mm to set the bolt heads back. The thickness of the panel is further reduced by the thickness of the steel plates, which is another 40 mm reduction.

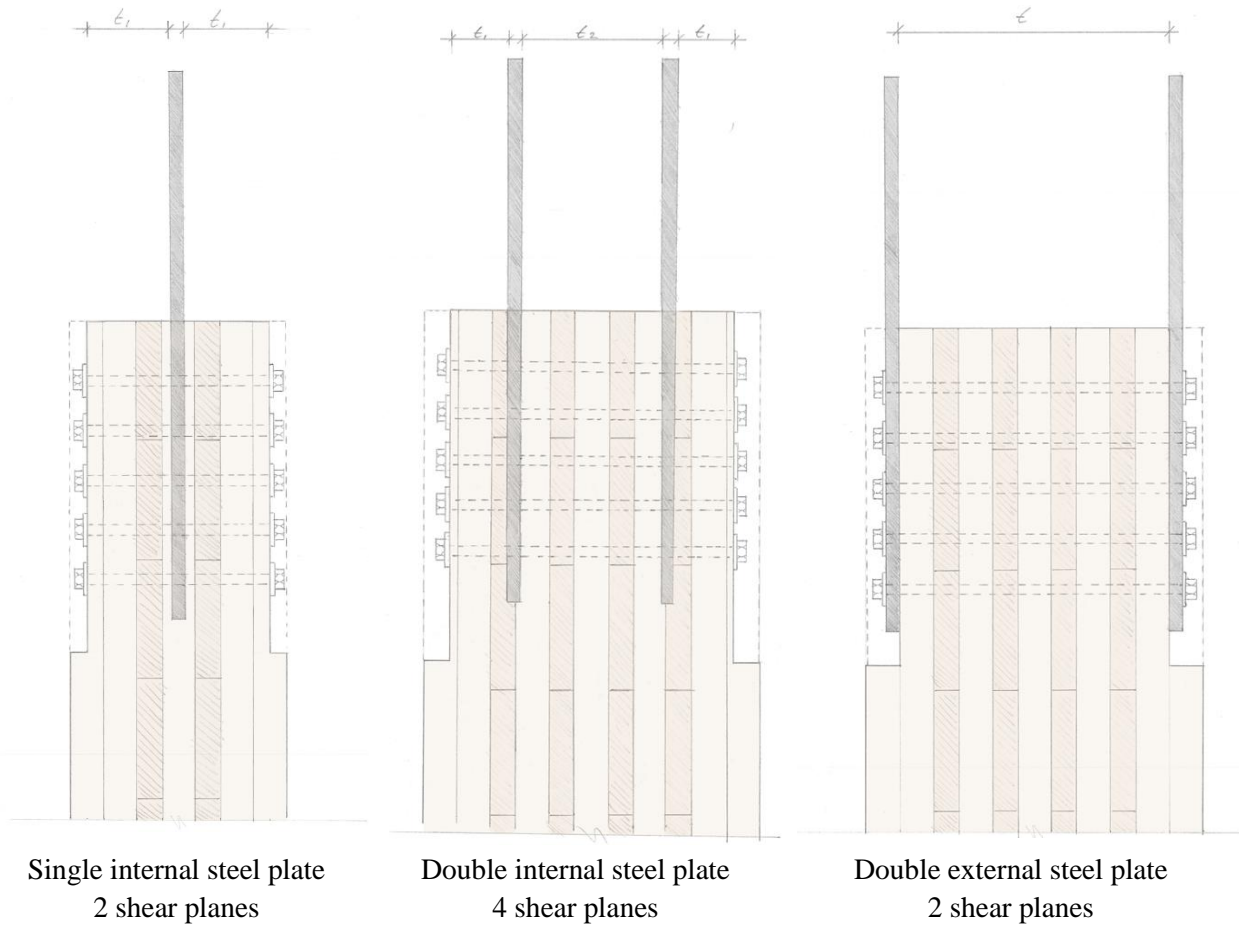


Figure 30, cross-sections of three connections

### 5.2.5 Spacing

Table 11 is presented below, showing the required spacing for timber according to Eurocode 5 and for CLT according to the ETA for CLT by Derix. Values of the ETA from Derix are used as these are given for CLT rather than for timber.

Table 11, spacings and end and edge distances for bolts

	Angle to the grain	Bolts in timber (EC5)	Distance [mm]	Bolts in CLT ETA Derix 2019	Distance [mm]
<b>a1</b>	0°	5d	80	5d	80
<b>a2</b>	0°	4d	64	4d	64
<b>a3,t</b>	0°	$\max\{7d; 80 \text{ mm}\}$	112	5d	80
<b>a3,c</b>	180°	$\max(3,5d; 40 \text{ mm})$	56	4d	64
<b>a4,t</b>	0°	4d	64	3d	48
<b>a4,c</b>	180°	3d	48	3d	48

### 5.3 Resistance of the applied connections

Connections on the horizontal edges of the CLT panels have been designed with slotted holes in order to only allow axial forces to be present in the connections. This means that the axial and shear force can be calculated by the number of bolts multiplied by the maximum resistance, since each bolt receives the same force. For the shear connection on the vertical edges of the panels a secondary step is required. The bending moment is resisted by all bolts, but those furthest from the center of rotation contribute most to the resistance. Hence, one of these bolts will yield first before the other bolts yield and this is determining the resistance of the connection.

The maximum bending moment on the connection can be calculated using equation (31) . Based on this equation, the maximum force on the outer bolt due to bending moments can be calculated.

$$M_{Ed} = \sum_{i=1}^n \frac{a_i^2}{a_{max}} * F_{max,d} \quad (31)$$

$$F_{max,d} = \sqrt{F_{m,x}^2 * (F_v + F_{m,y})^2} \quad (32)$$

Table 12, forces on the connections

Model height	Location	Connection	Horizontal edge		Vertical edge		
			N <sub>Ed</sub>	V <sub>Ed</sub>	V <sub>Ed</sub>	e	M <sub>Ed</sub>
			kN	kN	kN	m	kNm
77,5 meter	Foundation	C-S-T	1712	545	291	0,24	35
77,5 meter	Fifth floor	T-S-T	1040	467	250	0,24	30
62,0 meter	Foundation	C-S-T	918	410	219	0,24	26
62,0 meter	Fifth floor	T-S-T	418	332	177	0,12	11
46,5 meter	Foundation	C-S-T	388	287	153	0,12	9
46,5 meter	Fifth floor	T-S-T	80	209	112	0,12	7
31,0 meter	Foundation	C-S-T	87	176	94	0,12	6
31,0 meter	Fifth floor	T-S-T	0	98	59	0,12	4
15,5 meter	Foundation	C-S-T	0	78	42	0,12	3
15,5 meter	Fifth floor	T-S-T	-	-	-	-	-

The acting forces have been translated into a connection design for the hold-downs and shear connections. The number of bolts have been indicated in Table 13 by indicating the number of rows and the number of bolts per row. As all connections have similar width, the number of bolts in a row is 8 for all connections (contrary to the images where 9 bolts have been shown). Resistance of the connection is then the number of bolts multiplied with the resistance per bolt. Connections on the vertical edge are subjected to an additional bending moment hence some margin between the occurring shear force and resistance has been used.

Table 13, design resistances of the connections

Model height	Location	Connection	Hold-down	Horizontal edge			Vertical edge	
				$N_{Rd}$	Shear connection	$V_{Rd}$	Shear connection	$V_{Rd}$
				<i>kN</i>		<i>kN</i>		<i>kN</i>
77,5 meter	Foundation	C-S-T	5x8	2720	2x8	1088	2x8	640
77,5 meter	Fifth floor	T-S-T	3x8	1632	2x8	1088	2x8	640
62,0 meter	Foundation	C-S-T	3x8	1632	2x8	1088	2x8	640
62,0 meter	Fifth floor	T-S-T	2x8	1088	1x8	544	1x8	320
46,5 meter	Foundation	C-S-T	2x8	1088	2x8	1088	1x8	320
46,5 meter	Fifth floor	T-S-T	1x8	544	1x8	544	1x8	320
31,0 meter	Foundation	C-S-T	1x8	264	1x8	264	1x8	320
31,0 meter	Fifth floor	T-S-T	1x8	264	1x8	264	1x8	232
15,5 meter	Foundation	C-S-T	1x8	224	1x8	224	1x8	232
15,5 meter	Fifth floor	T-S-T	-	-	-	-	-	-

C-S-T concrete – steel – timber

T-S-T timber – steel – timber

5x8 5 rows of 8 bolts

## 5.4 Design stiffnesses of the connections

The stiffness of the connection is calculated based on the stiffness of the fasteners. The stiffness of the steel plate is not considered as it is much stiffer than the fasteners. The stiffness of a fastener is calculated below using equation (1). This value is then multiplied by 2 for a steel-to-timber connection.

$$k_{ser} = 2 * \frac{420^{1,5} * 16}{23} = 12 \frac{kN}{mm} \text{ per shear plane} \quad (33)$$

The stiffness of the connection is that of all bolts. But for the computer models a different stiffness will be used. In the computer model the CLT panels will be modelled with a steel plate in between. The interface between the CLT panels and the steel plate will then be given a spring stiffness that represents the bolt stiffnesses. This is shown in Figure 31. Where the left image shows the actual connection and the middle image shows the springs between the steel plate and the CLT panels.

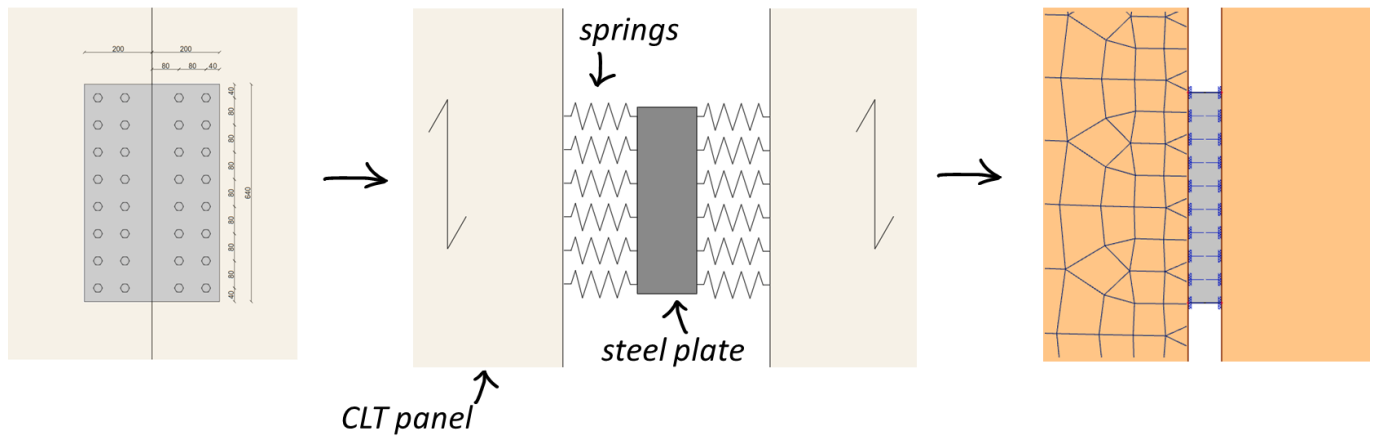


Figure 31, detail of the connection on the vertical edge (left), required spring stiffness (middle)

Table 14 shows the stiffness values of the fastener groups. The equation below shows how the linear elastic stiffness of the bolts on one side of the connection is calculated.

$$k_{fast,row} = \frac{k_{ser,fast} * n_{shear,pl} * n_{rows}}{a} \quad \left[ \frac{kN}{mm} \text{ per meter} \right] \quad (34)$$

Where,

$k_{ser,fast}$	serviceability stiffness $k_{ser}$ per fastener, per shear plane
$n_{shear,pl}$	number of shear planes per fastener
$n_{rows}$	number rows of bolts
$a$	spacing between fasteners

$$k_{fast,row} = \frac{12 * 4 * 5}{0,065} = 3692 \frac{kN}{mm} \text{ per meter} \quad (35)$$

Table 14, design stiffnesses of the connections

Model height	Location		Edge	Connection	$k_{ser}$	$D_{shear,pt}$	$k_{fast}$	$n$	$k_{fast,row}$	
					<i>kN/mm</i>		<i>kN/mm</i>		<i>kN/mm per meter</i>	
<b>77,5 meter</b>	Foundation	C-S-T	Hold-down	Horizontal	double internal steel plate	12	4	48	5	3692
<b>77,5 meter</b>	Foundation	C-S-T	Shear key	Horizontal	double internal steel plate	12	4	48	2	1477
<b>77,5 meter</b>	Foundation	T-S-T	Shear key	Vertical	double external steel plate	12	2	24	2	738
<b>77,5 meter</b>	Fifth floor	T-S-T	Hold-down	Horizontal	double internal steel plate	12	4	48	3	2215
<b>77,5 meter</b>	Fifth floor	T-S-T	Shear key	Horizontal	double internal steel plate	12	4	48	2	1477
<b>77,5 meter</b>	Fifth floor	T-S-T	Shear key	Vertical	double external steel plate	12	2	24	2	738
<b>62,0 meter</b>	Foundation	C-S-T	Hold-down	Horizontal	double internal steel plate	12	4	48	3	2215
<b>62,0 meter</b>	Foundation	C-S-T	Shear key	Horizontal	double internal steel plate	12	4	48	2	1477
<b>62,0 meter</b>	Foundation	T-S-T	Shear key	Vertical	double external steel plate	12	2	24	2	738
<b>62,0 meter</b>	Fifth floor	T-S-T	Hold-down	Horizontal	double internal steel plate	12	4	48	2	1477
<b>62,0 meter</b>	Fifth floor	T-S-T	Shear key	Horizontal	double internal steel plate	12	4	48	1	738
<b>62,0 meter</b>	Fifth floor	T-S-T	Shear key	Vertical	double external steel plate	12	2	24	1	369
<b>46,5 meter</b>	Foundation	C-S-T	Hold-down	Horizontal	double internal steel plate	12	4	48	2	1477
<b>46,5 meter</b>	Foundation	C-S-T	Shear key	Horizontal	double internal steel plate	12	4	48	2	1477
<b>46,5 meter</b>	Foundation	T-S-T	Shear key	Vertical	double external steel plate	12	2	24	1	369
<b>46,5 meter</b>	Fifth floor	T-S-T	Hold-down	Horizontal	double internal steel plate	12	4	48	1	738
<b>46,5 meter</b>	Fifth floor	T-S-T	Shear key	Horizontal	double internal steel plate	12	4	48	1	738
<b>46,5 meter</b>	Fifth floor	T-S-T	Shear key	Vertical	double external steel plate	12	2	24	1	369
<b>31,0 meter</b>	Foundation	C-S-T	Hold-down	Horizontal	single internal steel plate	12	2	24	1	369
<b>31,0 meter</b>	Foundation	C-S-T	Shear key	Horizontal	single internal steel plate	12	2	24	1	369
<b>31,0 meter</b>	Foundation	T-S-T	Shear key	Vertical	double external steel plate	12	2	24	1	369
<b>31,0 meter</b>	Fifth floor	T-S-T	Hold-down	Horizontal	single internal steel plate	12	2	24	1	369
<b>31,0 meter</b>	Fifth floor	T-S-T	Shear key	Horizontal	single internal steel plate	12	2	24	1	369
<b>31,0 meter</b>	Fifth floor	T-S-T	Shear key	Vertical	double external steel plate	12	2	24	1	369
<b>15,5 meter</b>	Foundation	C-S-T	Hold-down	Horizontal	single internal steel plate	12	2	24	1	369
<b>15,5 meter</b>	Foundation	C-S-T	Shear key	Horizontal	single internal steel plate	12	2	24	1	369
<b>15,5 meter</b>	Foundation	T-S-T	Shear key	Vertical	double external steel plate	12	2	24	1	369

## 5.5 Multi-linear load-displacement curves

The multi-linear load-displacement curves are defined by the resistance and stiffness of the fasteners. The stiffness from Table 14 are used. But these have to be compensated for the activation of bolts and the reduced stiffness in ULS.

### 5.5.1 Activation of bolts

Activation of bolts has been included by halving the stiffness for the first part of the load-displacement curve. For the first branch of the load-displacement curve only 50% of  $k_{ser}$  is applied until 40% of  $F_{max}$  is reached. The plastic deformation of the timber surrounding bolts is 0,15 mm, equal to the bolt misalignment in a connection. After 0,15 mm of deformation after initial slip has occurred, all bolts should contribute to the stiffness of the connection. Hence after 40% of the maximum load is reached the stiffness of  $k_{ser}$  is applied.

### 5.5.2 Stiffness in ULS

Connections in ULS have a stiffness that is two-thirds of the SLS stiffness. In order to model a single non-linear load-displacement curve for both SLS and ULS calculations, this difference is to be accounted for. The ULS stiffness is defined as the stiffness of the fastener between 67% of  $F_{max}$  and 100%  $F_{max}$  required in order to reach an effective stiffness at failure of  $2/3 k_{ser}$ . The value was found to be 40% of  $k_{ser}$ .

### 5.5.3 Non-linear load-deformation curve for a connection with multiple fasteners

The load-deformation behavior of fasteners has been summarized Figure 32. Several stages are defined.

Table 15, parameters for the non-linear load displacement curve

		Deformation		Stiffness	Until
<b>Stage 1</b>	Slip	$u_0$	1,0	<i>mm</i>	
<b>Stage 2</b>	Activation of bolts	$k_1$		$0,5 * k_{ser}$	<i>kN/mm</i> 40% $F_{max}$
<b>Stage 3</b>	Linear elastic stiffness	$k_2$		$k_{ser}$	<i>kN/mm</i> 67% $F_{max}$
<b>Stage 4</b>	ULS stiffness	$k_3$		$0,4 * k_{ser}$	<i>kN/mm</i> 100% $F_{max}$

### 5.5.4 Non-linear load-deformation curve compared to test results

Test results from three researches have been combined and presented in Figure 32. The non-linear load-displacement curve as defined according to the Eurocode is compared to these results.

Table 16, sources of load-deformation curves

Source	Year	Diameter	No. fasteners
<b>Liu et al.</b>	2020	M16 bolts	1
<b>Dobes et al.</b>	2022	M20 bolts	1
<b>Sandhaas</b>	2012	M12 dowels	1, 3 and 5

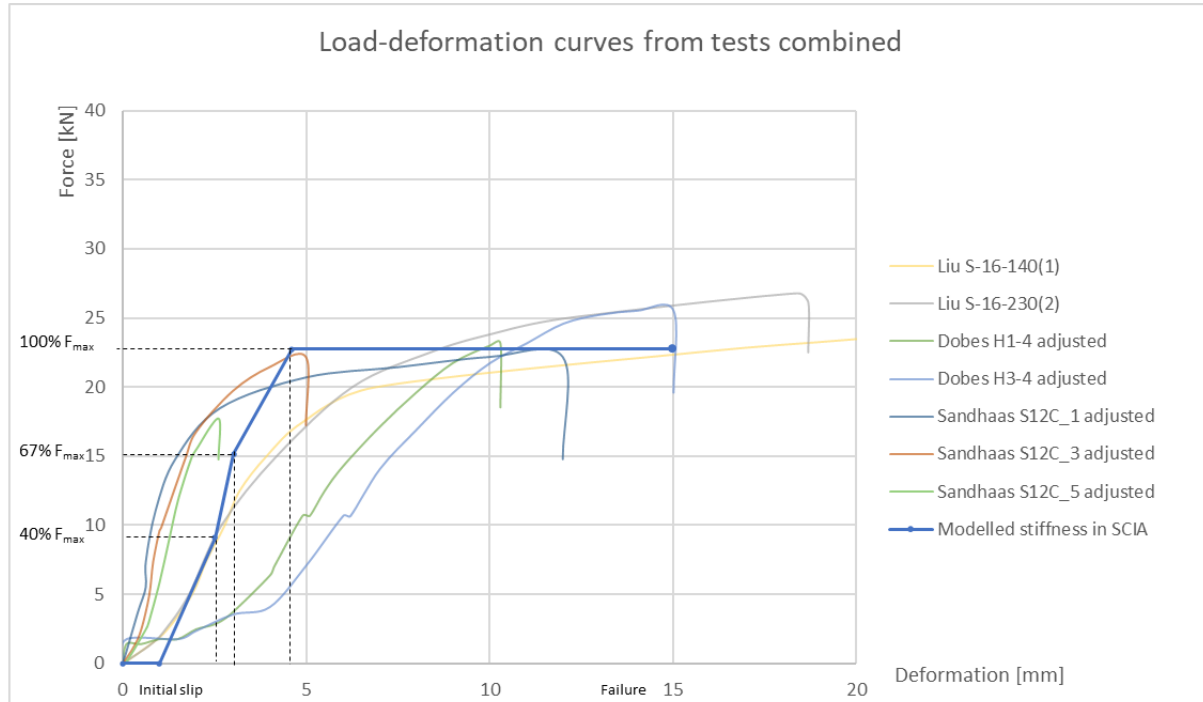


Figure 32, non-linear load-deformation curve for a multiple fastener connection

It can be observed that there is quite a significant difference between the test results. This is for a large part due to the initial slip. Results by Dobes show a linear stiffness only after 3 mm of deformation, whereas results by Sandhaas immediately have an elastic stiffness. The modelled initial slip and elastic stiffness in SCIA is a good average of all results. However, the increased stiffness after 40%  $F_{max}$  is not supported by the test results. Hence the modelled stiffness in SCIA is an overestimation of the connection stiffness.



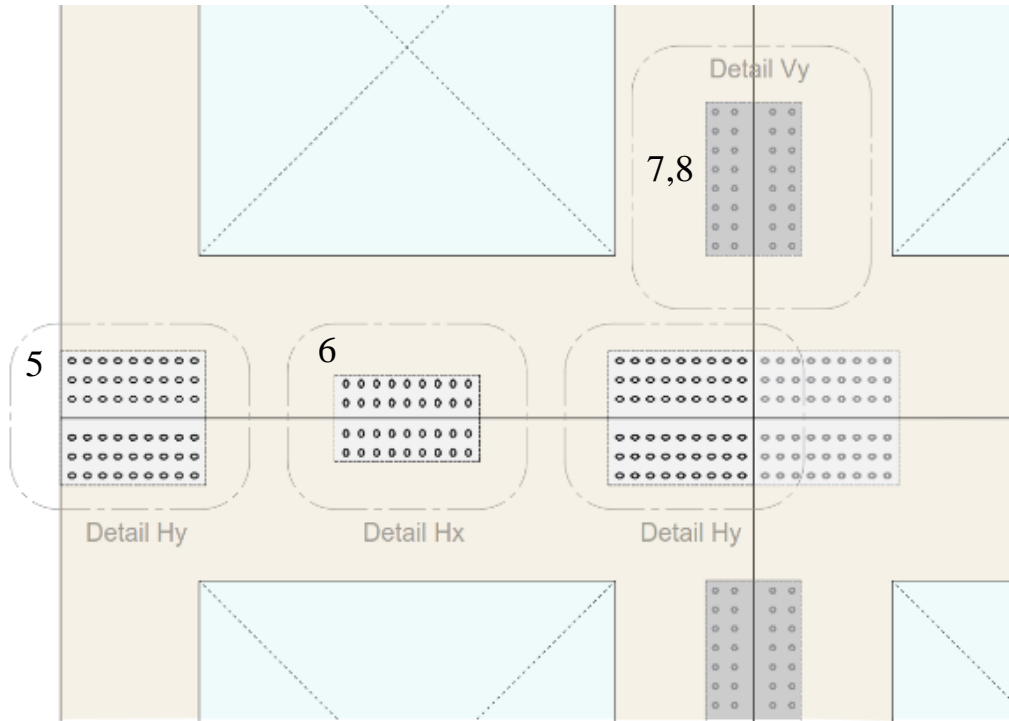
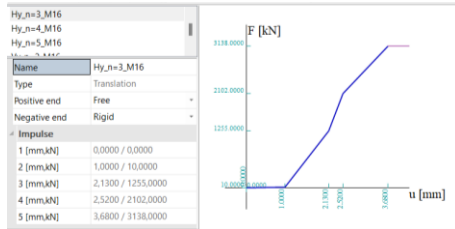
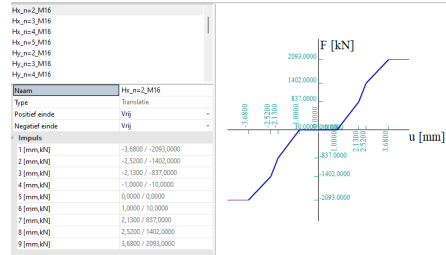


Figure 34, load-displacement curves for the model of 77,5 meter with connection stiffnesses for panel to panel connections

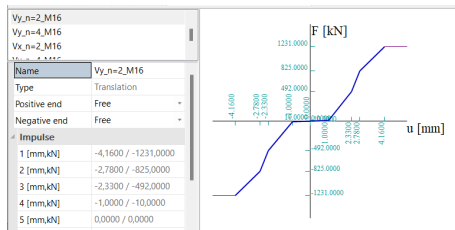
### 5 Hold-down double internal plate



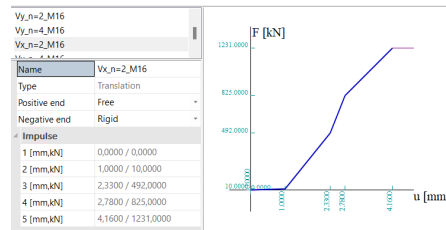
### 6 Shear key horizontal edge double internal plate



### 7 Shear key vertical edge double external plate Vertical stiffness



### 8 Shear key vertical edge double external plate Horizontal stiffness



The presented load-displacement curves are designed for a façade of 77,5 meter and resist the forces as specified in chapter 4.5. The resistance of the connections has been calculated in chapter 5.3 and the stiffnesses have been calculated in chapter 5.4. These values are used to define the different stages of the multi-linear load-displacement curve.

The design resistances of the connections have been calculated per connection. In order to use these for the multi-linear load-displacement curves in the computer model they have to be presented as forces per meter. That is why the resistances are divided by the width of the connections. For example, the resistance of the hold-down at the foundation for the model of 77,5 meter would then become.

$$N_{Rd,max} = \frac{N_{Rd}}{n * a} = \frac{2720}{8 * 0,065} = 5231 \frac{kN}{mm} \text{ per meter} \quad (36)$$

Doing this for all connections of the model of 77,5 meter the following parameters have been calculated.

Table 17, parameters per meter for the multi-linear load-displacement curves modelled in SCIA Engineer (model 77,5 meter)

No.	Connection type	Panels	n	m	$F_{v,Rd}$	$k_{ser}$	0,4F	0,67F	$N_{Rd,max}$	$u_0$	$u_1$	$u_2$	$u_3$
					<i>kN</i>	<i>kN/mm/m</i>	<i>kN/m</i>	<i>kN/m</i>	<i>kN/m</i>	<i>mm</i>	<i>mm</i>	<i>mm</i>	<i>mm</i>
1	Double int. Plate	LL-400/11s	8	5	68	3692	2092	3487	5231	1,0	1,13	0,38	1,17
2, 6	Double int. Plate	LL-400/11s	8	2	68	1477	837	1395	2093	1,0	1,13	0,38	1,17
3, 4, 7, 8	External plates	LL-400/11s	2	8	40	738	492	821	1231	1,0	1,33	0,45	1,38
5	Double int. Plate	LL-400/11s	8	3	68	2215	1255	2092	3138	1,0	1,13	0,38	1,17

Connections 1 and 5 are hold-down connections that have a spring behavior for tension forces but a rigid behavior for compression forces. In horizontal direction they do not have any stiffness. Connections 2 and 6 are shear connections that have a spring stiffness for shear forces in horizontal direction. In vertical directions they do not have any stiffness.

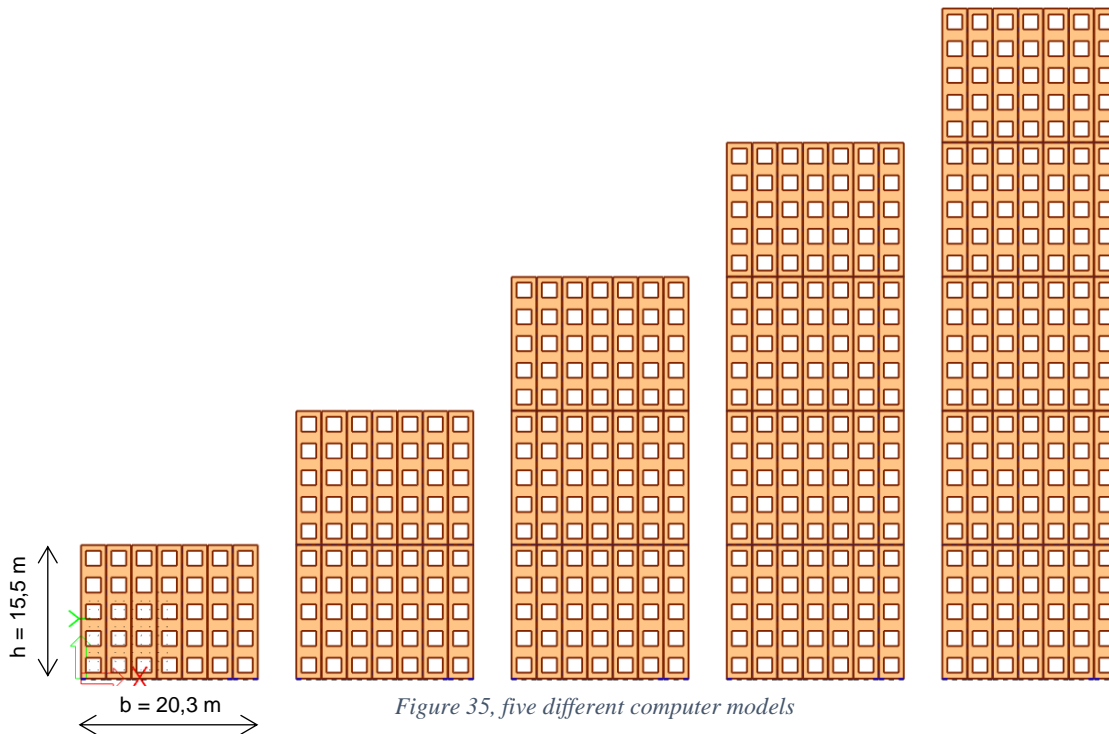
Connections 3, 4, 7 and 8 are shear connections that have a spring behavior for shear forces in vertical direction. In horizontal direction there is a spring behavior for tension forces but a rigid behavior for compression forces.

## 6 Computer model

SCIA Engineer is used to model the CLT façade and perform structural calculations. It is a finite element modelling software that is used for non-linear calculations of the structure. Analysis will be performed on the top deflection, maximum forces in the panels and in the connection. Connections will be modelled as steel plates with non-linear springs along the edges to represent the bolt stiffness. This chapter presents the input for the computer model.

*“How to model the CLT façade structure?”*

Several models have been made to compute the structural performances of the façade. The height of the façade is increased in steps of 15,5 meter, which is the height of one panel. Models are created in a 2D environment.



## 6.1 Setup of the structural model

The structural model will be discussed on several topics being the CLT panels, supports, connections and loads. A fragment of the CLT façade from SCIA Engineer is shown in Figure 36 with an additional close-up of the connections between the CLT-panels.

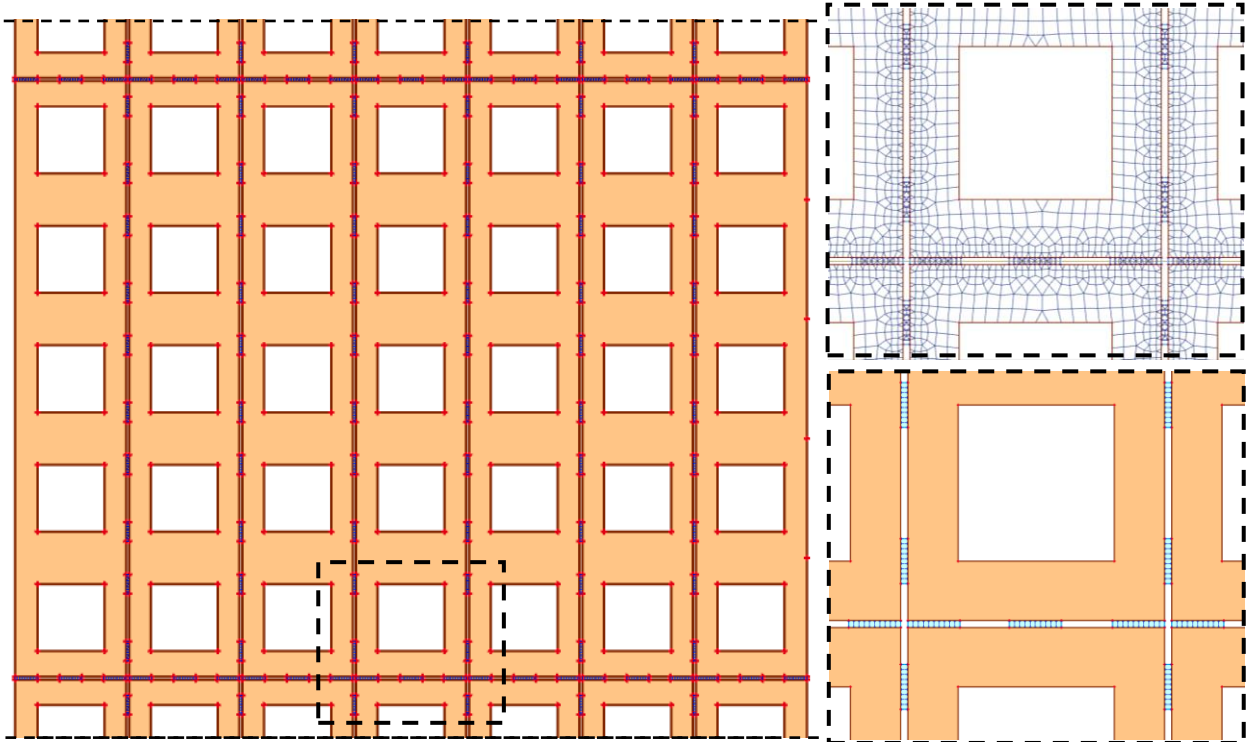


Figure 36, fragment of the CLT façade as modelled in SCIA with a close-up of the connections on horizontal and vertical edges

### 6.1.1 Orthotropic CLT plates

The CLT panels are modelled as orthotropic plates. There are three stiffness parameters required to describe the behavior of CLT as an orthotropic plate. These parameters are given in Appendix A2.6.

### 6.1.2 Mesh

The mesh of the CLT panels is a rectangular mesh of 0,15 meter. This dimension is based on the width of the vertical piers. These are 0,58 meter wide, so four mesh elements can be made to represent this element. At the edges of the CLT panels a mesh refinement has been applied. The number of mesh elements is locally increased by a factor 3. This means that at the location of the connections an effective mesh of 0,05 meter is applied. This finer mesh results in a more precise calculation of the forces near the connections. A close-up of the mesh of the CLT panels and connections is also shown in Figure 36.

### 6.1.3 Openings

Rectangular openings have been modelled. There are five openings in a single CLT panel. The model has been verified before openings were added. This verification (Appendix A6.1) showed results compatible with theoretical calculations. Which indicated that there were no major errors in the computer model.

### 6.1.4 Connections

CLT panels have been spaced from one another (80 mm). Small steel plates are then modelled in between the CLT panels. The interface between the steel plates and the CLT panels are given a continuous spring stiffness [kN/mm per meter] to represent the non-linear stiffness behavior of the fasteners. This continuous spring stiffness is the stiffness of a fastener divided by the spacing between fasteners.

The hold-down connections have a width that is equal to that of the vertical piers (580 mm). This allows forces in the piers to transfer in a straight line from panel to panel until they reach the foundation. The shear connections on the horizontal edge have been modelled with a width of 580 mm as well. Shear connections on the vertical edge have been modelled with a height of 500 mm.

The springs on the interface between the steel plate and the CLT panel represent the fastener stiffness. The stiffness of the total connection is half that of the springs modelled on the sides of the steel plate, since it is a system of two springs in series. The springs in horizontal direction are not shown in the figure on the right, but are present in the computer model. The mesh has been shown in the connection as modelled in SCIA only on the left panel.

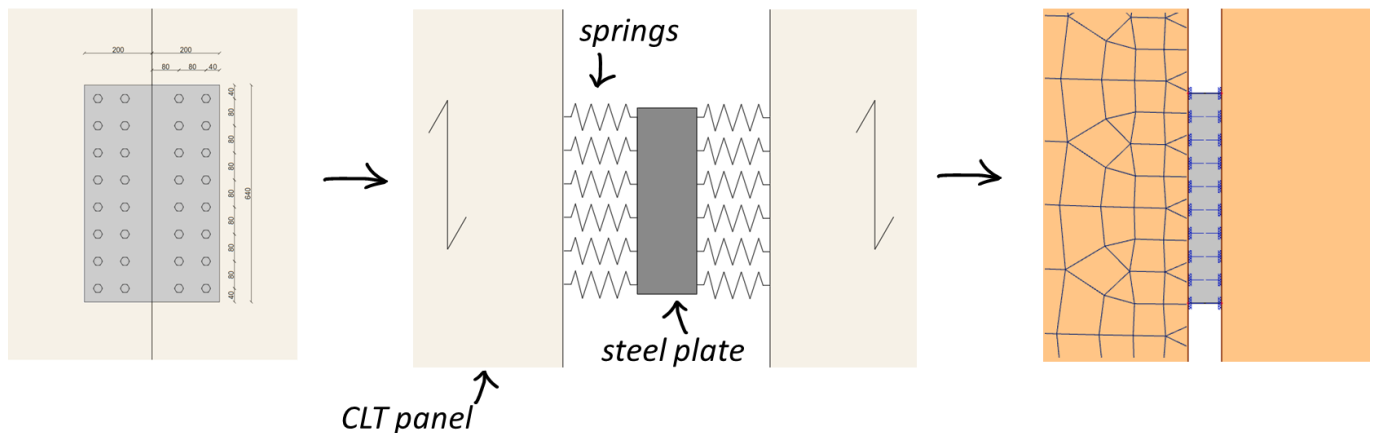


Figure 37, detail of the connection on the vertical edge (left), connection as modelled in SCIA (right)

### 6.1.5 Supports

The bottom CLT panels have hold-down connections similar to the ones between panels. However, only the interface between the steel plate and CLT panel has a stiffness of the fasteners modelled. The other side of the steel plate has rigid support conditions that represent the concrete foundation.

### 6.1.6 Non-linear load-displacement curves

The non-linear load-displacement curves have been modelled according to chapter 5.5.3. However, failure of the connection has not been modelled as this led to an unstable structure. This is caused by high local peak forces in the second iteration that exceed the resistance of the connection causing failure. Modelling connections without failure but with an infinite plastic behavior allowed for redistribution of these forces within the connection and between connections. If the final iteration shows that connections are not loaded by their maximum capacity, the deformation of the connection is by default less than 10 mm.

### 6.1.7 Loads

Five load cases have been defined for the structure. The first being the self weight of the structure, which is calculated by the computer itself, based on the thickness of the applied CLT panel. Load case 2 is the wind load. Load case 3 is the characteristic dead weight of the floor. Load case 4 is the variable floor load and load case 5 is the façade weight excluding the weight of the CLT itself. The floor load is applied at each floor height similar to the distribution shown in Figure 17. The façade load is applied at each floor height

Table 18, overview of load cases in the model

Load case		Load type	
LC 1	Self weight	Permanent	
LC 2	Wind load	Variable	
LC 3	Permanent floor load	Permanent	
LC 4	Variable floor load	Variable	Cat. A: domestic $\psi_0 = 0,4$
LC 5	Façade load	Permanent	

### 6.1.8 Load combinations

Load combinations have been defined according to the table below. The live floor load in serviceability limit state is excluded from the SLS load combination as the purpose of this load case is to find the maximum top deflection. The beneficial contribution of the live floor load on the rocking deformation has in this way been eliminated.

Table 19, load combinations

Name	Description	LC1 self weight	LC 2 wind	LC3 floor dead	LC4 floor live	LC5 façade load
SLS	No live load floor	1,00	1,00	1,00	0,00	1,00
ULS 1	Max compression	1,20	1,50	1,20	1,50	1,20
ULS 2	Max tension	0,90	1,50	0,90	0,00	0,90

## 6.2 Modelling of the additional elements

There are two additional elements considered in this research being a concrete core and the effective width of the transversal façade.

### 6.2.1 Modelling of the concrete core

The concrete core is considered to be a concrete 2D plate element (thickness of 300 mm) with properties of cracked concrete C30/37. The core is represented as a wall element parallel to the direction of the considered façade is used. No openings have been modelled in the concrete wall. The main purpose is to compute how a concrete slab interacts with the façade structure.

In between the façade and the concrete core “rigid links” have been modelled that transfer forces from the façade to the core and vice versa. These rigid links have an infinite axial stiffness. But they are connected to the façade and the core with hinges.

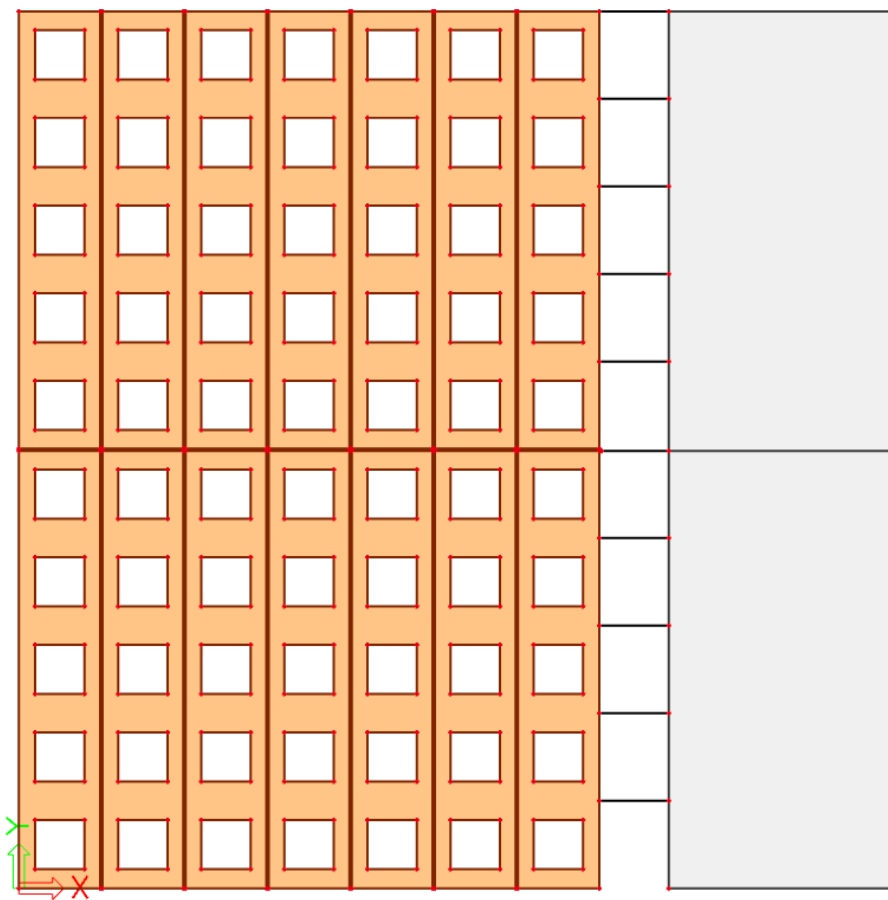


Figure 38, model of the façade of 31,0 meter with an additional concrete core

### 6.2.2 Modelling of the transversal façade

According to Chiewanichakorn et al. (2004) the effective width is defined as the width of the element that has a constant stress distribution equal to the maximum value of the actual stress distribution. In other words, the total force is divided by the maximum occurring stress.

$$b_{eff} = \frac{\int_{\frac{1}{2}b}^b n_y}{n_{y,max}} = \frac{0,5 * R_y}{n_{y,pier}} \quad (37)$$

Using this approach, the effective width values from the table below have been found (appendix A6.3). The percentage presented is the percentage of the width of the façade that is contributing as the effective width.

The effective width that has been applied in the models deviates from the calculated values. This is due to the fact that during the research an alternative calculation was used that in hindsight was deemed unsuitable.

*Table 20, parameters used to define the effective width*

<b>Model</b>	<b>R<sub>y</sub></b> <i>kN</i>	<b>n<sub>y,max</sub></b> <i>kN/m</i>	<b>b<sub>eff</sub></b> <i>m</i>	<b>Percentage</b>	<b>b<sub>eff</sub> applied</b> <i>m</i>
<b>15,5 meter</b>	3100	1483	1,0	20%	1,1
<b>31,0 meter</b>	6200	2143	1,4	28%	1,3
<b>46,5 meter</b>	9300	2533	1,8	35%	2,0
<b>62,0 meter</b>	12.400	2864	2,2	41%	2,7
<b>77,5 meter</b>	15.500	3185	2,4	47%	3,4

### 6.2.3 Connections of the transversal façade

The transversal façade is modelled as a 1D timber beam elements with a thickness equal to the  $t_0$  thickness of the CLT panel and a width equal to the effective width as defined above. There are shear key connections on the vertical edges similar as those between the other CLT panels.

At the foundation and in between elements node supports have been modelled with a stiffness value representing the connection stiffness. The stiffness values of these connections is based on the hold-down connections applied on the façade, multiplied with the value of the effective width. The deformation of the connection was doubled as the modelled connection represented two sides of the CLT plate with fasteners.

Shear key connections on the horizontal edge have not been modelled for the transversal façade. A free deformation in horizontal direction was assumed in order to prevent the transversal wall of contributing to the shear force distribution.

## 6.3 Calculations

There are multiple models used to make calculations. An overview is given below.

Table 21, overview of the different models

<b>Verification of panels</b>	CLT façade panels without connection stiffness or openings
<b>Verification of connection stiffness</b>	CLT façade panels including connection stiffnesses, but without openings
<b>Rigid models</b>	Models without fastener stiffnesses modelled, including openings
<b>Spring models</b>	Models with fastener stiffnesses modelled <ul style="list-style-type: none"> <li>• Without initial slip</li> <li>• Including initial slip</li> </ul>
<b>Models with core</b>	Models with fastener stiffnesses modelled (including slip) and a concrete core
<b>Models with effective width</b>	Models with fastener stiffnesses modelled (including slip) and an effective width
<b>Complete models</b>	Models with fastener stiffnesses modelled (including slip) and both a concrete core and an effective width

### 6.3.1 Non-linear calculations

Non-linear calculations are performed including geometrical nonlinearity. This means that the results are based on an iterative calculation that includes the behavior of the fasteners that are modelled as springs, as well as the additional forces (and deflections) due to eccentricities. Models with geometrical nonlinearity did not lead to converging results in case failure was modelled in the connection, as peak forces in iterative steps caused connections to fail. Hence failure has been excluded from the non-linear load-displacement curve.

### 6.3.2 Verifications

Simplified versions of the model have been used for verifications. Openings that are present in the final models have been excluded in order for an easier comparison to theoretical calculations. Also the non-linear load-displacement curves of the connections have been simplified to linear load-displacement curves.

The goal of these verifications is threefold. First to show that the behavior of the orthotropic plates is comparable to the expected behavior in terms of force transfer and deformations. Secondly to show that the connections in between CLT panels do behave as expected. Once these models have been verified it can be concluded that the models including openings and non-linear load-displacement curves work as expected. Lastly, the deviations between theoretical calculations and computer models can be compared. Large deviations should not occur, but smaller deviations can be interpreted in order to understand how several factors can be included in a preliminary design.

Appendix A6.2 entails these verifications. The behavior of the structure for sliding, rocking and additional bending deformation have been compared to theoretical results.

Sliding	<i>good correlation</i>
Rocking	<i>decent correlation for larger connection stiffness</i>
Additional bending deformation	<i>good correlation</i>

The verification of rocking deformation showed that for decreasing connection stiffnesses, the forces in the connections decrease as well. This in turn influences the elongation of the connection and thus the rocking deformation. For large connection stiffnesses (1000 kN/mm per m) the reduction of the force on the connection is 24%. Theoretical hand calculations of the rocking deformation showed to be conservative.

## 6.4 Model workflow

The workflow of the model is shown in Figure 39. It shows the steps and information related to the model in blue. The relation between the model and the structural design is included in the workflow as it directly relates to the use of the model(s).

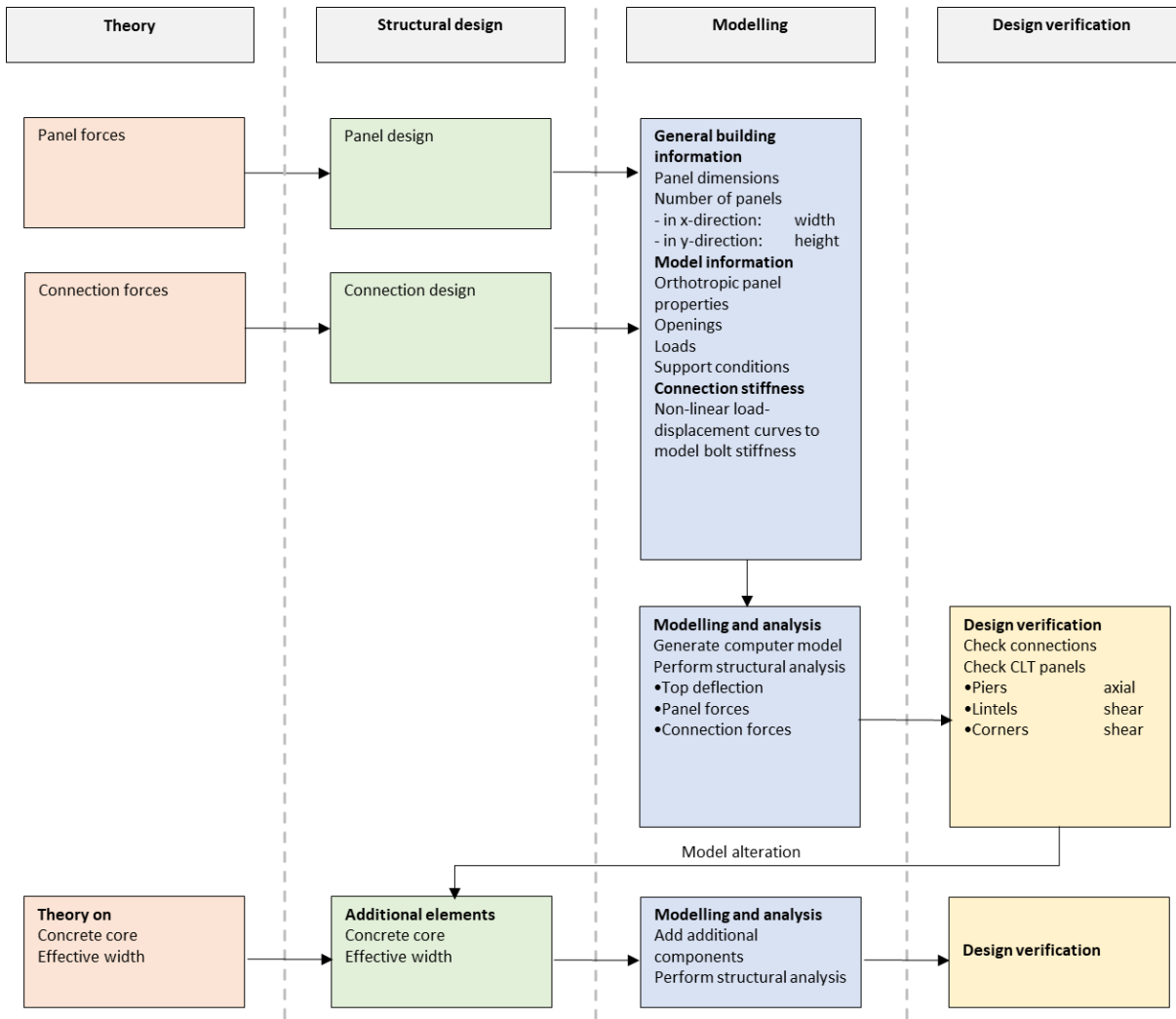


Figure 39, workflow of the model

## 7 Results

Results of the structural computer models will be presented in this chapter. The interpretation of the results will be given in the next chapter. The results are according to the research questions stated in chapter 1.3.

*“What is the top deflection of the CLT façade?”*

*“What are the forces in the CLT panels?”*

*“What are the forces in the connections?”*

Results are presented for CLT façades with and without fastener stiffness modelled. For the fastener stiffness two options were examined. One option with initial slip deformation of the fastener and one option without slip deformation of the fastener. The results for the façade models including connection deformation and initial slip will then be compared to models with additional elements.

## 7.1 Results for models without fastener stiffness

Results are presented in Table 22. Top deformations are based on the deformations of panels with openings. Forces on the structure are the reaction forces at the foundation in horizontal and vertical direction as well as the bending moment. Axial forces per meter on the panels have been calculated for the piers and shear forces per meter for both piers and lintels. Connection forces have been calculated in the program as well.

Table 22, results for the rigid plate models

	Structure				Panels				Connections			
	$w_x$	$R_{x,d}$	$R_{y,d}$	$M_{y,d}$	$n_{y,t,d}$	$n_{y,c,d}$	$n_{xy, pier,d}$	$n_{xy, lintel,d}$	$N_{y,t,d}$	$N_{y,c,d}$	$V_{xy,d}$	$V_{yx,d}$
	<i>mm</i>	<i>kN</i>	<i>kN</i>	<i>kNm</i>	<i>kN/m</i>	<i>kN/m</i>	<i>kN/m</i>	<i>kN/m</i>	<i>kN</i>	<i>kN</i>	<i>kN</i>	<i>kN</i>
<b>15,5 meter</b>	6,7	404	2.548	3.159	72	-345	77	44	+56	-220	72	56
<b>31,0 meter</b>	25,4	896	5.288	14.649	429	-1220	169	119	+279	-757	177	111
<b>46,5 meter</b>	48,6	1445	8.381	36.034	1086	-2550	279	211	+684	-1556	284	181
<b>62,0 meter</b>	113,3	2039	11.191	68.359	2195	-4264	407	324	+1364	-2586	408	244
<b>77,5 meter</b>	230,0	2666	13.847	112.245	3763	-6398	548	455	+2298	-3856	543	344

$R_{x,d}$  reaction at the foundation in x-direction [kN] *total horizontal wind force on the foundation*

$R_{y,d}$  reaction at the foundation in y-direction [kN] *total vertical force on the foundation*

$M_{y,d}$  Moment on the foundation [kNm]

$n_{y,t,d}$  maximum tensile force per meter on the panels [kN/m]

$n_{y,c,d}$  maximum compression force per meter on the panels [kN/m]

$n_{xy,d}$  maximum shear force per meter on the panels [kN/m]

$N_{y,t,d}$  maximum tensile force on the connection [kN]

$N_{y,c,d}$  maximum compression force on the connection [kN]

$V_{xy,d}$  maximum shear force on the connection (horizontal edge) [kN]

$V_{yx,d}$  maximum shear force on the connection (vertical edge) [kN]

## 7.2 Results for models with fastener stiffness

Similar results as those in chapter 7.1 have been calculated for the model including fastener stiffness. Two types of non-linear load-displacement curves have been modelled. One with initial slip of 1,00 mm and one without this initial slip.

### 7.2.1 Results without slip of the fastener

The non-linear load displacement curves were defined in chapter 5. The resulting top deformation and forces in panels and connections are shown below.

Table 23, results for the 2D plates models with bolt stiffnesses modelled without slip

	Structure				Panels				Connections			
	$w_x$ <i>mm</i>	$R_{x,d}$ <i>kN</i>	$R_{y,d}$ <i>kN</i>	$M_{y,d}$ <i>kNm</i>	$n_{y,t,d}$ <i>kN/m</i>	$n_{y,c,d}$ <i>kN/m</i>	$n_{xy, pier,d}$ <i>kN/m</i>	$n_{xy, lintel,d}$ <i>kN/m</i>	$N_{y,t,d}$ <i>kN</i>	$N_{y,c,d}$ <i>kN</i>	$V_{xy,d}$ <i>kN</i>	$V_{yx,d}$ <i>kN</i>
<b>15,5 meter</b>	8,8	404	2.625	3.175	52	-367	77	52	51	-243	57	28
<b>31,0 meter</b>	33,7	896	5.288	14.828	393	-1314	173	130	279	-840	135	62
<b>46,5 meter</b>	73,4	1445	8.610	36.575	1127	-2888	284	223	727	-1770	221	103
<b>62,0 meter</b>	148,9	2039	11.496	69.853	2238	-4716	419	321	1413	-2865	318	204
<b>77,5 meter</b>	281,3	2666	14.229	115.568	3941	-7029	558	438	2439	-4247	413	238

### 7.2.2 Results with 1,0 mm slip of the fastener

The same non-linear load-displacement curves from chapter 7.2.1 were used, but now with an additional initial slip of 1,0 mm.

Table 24, results for the 2D plates models with bolt stiffnesses modelled including slip of 1,00 mm

	Structure				Panels				Connections			
	$w_x$ <i>mm</i>	$R_{x,d}$ <i>kN</i>	$R_{y,d}$ <i>kN</i>	$M_{y,d}$ <i>kNm</i>	$n_{y,t,d}$ <i>kN/m</i>	$n_{y,c,d}$ <i>kN/m</i>	$n_{xy, pier,d}$ <i>kN/m</i>	$n_{xy, lintel,d}$ <i>kN/m</i>	$N_{y,t,d}$ <i>kN</i>	$N_{y,c,d}$ <i>kN</i>	$V_{xy,d}$ <i>kN</i>	$V_{yx,d}$ <i>kN</i>
<b>15,5 meter</b>	16,1	404	2624	3.197	62	-440	82	59	56	-289	59	16
<b>31,0 meter</b>	55,8	896	5723	14.843	416	-1440	182	144	293	-923	134	51
<b>46,5 meter</b>	101,7	1445	8610	36.034	1090	-2974	300	242	737	-1878	220	96
<b>62,0 meter</b>	199,3	2039	11.496	70.156	2307	-5034	428	342	1467	-3027	312	195
<b>77,5 meter</b>	352,4	2666	14.229	116.093	4089	-7429	573	449	2543	-4437	409	218

### 7.3 Results compared

The results of the models without fastener stiffness are compared to those of the models with fastener stiffness (both with and without initial slip). The tables in chapters 7.1 and 7.2 are translated into graphs in order to have a more visual interpretation of the results. The results of the models without fastener stiffness are shown in the blue bars, results of the models with fastener stiffness (no slip) are shown in the orange bars and models including slip are shown in the grey bars.

#### 7.3.1 Top deformations

Answering the first question of this chapter, the results from the tables before are compared to one another. The maximum top deformation is considered to be  $H/500$ .

*“What is the top deflection of the CLT façade?”*

The left figure shows the absolute values of the top deformation as calculated with the computer models. The right figure shows how these values relate to the allowable top deformation by comparing unity checks.

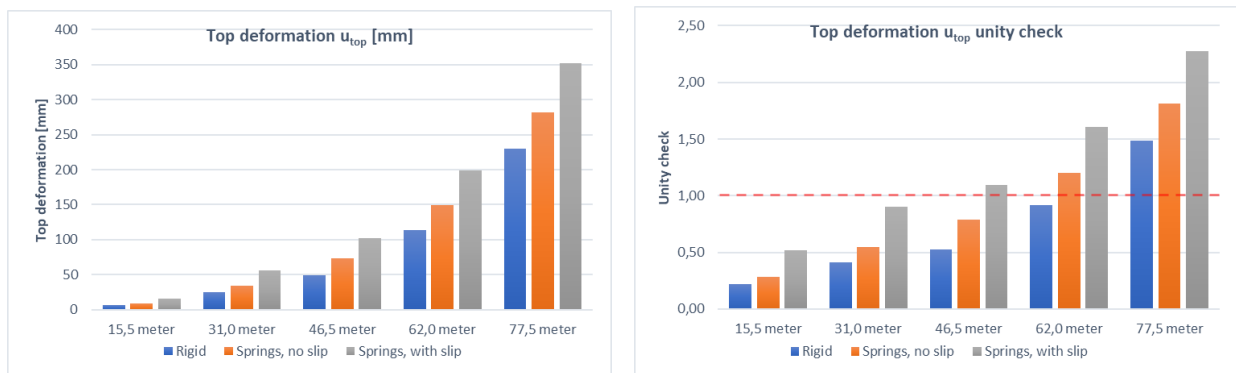


Figure 40, top deflection of the CLT façade for different models

The top deflection of the structure increases as the stiffness of the connections decreases. A significant contribution of the connections can be observed. Top deflections are not governing for models of 15,5 and 31,0 meter. For a structure of 46,5 meter the top deflection can exceed allowable deformation in case the connections have an initial slip of 1,0 mm. For structures of 62,0 and 77,5 meter the top deflection is an important factor to consider. Especially the model with a height of 77,5 meter has an unfeasible top deflection.

The top deformations of the façade are also compared to theoretical calculations that include the influence of the connection stiffnesses. The top deformation of the façade without connection stiffnesses modelled is slightly underestimated using the theoretical approach (appendix A4.4). Whereas the top deformation of the façade including connection stiffnesses (with slip) is a slight overestimation of the top deformation (appendices A7.1 and A7.2). However, the general conclusion on the comparison between computer results and theoretical calculations is that the hand calculations provide a good insight in the top deformation of the façade, and therefor also for the contribution of each component.

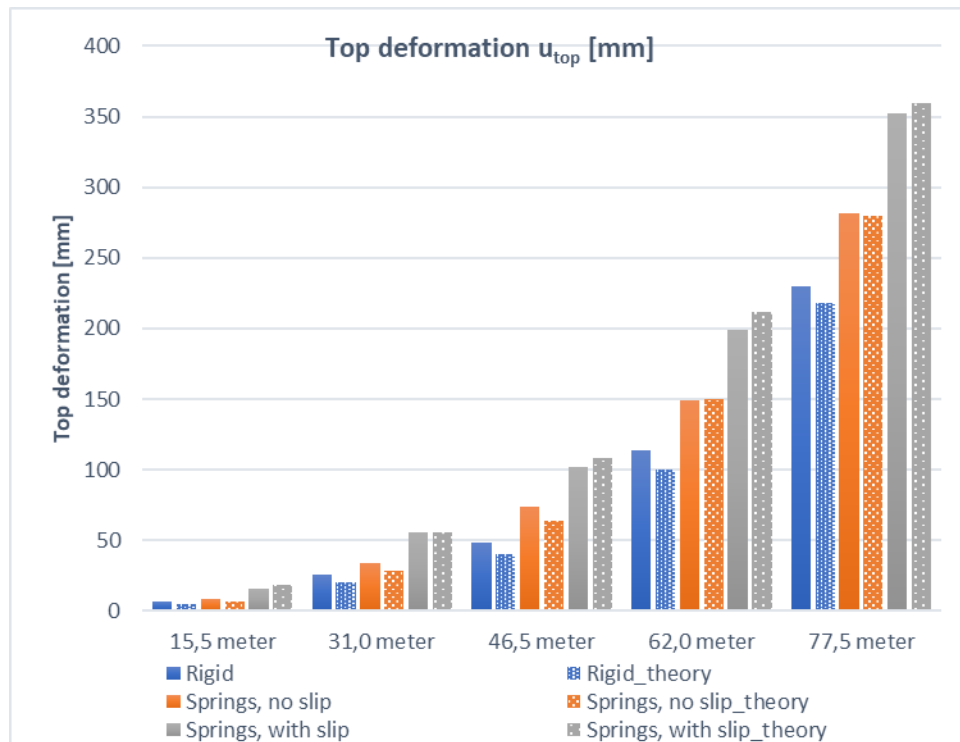


Figure 41, top deflection of the CLT façade for different models – compared to theory

### 7.3.2 Connection influence on top deformation

The increase of top deformation as a result of connection deformation is significant. The models however do not explain which connection is most of influence on the top deformation. In order to explain which connections are most contributing to the additional top deformation, the theoretical results are used. The top deformations from the theoretical results were found to be comparable to the computer results (as shown in 7.3.1).

Theoretical results indicate that most of the deformation due to connection deformation is caused by shear connections on the vertical edges of the panels. Connections that do not have any initial slip contribute to 20-25% additional deformation of the top as can be seen in the figures below in the yellow bars. The structure of 77,5 meter only has 12% additional top deformation due to this connection. This is explained by the fact that the model of 77,5 meter has a higher connection stiffness. Showcasing that an increased stiffness of the connection reduces the additional top deformation. For connections including initial slip this contribution increases even further. The contribution of additional bending deformation increases to 25-60% computed with the method of Schelling. This contribution of additional bending deformation reduces for increasing heights, but remains the main contributor of all connections to the increased top deformation.



Figure 42, contribution of connection slip on the top deformation without initial slip

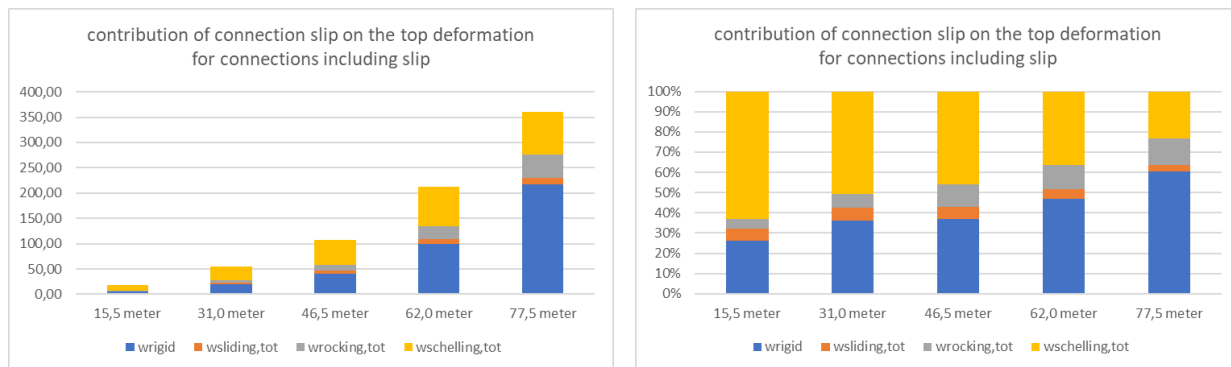


Figure 43, contribution of connection slip on the top deformation including initial slip

Rocking deformation is the second largest contributor to the increased top deformation. Its contribution increases with the height of the structure. But the inclusion of slip in the connection does not significantly increase the rocking contribution to the top deformation. A maximum contribution of 13% was observed, with a 10% contribution on average.

Sliding of the connections on the horizontal edge does not play a significant role on the top deformation. the observed sliding deformation is only a fraction of the total deformation. When including the initial slip in the load-displacement curve it is shown that the contribution of the sliding deformation increases, but that it is at most 5% of the total deformation. The sliding deformation is practically equal to the free initial slip of the horizontal shear key connections. The calculations do not include friction of the connections, indicating that the actual deformation will be even smaller.

### 7.3.3 Panel forces

Answering the second question of this chapter, the results from the tables are compared to one another. Figure 44 until Figure 47 with the maximum panel forces are shown on the next page.

*“What are the forces in the CLT panels?”*

The influence of the connections on the panel forces is less significant than on the top deformations. But there is still an influence of the connections noticeable on the results.

Axial forces in the panels increase both for compression and tension. Theoretical results for panel forces were presented in Table 7 of chapter 4.2.5. A comparison between the theoretical results and computer results shows that there is a significant underestimation of the panel forces.

Tension forces were underestimated significantly with the model for 31,0 meter being the most significant difference as the maximum tensile force per meter of 416 kN/m found in the computer model exceeds the expected maximum tensile force of 149 kN by more than double.

Compression forces are found to be underestimated by theoretical calculations for most models by 30%. Only the model of 15,5 meter showed a lower maximum compression force compared to theoretical results.

Shear forces in the piers were underestimated consistently by 20% for all models. Shear forces in the lintels on the other hand were underestimated by 5% at most for most models. Only the model of 15,5 meter showed an overestimation (5%).

The conclusions above are influenced by the difference between hand calculations and the computer models without connection stiffness modelled. Which should be the same. When comparing the axial forces between the computer models with and without connection stiffnesses modelled, a better comparison can be made.

The maximum tension force in the panels is in this case increased by 10% for larger heights. Only the model of 15,5 meter showed a reduced maximum tension force in the panels. The maximum compression force in the panels is increased by 15 to 25% for all models.

Shear forces in piers increase slightly by 5 to 8% for all heights. This is in case initial slip is included in the connection stiffness. Shear forces in lintels increase more significantly for lower models. An average of 20% increase is found. Models with a height of 62,0 and 77,5 meter do not indicate an increase of shear forces in the lintels.

Considering the unity checks that are also provided on the next page, it can be seen that the model of 77,5 meter does not satisfy safety requirements. Both tension and compression forces in the CLT panels exceed allowable limits. Top deformations already indicated that the models of 62,0 and 77,5 meter are not feasible.

Shear forces in the piers and lintels do not exceed the unity check limit, but it is known that the shear forces in the corners of the openings are larger. Measured shear forces in the computer model however indicated values up to 3 times the values found in piers and lintels. This is partly due to singularities in the corners of the panels. So there is an exceedance of the unity check for shear forces as well, but realistic values could not be calculated using the computer model.

The increased shear force in the corners is therefor included by increasing the observed shear force by 50% as explained in chapter 4.2.4.

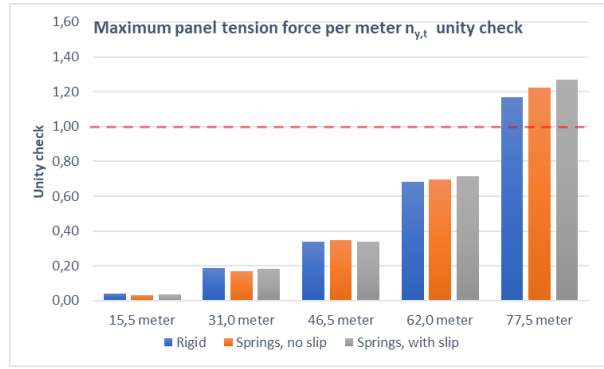
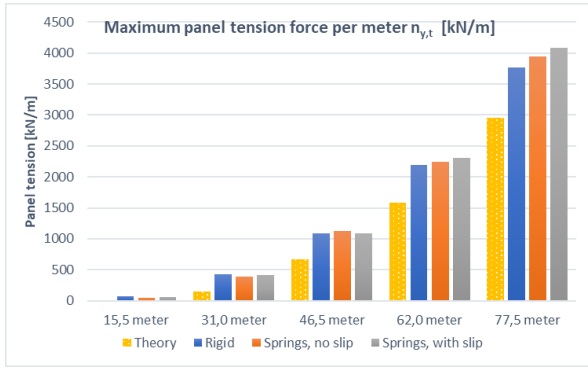


Figure 44, maximum tension force per meter in the CLT panels of the façade for different models

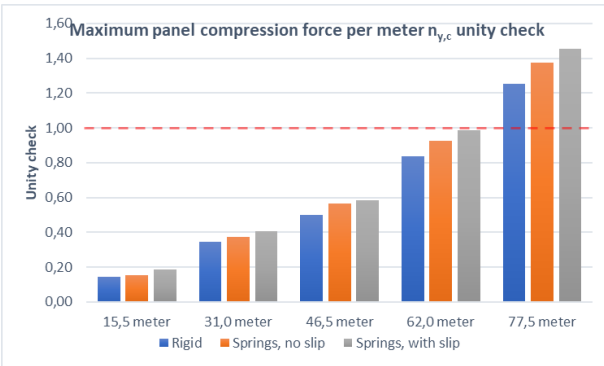
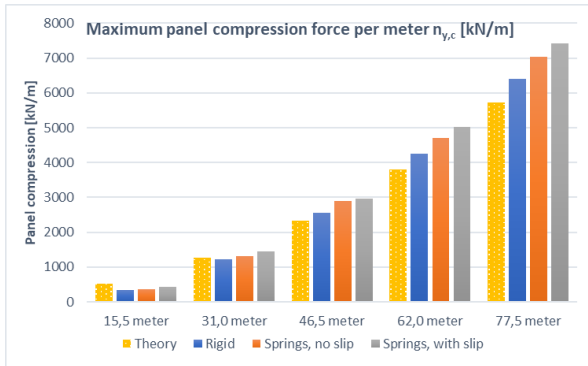


Figure 45, maximum compression force per meter in the CLT panels of the façade for different models

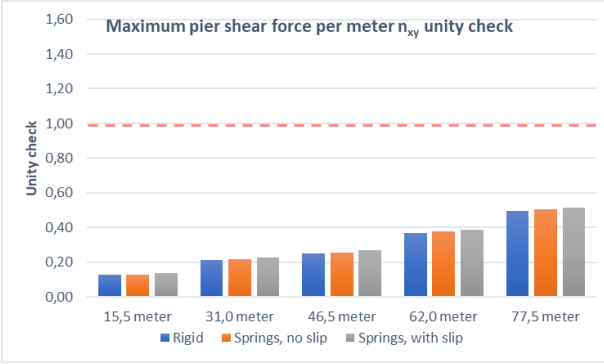
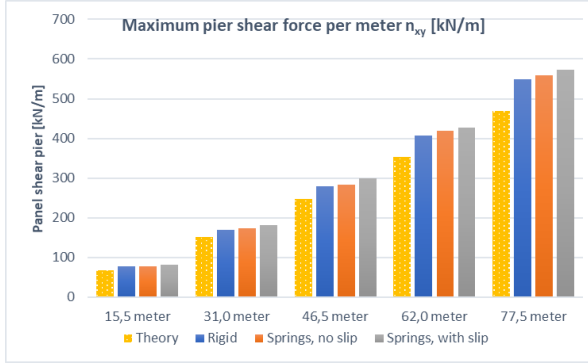


Figure 46, maximum shear force per meter in the piers of the façade for different models

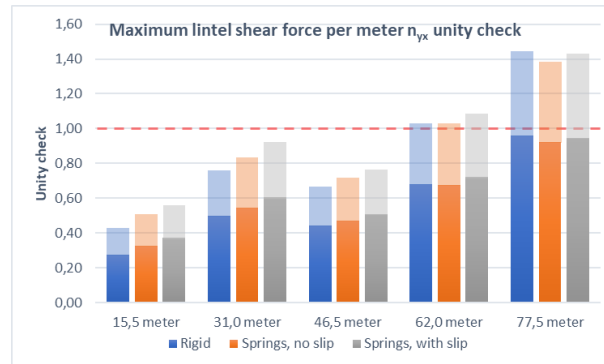
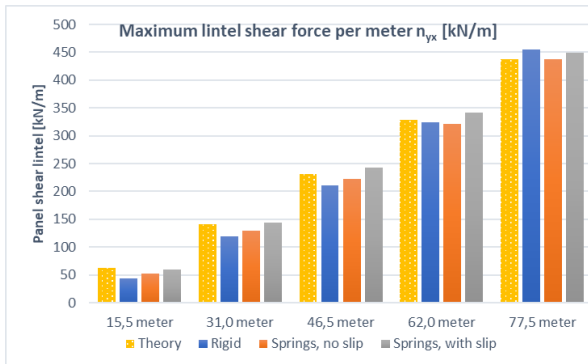


Figure 47, maximum shear force per meter in the lintels and corners of the façade for different models

Panels for the models of 15,5 meter and 31,0 meter have a lower resistance as these are panels with a smaller cross section. Shear forces are governing for the design of the façade panels for these models. Shear forces in the lintels have a unity check of 0,60 (model of 31,0 meter).

The unity check for shear forces in corners is calculated with an additional factor of 1,5 and becomes 0,90. Which makes that the panels still satisfy safety conditions.

The panels for 46,5 meter, 62,0 meter and 77,5 meter have a larger cross section hence larger resistance. For the larger structures shear no longer is the governing force on the structure. For the model of 62,0 meter compression forces on the façade are governing. The resistance of the panels suffices, albeit that the compression forces increase due to connection slip. The maximum unity check for the model of 62,0 meter increases from 0,83 to 0,98 due to the influence of the connection stiffness. For the model of 77,5 meter both compression forces and tension forces surpass the resistance of the façade panels.

### 7.3.4 Connection forces

Answering the third question of this chapter, the results from the tables before are compared to one another.

*“What are the forces in the connections?”*

The graphs in Figure 48 to Figure 50 show the resistance of the connections of the bottom CLT panels. The tensile forces in the connections show a similar pattern as the tensile force in the CLT panels. Which stands to reason as this is basically the same force that has to be transferred. Although in case of the CLT panels it is denoted as a force per meter, whereas in case of the hold-down connections it is denoted as a force on the connection. Still, just like with the tensile forces in the panels, the tensile force in the connection is underestimated using the theoretical calculations. So much so that the connections of the 31,0 meter model do not satisfy the unity check. Keep in mind that the connections were designed with a maximum unity check of 0,70. The increase of tensile forces is over 30% resulting in the failure of the connection due to underestimating the tensile force in the connection. The tension force in the connections for both the models with and without fastener stiffness deviated from the expected tension force. This shows that the theoretical calculation used to compute the axial forces in panels and connection should be revised. As the deviation is not the result of the fastener stiffness being added to the models. This only increased the force in the connection slightly.

The failure of the connection did not lead to failure of the structure in the computer model given that no failure was modelled. This would have led to failure of the calculation due to temporary peak forces in the iterative calculation. The connection underwent a plastic deformation which allowed the load to be resisted by other connections.

Shear key connections on the horizontal edges of the panels show a good correlation between theoretical results and computer results for the models without connection slip. Once the connection deformation is included in the computer models, a reduction of 30% of the shear forces is observed for all models. This reduction is credited to the fact that the forces no longer distribute in a parabolic shape, but rather distribute more evenly over the connections. Still, this distribution is not perfectly equal over all connections. The middle connections are still loaded by 20% more than those at the edges.

Shear key connections on the vertical edges of the panels show an underestimation of the theoretical forces compared to computer results in case no connection stiffness is included (blue bars). But once the connection stiffness is included in the model a reduction of the force on these connections is observed. This is due to the fact that the panels no longer fully cooperate, and therefore don't transfer all the forces from one panel to the next. This makes that the forces on the connections calculated by hand do give a good indication of the actual forces to be considered.

The shear key connections on the vertical edges of the panels have been checked for bending forces due to an additional eccentricity. Equation (32) from chapter 5.3 is applied to calculate the additional bending moment on the connection. The additional force on the connection is added in the figure of the unity check as the transparent bars. All shear key connections have a unity check below 1,0, hence the connection is safe. The connections for the models with a height of 15,5; 31,0 and 46,5 meter have one row of fasteners whereas the connections for the models with a height of 62,0 and 77,5 meter have two rows of fasteners (for the shear keys at the foundation).

Comparing the shear forces in the CLT panels to the shear forces in the connections it can be seen that shear forces in panels increase, but shear forces in connections decrease.

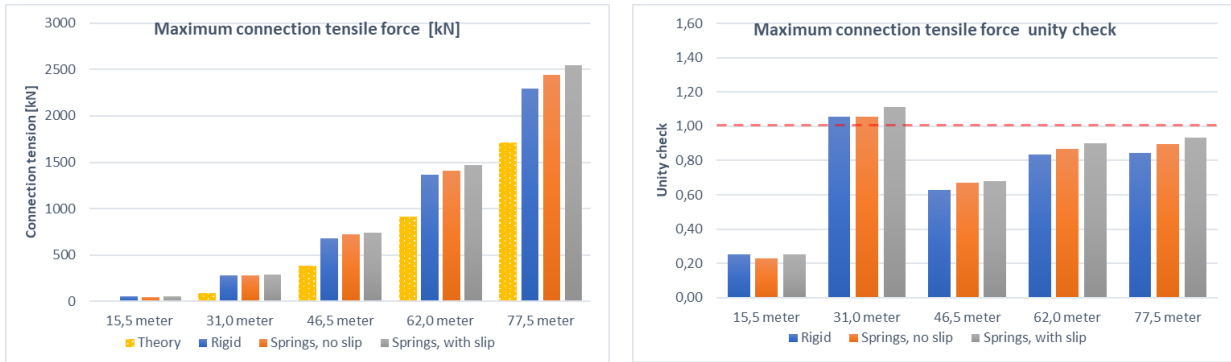


Figure 48, maximum tension force in the hold-down connections for different models

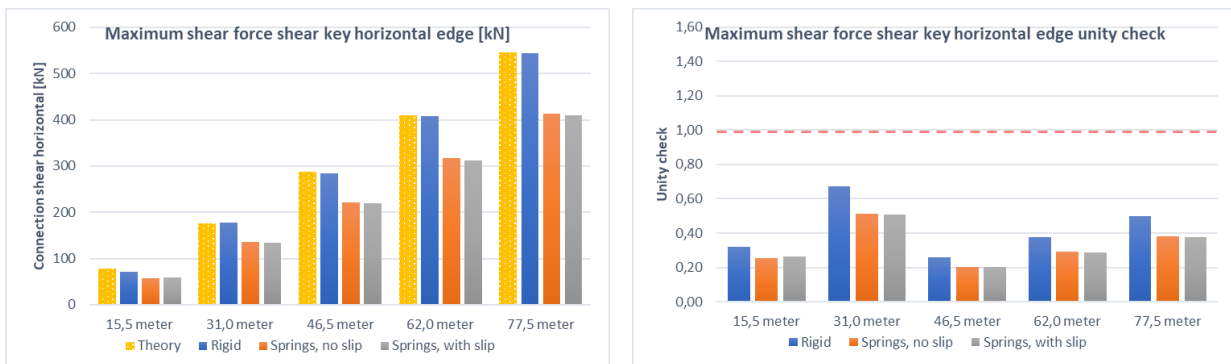


Figure 49, maximum force in the shear key connection on the horizontal edges for different models

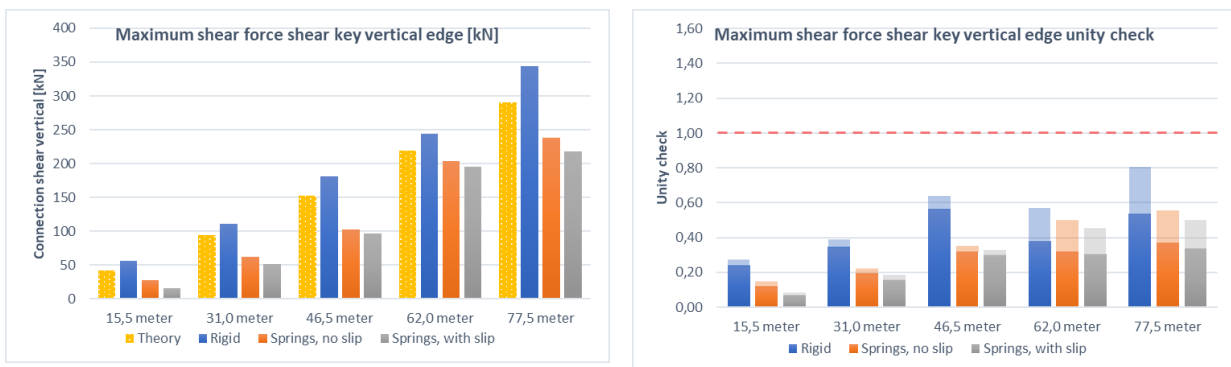


Figure 50, maximum force in the shear key connection on the vertical edges for different models

#### 7.4 Results of models with additional elements

The additional elements have been added to the façade model with connection deformation and initial slip. Results are presented for the façade model with only a concrete core, only the effective width and both the concrete core and effective width added to the model.

Results have been gathered and are presented in a similar way as the previous chapter. Again the top deformation, forces in the façade, panels and connections are compared to one another. Additionally, the forces on the façade are compared for each model as the concrete core reduces the horizontal force at the foundation and the bending moment on the façade. In case of the effective width, the force per meter in the flange and the force in the shear key connection to the transversal façade are of interest.

#### 7.4.1 Results of the façade model with an additional concrete core

The results of the façade model including connection stiffness and a concrete core have been presented in the tables below. The horizontal shear force in the concrete core and the bending moment in the core are also presented.

Table 25, results for the 2D plates models with bolt stiffnesses modelled with slip and concrete core

	Structure				Panels				Connections			
	$w_x$ <i>mm</i>	$R_{x,d}$ <i>kN</i>	$R_{y,d}$ <i>kN</i>	$M_{y,d}$ <i>kNm</i>	$n_{y,t,d}$ <i>kN/m</i>	$n_{y,c,d}$ <i>kN/m</i>	$n_{xy,pier,d}$ <i>kN/m</i>	$n_{xy,lintel,d}$ <i>kN/m</i>	$N_{y,t,d}$ <i>kN</i>	$N_{y,c,d}$ <i>kN</i>	$V_{xy,d}$ <i>kN</i>	$V_{yx,d}$ <i>kN</i>
<b>15,5 meter</b>	2,1	70	2837	448	0	248	21	19	0	142	9	3
<b>31,0 meter</b>	15,5	112	5725	3077	0	779	39	41	0	437	16	5
<b>46,5 meter</b>	57,2	182	8.616	14.337	29	1727	110	87	15	982	32	44
<b>62,0 meter</b>	130,9	275	11.513	35.800	552	3057	189	160	274	1648	46	73
<b>77,5 meter</b>	251,2	394	14.262	68.492	1688	4793	308	255	935	2613	56	128

Table 26, forces on the concrete core

	Core	
	$R_{x,d}$ <i>kN</i>	$M_{y,d}$ <i>kN</i>
<b>15,5 meter</b>	334	2690
<b>31,0 meter</b>	784	11.614
<b>46,5 meter</b>	1263	22.115
<b>62,0 meter</b>	1764	34.015
<b>77,5 meter</b>	2272	47.344

#### 7.4.2 Results of the façade model with an effective width of the transversal wall

Results of the façade model with connection stiffness and an effective width are presented in Table 28 below. The maximum axial forces in the transversal walls are presented in Table 28. A force per meter has been calculated by dividing this axial force by the effective width.

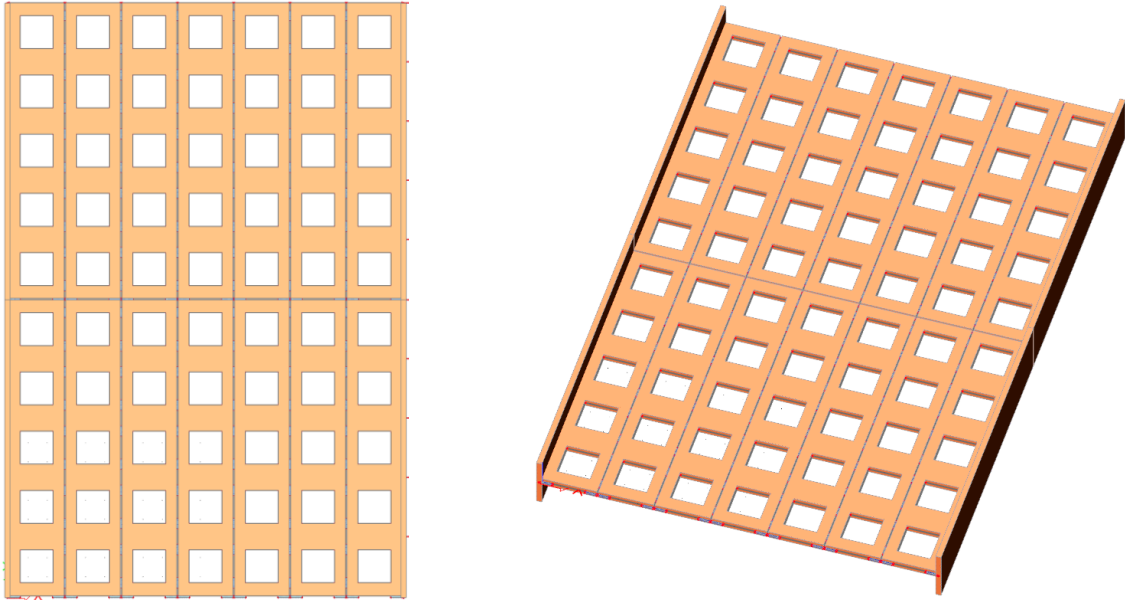


Figure 51, façade model with flange (left: 2D; right: 3D)

Table 27, results for the 2D plates models with bolt stiffnesses modelled with slip and effective width

	Structure				Panels				Connections			
	$w_x$ <i>mm</i>	$R_{x,d}$ <i>kN</i>	$R_{y,d}$ <i>kN</i>	$M_{y,d}$ <i>kNm</i>	$n_{y,t,d}$ <i>kN/m</i>	$n_{y,c,d}$ <i>kN/m</i>	$n_{xy, pier,d}$ <i>kN/m</i>	$n_{xy, lintel,d}$ <i>kN/m</i>	$N_{y,t,d}$ <i>kN</i>	$N_{y,c,d}$ <i>kN</i>	$V_{xy,d}$ <i>kN</i>	$V_{yx,d}$ <i>kN</i>
<b>15,5 meter</b>	8,7	404	3241	3184	7	484	54	58	18	276	59	4
<b>31,0 meter</b>	44,1	896	6561	14.861	173	1459	121	146	129	911	134	43
<b>46,5 meter</b>	93	1445	9697	36.034	638	2204	184	244	429	1201	220	84
<b>62,0 meter</b>	161,2	2039	13.476	70.067	934	2898	253	354	626	1818	312	156
<b>77,5 meter</b>	248,9	2666	16.853	115.566	1620	4130	386	461	907	2313	409	190

Table 28, forces on the transversal walls

	Flange			Flange		
	$R_{y,t,d}$ <i>kN/m</i>	$b_{eff}$ <i>m</i>	$n_{y,t,d}$ <i>kN/m</i>	$R_{y,c,d}$ <i>kN/m</i>	$b_{eff}$ <i>m</i>	$n_{y,c,d}$ <i>kN/m</i>
<b>15,5 meter</b>	0	1,1	0	219	1,1	199
<b>31,0 meter</b>	4	1,3	3	512	1,3	394
<b>46,5 meter</b>	128	2,0	64	1636	2,0	818
<b>62,0 meter</b>	694	2,7	257	3410	2,7	1263
<b>77,5 meter</b>	1707	3,4	502	5835	3,4	1716

### 7.4.3 Results of the façade model with an effective width and concrete core

The results for the façade models with connection stiffness and both an effective width and concrete core added are shown in Table 29 and Table 30.

Table 29, results for the 2D plates models with bolt stiffnesses modelled with slip and effective width

	Structure				Panels				Connections			
	$w_x$ <i>mm</i>	$R_{x,d}$ <i>kN</i>	$R_{y,d}$ <i>kN</i>	$M_{y,d}$ <i>kNm</i>	$n_{y,t,d}$ <i>kN/m</i>	$n_{y,c,d}$ <i>kN/m</i>	$n_{xy, pier,d}$ <i>kN/m</i>	$n_{xy, lintel,d}$ <i>kN/m</i>	$N_{y,t,d}$ <i>kN</i>	$N_{y,c,d}$ <i>kN</i>	$V_{xy,d}$ <i>kN</i>	$V_{yx,d}$ <i>kN</i>
<b>15,5 meter</b>	2,1	71	3241	452	0	458	19	18	0	254	9	2
<b>31,0 meter</b>	15,4	114	6561	3.130	0	1009	40	42	0	530	16	6
<b>46,5 meter</b>	54,8	187	10.004	15.069	124	1474	118	94	3	794	32	29
<b>62,0 meter</b>	112,9	295	13.476	38.258	209	2023	200	159	76	1173	46	79
<b>77,5 meter</b>	161,5	457	15.837	56.983	550	2337	287	270	204	1313	56	122

Table 30, results for the 2D plates models with bolt stiffnesses modelled with slip and effective width

	Flange			Flange			Core	
	$R_{y,t,d}$ <i>kN</i>	$b_{eff}$ <i>m</i>	$n_{y,t,d}$ <i>kN/m</i>	$R_{y,c,d}$ <i>kN</i>	$b_{eff}$ <i>m</i>	$n_{y,c,d}$ <i>kN/m</i>	$R_{x,d}$ <i>kN/m</i>	$M_{y,d}$ <i>kN/m</i>
<b>15,5 meter</b>	0	1,1	0	188	1,1	171	333	2685
<b>31,0 meter</b>	0	1,3	0	431	1,3	332	782	11.548
<b>46,5 meter</b>	0	2,0	0	1203	2,0	602	1259	21.311
<b>62,0 meter</b>	14	2,7	5	2561	2,7	949	1744	31.259
<b>77,5 meter</b>	219	3,4	64	3857	3,4	1134	2081	37.033

The sum of bending moments of the façade structure and concrete core is less than the acting bending moment on the structure. This indicates that there is an additional component resisting bending moments.

## 7.5 Results compared

The results of the models with additional elements are compared to one another. The results of the façade model with connection stiffness and initial slip serves as a benchmark. Similar graphs as previously have been made for the comparison. Results of only the façade structure (including connection stiffness) are shown in grey bars. The results including the concrete core are given in green bars. The results with the effective width are shown in orange. Finally, the results for the models including both a concrete core and the effective width are presented in the blue bars.

### 7.5.1 Top deformations

Just like for the previous models the top deformations for the façade with additional elements are compared. The top deformation of the façade is reduced due to the addition of a concrete core and the addition of an effective width. When both additional structures are added to the model, the top deformation is further reduced.

A reduction of the top deformation is observed for all models with additional elements. If both a concrete core and the effective width are modelled, the top maximum height of the structure can be increased from 45 meter to 75 meter. This is an increase of the maximum height of 67%.

For most models the addition of a concrete core is more beneficial to the stiffness of the structure. This is due to higher shear stiffness of the core. The shear stiffness is more important for lower levels. The higher the building, the more important the bending stiffness becomes. For the model of 77,5 meter the concrete core and effective width both contribute equally to the reduction of the bending stiffness.

The contribution of the effective width of the transversal façade is most noticeable for the models of 62,0 meter and 77,5 meter. This is due to the increasing contribution of bending deformation on the total deformation of the structure for higher buildings. But also due to the fact that the effective width of the transversal façades increases for higher structures. Lastly, the shear keys on the vertical edges for the model of 77,5 meter have a higher stiffness. This makes that the bending stiffness of the structure is higher as there is better cooperation between panels.

The top deformation is significantly reduced for the models of 15,5 meter and 31,0 meter in case a concrete core is applied. This is credited to the bending stiffness of the concrete core being larger than that of the individual panels. Figure 42 indicates that the initial slip results in a large deformation due to free additional bending panels. Only once this initial slip has occurred will the panels start to cooperate. So before this point, the bending stiffness of the structure is that of the seven panels individually. Compared to the bending stiffness of the core the bending stiffness of the individual panels is rather low. Hence the core will resist most of the bending forces as well as providing most of the stiffness to this bending deformation.

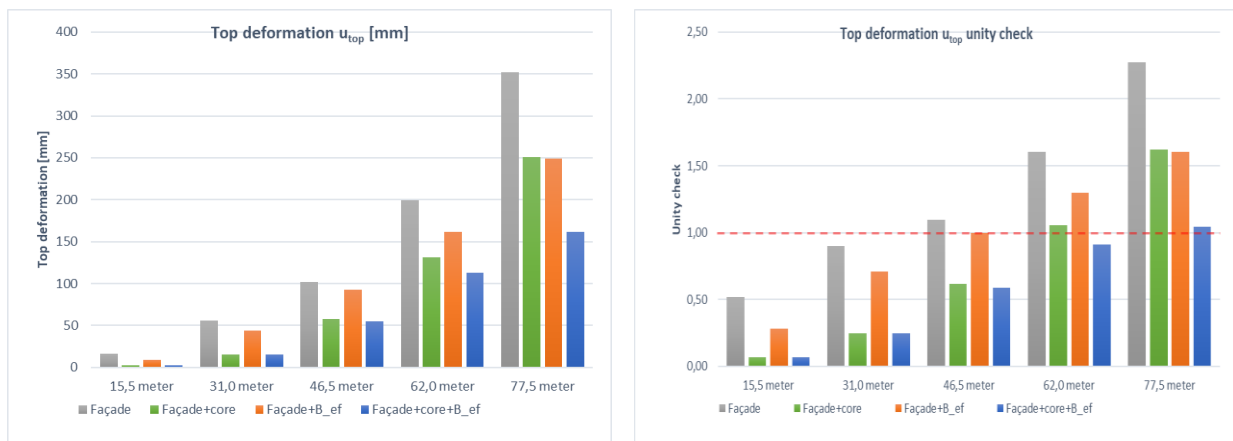


Figure 52, top deformation for different models with additional components

### 7.5.2 Resultant forces on the foundation

The resultant forces on the foundation of the façade structure have been presented in order to show how the horizontal shear force and bending moment are reduced. This is due to the concrete core which has additional shear and bending stiffness. Most of the shear forces are resisted by the concrete core and are not acting on the façade structure. This has a beneficial effect for the shear forces in the façade.

The same can be said for the bending moments on the façade. The core will resist a part of the bending moments acting on the structure. This will have a beneficial effect on the shear forces on the shear keys on the vertical edges.

The bending stiffness of the core is only 12% of that of the total façade. However, due to slip in the connections, the cooperation between façade panels can reduce and the corresponding bending stiffness of the façade also reduces. This in turn can increase the bending stiffness contribution of the core.

This can be clearly seen for the lower models where the bending moment acting on the façade is reduced significantly. This has already been explained in 7.5.1 to be caused by the initial slip of the connection.

Table 31, contribution of the façade when combined with a concrete core

Model	$R_x$ – façade	$M_{y,d}$ – façade	$M_{y,d}$ – core
15,5 meter	17%	16%	84%
31,0 meter	13%	22%	78%
46,5 meter	13%	41%	59%
62,0 meter	13%	55%	45%
77,5 meter	15%	68%	32%

The shear force on the façade is only 13 – 17% of the initial calculated shear force. Appendix A7.3 calculated the shear stiffness to be 27% of the total shear stiffness of the structure. But this is based on the shear stiffness of the façade without connection stiffness contribution.

The contribution of the façade on the bending moment resistance increases for higher models, indicating that the effect of the initial slip decreases for these higher models. Still, the bending stiffness of the core is only 12% of the bending stiffness of the façade (without connection stiffness or effective width). So the expected bending moment on the façade is 88% of the initial bending moment. All values in Table 31 are considerably lower.

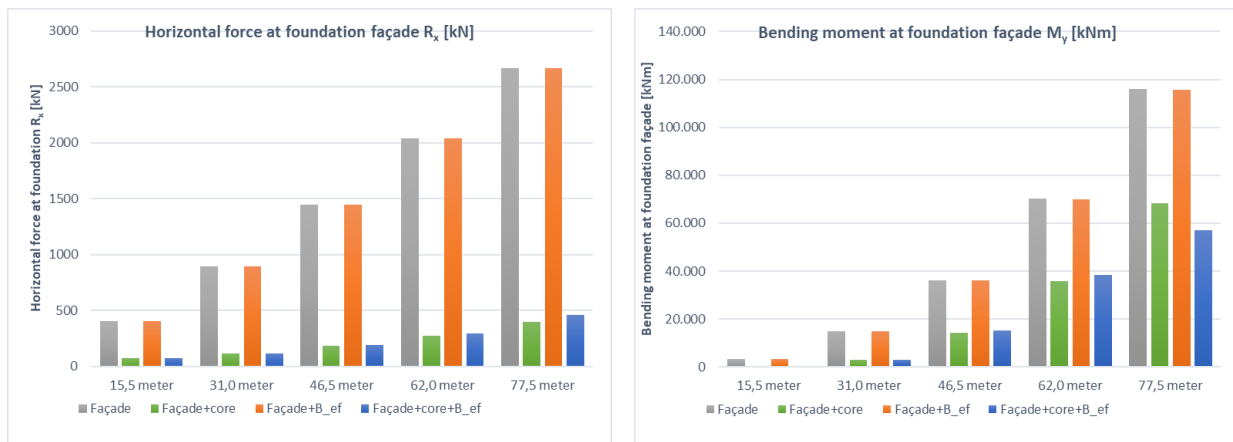


Figure 53, forces on the façade structure for different models with additional components

One note should be added regarding the bending moment on the façade when a concrete core is included. Which is that the sum of bending moments of the façade and core does not equal the total bending moment on the structure. Additional mechanisms seem to be resisting a part of the bending moments.

### 7.5.3 Panel forces

Changes of the forces acting on the façade panels have been observed as a result of the additional elements. Bending moments on the façade have reduced by 32-84% due to the addition of the core. Hence tension forces on the façade panels have also reduced. Just like the tension forces in the façade, also the compression forces reduce.

The observed forces per meter in the transversal façade are lower than the forces per meter in the main façade. Tensile forces per meter in the transversal façade lie between 0% and 31% of the forces per meter observed in the main façade. For compression forces per meter on the transversal façade this lies between 27% and 44%

Shear forces in the piers of the CLT panels reduce significantly. All unity checks show low values. Shear forces were found to be governing for the required panel thickness. Additional elements can contribute to the shear resistance of the façade allowing for thinner CLT panels to be used.

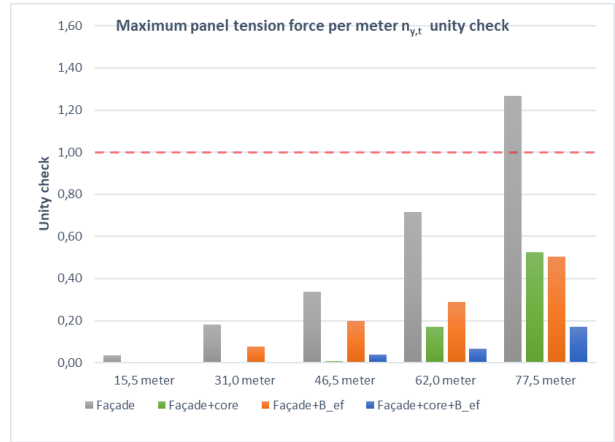
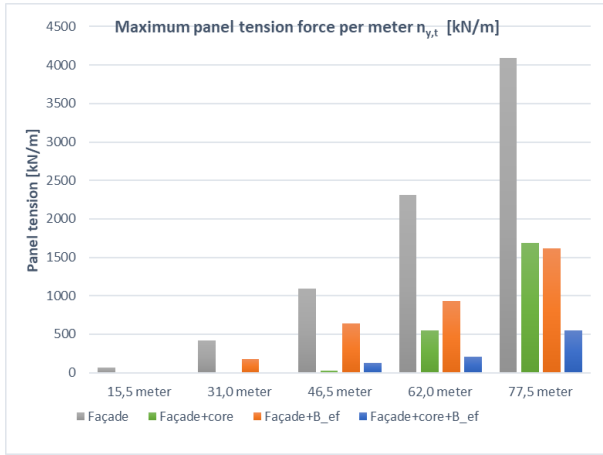


Figure 54, tension forces per meter on the façade panels for different models with additional components

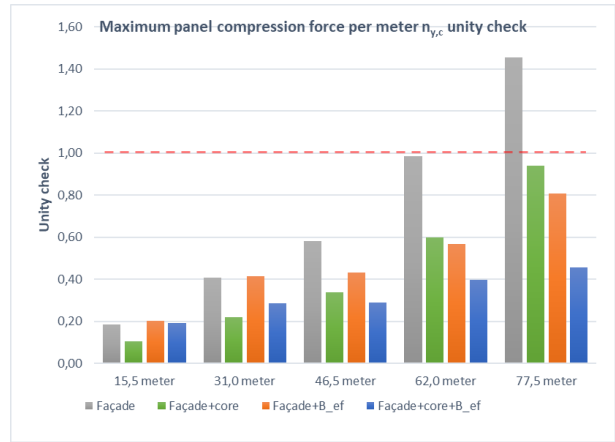
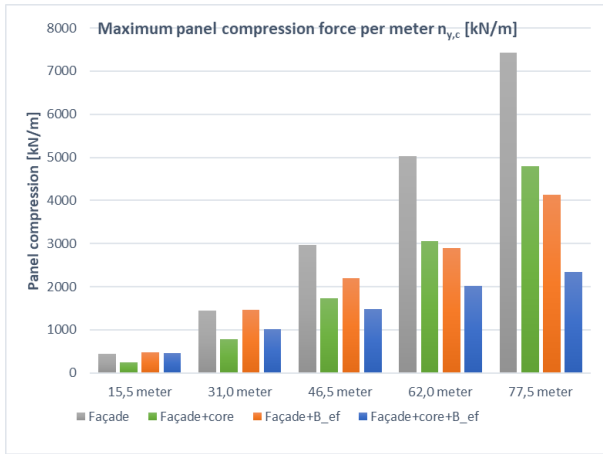


Figure 55, compression forces per meter on the façade panels for different models with additional components

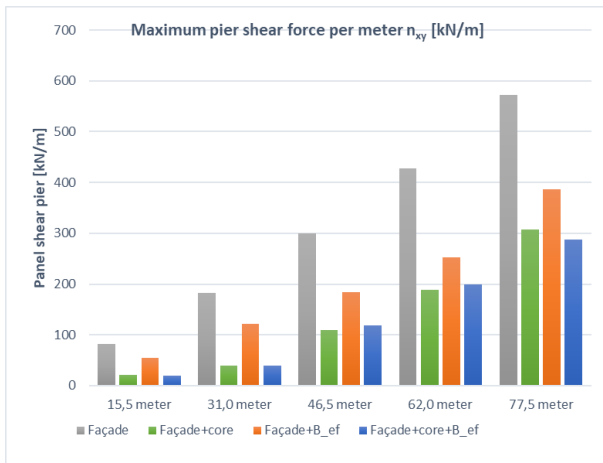


Figure 56, shear forces per meter on the piers in the façade for different models with additional components

#### 7.5.4 Connection forces

Connection forces are gathered in this chapter. Maximum tensile forces in hold-down connections at the foundation are given in Figure 57. Maximum shear forces in shear key connections on the horizontal edges at the foundation are given in Figure 58. Figure 59 shows the maximum shear forces in the shear key connections on the vertical edges.

Tension forces in the hold-down connections at the foundation reduce by at least 63% when a concrete core is added to the structure. Lower models indicate that for structures below 46,5 meter including a concrete core, there are no tensile forces in the connections.

The models with an effective width show reduced tensile forces of 42-68%.

When both a concrete core and an effective width are applied, the tensile forces in the connection are reduced by over 90%.

Shear forces on the shear keys on the horizontal edges are largely resisted by the concrete core at the foundation level. Shear forces on the shear keys on the vertical edges are also reduced by the addition of a concrete core. A reduction of at least 44% is observed. However, compared to the horizontal shear keys and hold-down connections there is still a significant part of the force present in the connection.

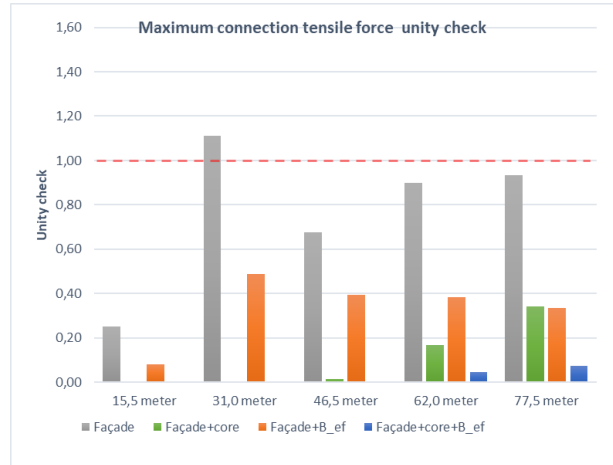
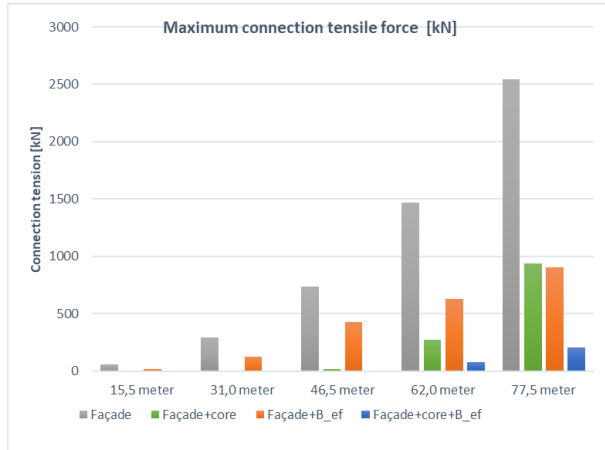


Figure 57, maximum tension force in the hold-down connections for different models with additional components

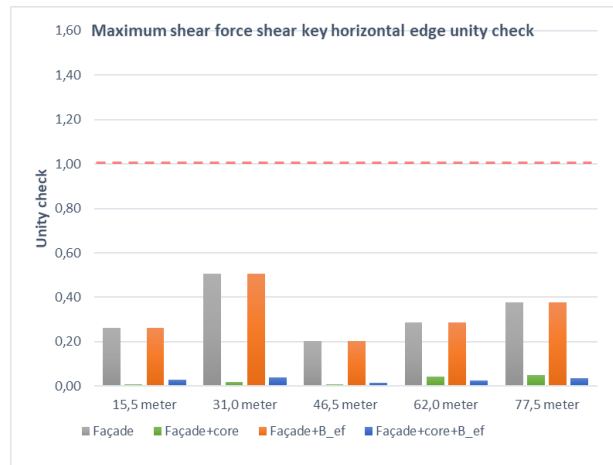
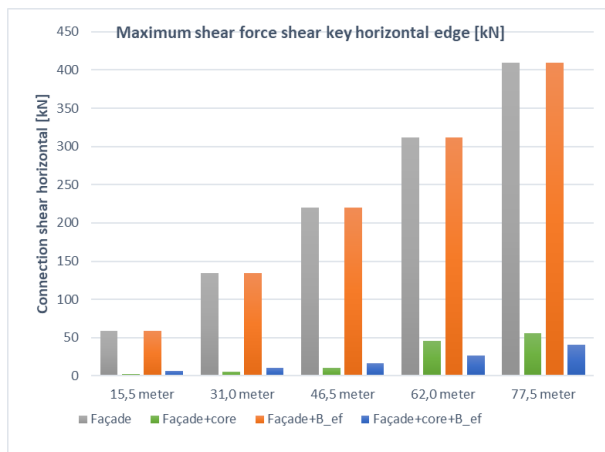


Figure 58, maximum force in the shear key connections on the horizontal edges for different models with additional components

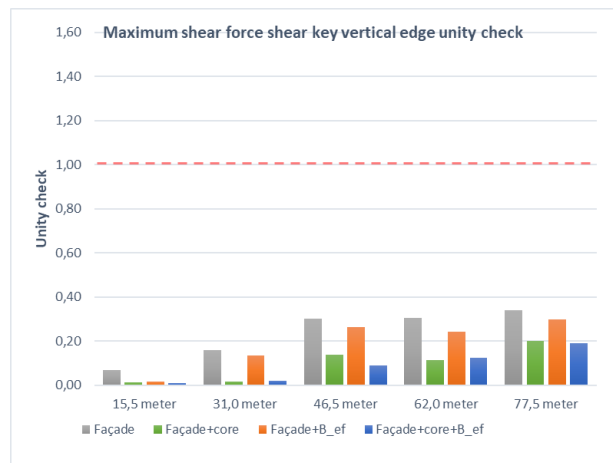
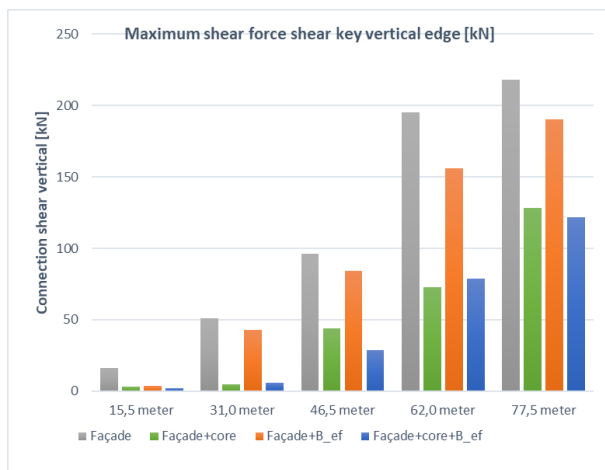


Figure 59, maximum force in the shear key connections on the horizontal edges for different models with additional components

## 8 Discussion

This research has been conducted according to the methodology stated in chapter 1.6. Looking at the results some remarks regarding the methodology and approach of the research can be made.

The stiffness parameter  $k_{ser}$  of the multi-linear load-displacement curves of the connections has been based on the current Eurocode 5 (version 2020). To account for the activation of bolts, the first stiffness trajectory of the load-displacement curve had a reduced stiffness of 50%  $k_{ser}$  until 40% of  $F_{max}$  was reached. Between 40% and 67% of  $F_{max}$  the value of  $k_{ser}$ , defined according to the Eurocode was used. This non-linear load-displacement curve was later compared to load-displacement curves from several test specimen. This showed that the stiffness reduction should also have been applied after 40% of  $F_{max}$  was reached as well as for the plastic stage of the load-displacement curve. This makes that the modelled connections behave too stiff.

Most connections however do not get loaded by more than 50% of the maximum resistance. Hold-down connections are designed for the tension forces at the outer panels at the lower levels. The forces occurring in these connections is significantly higher than the forces in the middle panels or the panels at higher locations.

Shear key connections are designed with a maximum unity check of 0,7 and the actual forces in the connections were found to be lower in the computer models including slip.

This leads to conclude that the overly stiff modelling of the fastener stiffness has not lead to significant deviations for top deformations and force distribution in the façade.

The reduction of the first stiffness trajectory of 50% was based on researches on multi-fastener connections up to 5 fasteners. However, research by Reynolds et al. (2022) shows that the calculated stiffness of a multi-fastener connection with significantly more than 5 fasteners can be much lower ( $n_{ef} = 0,2 n$ ). This effective number of bolts was found for a test specimen with 35 dowels and three steel plates. Only one such connection was tested.

Assumption  $n_{ef} = n$  for strength of fasteners from ETA2019 is not supported by the new Eurocode 5 draft. Here it is noted that the effective number should be calculated using the equation below. This would result in an effective percentage of the resistance of 67-73% for spacing  $a_1 = 5d$  and 2 to 5 rows of bolts.

$$n_{ef} = n^{0,9} * \sqrt[4]{\frac{a_1}{13d}} \quad (38)$$

The floor was assumed to be a timber-concrete composite floor. The assumed load distribution on the east façade was therefor assumed to be a trapezoidal distribution. However, a linear distribution over the whole width of the façade is more realistic given that the timber-concrete composite floor is not capable to carry loads in two directions as long as the CLT panels span in one direction and cannot transfer tension and shear forces from one panel to another.

The effective width of the façade was overestimated for the models of 62,0 meter and 77,5 meter. The width of the model of 62,0 meter was calculated to be 2,2 meter but 2,7 meter was applied. The width of the model of 77,5 meter was calculated to be 2,4 meter but 3,4 meter was applied. The bending deformation is thus underestimated. The bending stiffness of a façade with an effective width of 2,4 meter

is 18% lower than that of a façade with an effective width of 3,4 meter. Therefor the bending deformation is 22% higher.

The top deformation calculations do not contain the influence of the stiffness of the foundation. This will increase the top deformation directly and indirectly (2<sup>nd</sup> order factor).

As the stiffness of the foundation is not included in the models, the beneficial contributions of both the concrete core and effective width of the transversal wall may differ.

The unity checks of maximum tensile and compressive stresses in the CLT panel have been made without taking into account that the cross-section of the panel is reduced at the location of the connection. For a panel LL-400/11s, the effective thickness reduces from 280 mm to 240 mm. This is a reduction of 14%. This can be solved in the design of the connection by increasing the width of the hold-down connections.

Verifications of the models were made for the façade without openings and showed that the computer models presented predictable results. Verifications of the models with openings have not been made. If this would have been done, a deviation between theoretical calculations and computer models would have been found. Connections could then have been designed for the maximum loads found in the computer models and the theoretical calculations could have been improved by including the influence of lintel deformation on the load distribution in the façade.

All connections have been designed with a maximum unity check of 0,7 in order to avoid failure due to unforeseen deviations between theoretical hand calculations and computer results. This value of 0,7 is not conservative enough as one of the models showed failure of the hold-down connection. This is due to the underestimation of the tensile forces in the connections with the theoretical calculation. Either the theoretical calculations are to be improved, or the maximum unity check during first design should be even lower.

The connections of the different models have been compared at the foundation level. In hindsight this comparison should have been done for the maximum force in all connections. The shear key connections on the horizontal edges of the CLT panels are loaded by larger forces at higher levels when a concrete core is present.

## 9 Conclusions and recommendations

This research has focused on the research questions presented in chapters 1.4 and 1.5. Conclusions will be presented in the following chapter. Chapter 9.2 will then go into the recommendations that result from these conclusions.

### 9.1 Conclusions

The main research question stated in chapter 1.4 is:

*“What is the influence of mechanical fastener connections on the strength and stiffness of CLT façades that function as the main stability system?”*

This question has been divided into sub-questions which were first presented in chapter 1.5. Chapters 2 until 7 then answered one sub-question each. The sub-questions of chapters 4 until 7 contribute to answering the main research question. The conclusions of these chapters will be presented below.

Chapter 4      structural design of CLT façades

*“How to design a façade with CLT panels?”*

Current theories on CLT structures provided answers to the strength and stiffness behavior of CLT panels. The presence of openings however has not fully been described in literature for façades of CLT walls in multistory buildings. The deformation of a CLT façade is the sum of the deformation caused by individual components. Similarly, forces in the structure can be explained and calculated using the same components. The following components are defined:

- Bending of the façade      *bending stiffness adjusted for openings*
- Shear of the façade      *shear stiffness adjusted for openings*
- Bending of lintels      *derived to calculate top deformation*
- Bending of piers      *calculated using the method of Schelling*
- Sliding of connections      *shear key connections on the horizontal edges of the panels*
- Rocking of connections      *elongation of hold-down connections*
- Additional bending deformation      *calculated using the method of Schelling*

Bending stiffness and shear stiffness of the façade have been adjusted for the presence of openings. The influence of openings on the façade deformation has been derived. Bending of piers and lintels have an additional contribution to the deformation. The effective dimensions of these piers and lintels can be calculated using the equations by Hsiao (2014). Piers result in a horizontal sway per story. Equation (22) was derived to calculate the resulting deformation at the top. Bending of lintels also increased the deformation of the structure. The method of Schelling was used to calculate this deformation. Using this theory provided accurate results for the top deformation. However, the contribution of the bending of lintels on the force distribution in the façade has to be included in order to get correct axial forces in the CLT panels and connections. The method of Schelling does not provide sufficient insight regarding the influence of the lintels on the force distribution in the façade.

The individual contributions of each component has not been checked. Only the sum of all components (maximum top deformation) was compared to computer results. The comparison showed in Figure 41 indicated that for all heights the theoretical hand calculations showed comparable results.

Contributions of connections on the top deformation was divided into three components: sliding, rocking and additional bending deformation. Sliding deformation is the result of shear forces on the shear key connections on the horizontal edges of panels. Its contribution is negligible. In case connections have an initial slip the sliding deformation is predictable and was found to be equal to the sum of the initial slip. Rocking deformation is found to be the most difficult to be calculated by theoretical calculations. Chen and Popovski presented a series of equations. For large connection stiffnesses ( $k = 1000$  kN/mm per meter) the theoretical hand calculation for rocking deformation is acceptable for a first indication of the rocking deformation of a CLT façade. However, realistic hold-down connection stiffnesses might not reach this stiffness value.

Deformations of the connections on the vertical edges of the CLT panels were found to be the most important contributor to the top deformation.

According to theoretical calculations, the required thickness of the CLT panels is governed by shear forces in the corners of openings.

## Chapter 5      Connection design

*“What are the required connections for the CLT façade structure to resist the forces acting on them?”*

The connections have been designed based on forces that were calculated using theoretical hand calculations. Computer results then verified these connections. The hold-down connections designed for the façade of 31,0 meter had to be altered as the computer calculations showed the initial design to be unsafe. An additional row of bolts was added to halve the utilization of the connection.

## Chapter 6 Computer model

*“How to model the CLT façade structure?”*

The models used to calculate the façade structure have been explained in chapter 6. Modelling the connection as a steel plate with the fastener stiffness modelled on both sides is a suitable method to calculate the structural behavior of the façade. The fastener stiffness was modelled as multi-linear load-displacement curves based on the stiffness definitions in Eurocode 5 and a reduced stiffness (50%) for the initial loading trajectory given that not all fasteners contribute immediately after loading.

The effective width of the transversal walls have been modelled as 1D beam elements with connection stiffness based on the load-displacement curves for the connections on the main façade. The effective width was overestimated in initial calculations. Results of the computer model therefor have a underestimation of the bending deformation.

The core has been modelled as a 2D concrete plate with cracked concrete properties without openings or flanges. The foundation stiffness has not been modelled.

## Chapter 7 Results of the computer model

*“What are the forces in the CLT panels according to the computer models?”*

*“What is the top deflection of the CLT façade according to the computer models?”*

Forces in CLT panels and connections have been presented in Chapter 7, just like the maximum top deflections of the CLT façades for several models. Comparisons to theoretical hand calculations were made to analyze how the more accurate computer models relate to the expected behavior of the structure. Comparing the forces in the connections for models with and without connection stiffnesses, the following conclusions were made:

Axial forces in hold-down connections calculated in the computer models are significantly higher than calculated with theoretical calculations. This results in failure of the designed connection for the model of 31,0 meter. Designing connections with a maximum unity check of 0,7 is not sufficient. The effect of the lintels on the distribution of the bending forces is to be taken into account.

Shear forces in the shear keys on the horizontal edges decrease by 19 to 25%. This shows that the connections can be designed in an early design phase with a unity check of 1,0.

Shear forces in the shear keys on the vertical edges decrease by 11 to 62%. There is a large deviation between the reduced forces in the connections. But in general, all connections are loaded by a lower force than initially calculated. This shows that also the shear keys on the horizontal edges can be designed in an early design phase with a unity check of 1,0. As these shear keys on the vertical edges have the largest influence on the stiffness of the façade it is more important to design these connections for stiffness instead, especially for higher structures. Initial slip in the fastener should be avoided.

The deformation of the top of the façade has been calculated for several models. The following conclusions were made:

- Connections with slip increase the top deformation by 53 to 140% compared to the façade model without fastener stiffness. The initial slip of the fasteners is the largest contributor to the increased top deformation. Primarily the shear key connections on the vertical edges have a significant influence on the top deformation.
- The addition of a core reduces the top deformation of the façade by 29 to 87% compared to the façade model including fastener stiffness. The reduction of the top deformation reduces for higher models.
- The effective width reduces the top deformation of the façade by 9 to 29% for the models larger than 40 meter. The reduction of the top deformation increases for higher models.

The top deformation of the façade exceeds the limit of  $H/500$  for a height of 40 to 45 meter. In case the effective width is included and a concrete core is added to the design, a height of 70 to 75 meter can be obtained. However, there is no contribution of the foundation stiffness included in this analysis. This can reduce the stiffness of the overall structure, increasing the top deformations. Also, the stiffness of the structure is related to the dynamic behavior of the structure. A dynamic analysis has not been included in this research.

Additional elements in the model reduce the maximum shear force in the CLT panels. As the CLT panel thickness is governed by shear forces on the panels, this provides the possibility to reduce the panel thickness.

The contribution of the concrete core on the acting bending moment on the façade (41% to 86%) is more than expected when comparing the bending stiffness of the core to the bending stiffness of the façade. This makes that the theoretical calculation is on the conservative side.

The addition of an effective width shows potential regarding the additional bending stiffness and reduction of forces in the panels and connections.

## 9.2 Recommendations

The following recommendations for further research have been made:

### Chapter 2

- The fastener stiffness  $k_{ser}$  as described in Eurocode 5 does not explain all parameters that influence this stiffness. The stiffness of multi-fastener connections is not elaborated on in Eurocode 5. It is not described whether an effective number of fasteners is to be considered.
- Research by Reynolds et al. (2022) indicated that there is a significant reduction of the stiffness of multi-fastener connections ( $n_{ef} = 0,2 n$  to  $0,5 n$  depending on the number of fasteners). Design guidelines are needed on the stiffness of multi-fastener connections.
- Brittle failure due to block shear was found to be governing for the connection when including brittle failure mechanisms according to the new Eurocode draft. Brittle failure was calculated to occur at 67% of the ductile failure that is expected. However, the equations specified in the Eurocode are given for standard timber and parallel laminated timber, and are not mentioned for CLT. Results highly depend on the interpretation of the equations and translation in the case of CLT. More research is required with regard to the brittle failure modes for CLT panels and is to be translated into design guidelines. In case the current equations for timber also are deemed fit for determining the brittle failure behavior of CLT, the spacing can be increased by 50% in order to avoid brittle failure calculated according to the new Eurocode draft. .
- The method of Schelling is a very useful method that extends past the applications of the gamma-method. But the method is not complete with regards to the bending stresses in the individual members. This should be further developed based on the gamma-values of each member. In this research, a more simplified approach was used based on the equilibrium of section forces.

### Chapter 4

- There is no accurate method to calculate rocking deformation that includes the influence of the connection stiffness on both the forces in the connections and the width of the façade that is loaded in tension. More research is required on the change of the forces in the connections related to the stiffness of the connection.
- More research is required on the influence of altering width and height of the panels

### Chapter 5

- The assumption for the effective number of bolts  $n_{ef} = n$  for strength of fasteners as given in ETA-11/0189 (2019) of Derix panels does not correspond with the Eurocode draft, where  $n_{ef}$  of CLT panels is identical to that of standard timber elements. The connection resistance was calculated for  $n_{ef} = n$ , indicating that this might be an overestimation of the actual resistance. Conclusions from this thesis need to be revised in case the assumption  $n_{ef} = n$  is deemed incorrect.

## Chapter 7

- Additional bending deformation is a large contributor to the deformation of the façade as a result of connection deformations. Friction in the interface between panels may reduce this deformation. Research including this friction component may increase the insight into the actual deformation of a CLT façade.
- Large top deformations were found. No research was done with regard to the dynamic behavior of the design. But this is a well known issue for timber high-rise. More research is required on this topic to find the limitations of this type of stability system.
- The addition of an effective width shows potential regarding the additional bending stiffness and reduction of forces in the panels and connections. But the width of the effective flange was overestimated. Also, the connections between the façade and effective width were assumed to be similar to the shear keys on the vertical edges. Shear forces have been checked and showed to be lower than the shear forces that the connections were designed for. But the force transfer in these connections should be further researched. A 3D model is better suited than the 2D model used in this research.
- The stiffness of the foundation has not been included in this research. This can have a significant influence on both the top deformation of the structure, as well as the contribution of the additional elements to the structure in general.

## 10 Sources

### 10.1 Sources chapter 1

- [1] Blaß, H.J., & Sandhaas, C. (2017). Timber Engineering V2, principles for design. Karlsruhe: KIT Scientific Publishing.
- [2] Breach, M. (2009). Dissertation writing for engineers. Essex: Pearson Education Limited
- [3] NEN-EN-1995 Eurocode 5 (2011). Design of timber structures – part 1-1: General - common rules and rules for buildings. Delft: Nederlands Normalisatie-instituut
- [4] NEN-EN-1995 Eurocode 5 (2013). Nationale bijlage bij NEN-EN 1995-1- Delft: Nederlands Normalisatie-instituut.
- [5] prEN-1995 Eurocode 5. (2021). Design of timber structures – part 1-1: General - common rules and rules for buildings.

### 10.2 Sources chapter 2

- [6] Derix website. (2021). Retrieved from <https://nl.derix.de/nl/>
- [7] Brandner, et al. (2016). Cross laminated timber (CLT): overview and development. Berlin: Springer, vol. 2016, p.21.
- [8] Wallner-Novak, M., Koppelhuber, J., Pock, K. (2014). Cross-Laminated Timber Structural Design: Basic design and engineering principles according to Eurocode. Vienna: ProHolz Austria.
- [9] Schelling, W. (1982). Zur Berechnung nachgiebig zusammengesetzter Biegeträger aus beliebig vielen Einzelquerschnitten. Karlsruhe.
- [10] Augustin, M. (2008). Handbook 1 – Timber structures. Graz.
- [11] RCSC Committee (2014). RCSC Specification for Structural Joints using High-Strength Bolts. Chicago: Research Council on Structural Connections.
- [12] Klomp, M. (2020). Hybrid interaction of timber decks in movable bridges. Delft: TU Delft.
- [13] Reynolds, et al. (2022). Stiffness and slip in multi-dowel timber connections with slotted-in steel plates. Elsevier, Engineering structures 268.
- [14] Jorissen, A. (1998). Double shear timber connections with dowel type fasteners. Delft: TU Delft.
- [15] Sandhaas, C. and Van de Kuilen, J.W.G. (2017). Strength and stiffness of timber joints with very high strength steel dowels. Karlsruhe: Elsevier, Engineering structures 131.
- [16] EN 26891 (1991). Timber structures – joints made with mechanical fasteners.
- [17] Hartl, H., Leijten, A.J.M., Hilson, B.O. (2017). Timber Engineering V2, principles for design – E15 Joints with multiple shear planes. Karlsruhe: KIT Scientific Publishing.
- [18] DIBt (2019). ETA-11/0189. Berlin.
- [19] Uibel, T. and Blaß, H.J. (2006). Load Carrying Capacity of Joints with Dowel Type Fasteners in Solid Wood Panels. Karlsruhe: KIT Scientific Publishing.
- [20] Znabei, T. (2020). A post-tensioned Cross-Laminated Timber core. Delft: TU Delft.
- [21] Hsiao, K. J. (2014). Hand-Calculated Procedure for Rigidity Computation
- [22] Chen, Z., & Popovski, M. (2020). Mechanics-based analytical models for balloon-type cross-laminated timber (CLT) shear walls under lateral loads. Engineering structures, 208, Vancouver: Elsevier.

### 10.3 Sources chapter 3

[23] NEN-EN-1990 (2011). Eurocode. Grondslagen van het constructief ontwerp. Delft: Nederlands Normalisatie-instituut.

[24] NEN-EN-1991-1-4/NB (2011). Eurocode 1: Nationale bijlage bij NEN-EN 191-1-4: Eurocode 1: Belastingen op constructies – Deel 1-4: Algemene belastingen – windbelasting. Delft: Nederlands Normalisatie-instituut.

[25] Bouwbesluit. (2021). Retrieved from <https://www.bouwbesluitonline.nl/>

### 10.4 Sources chapter 4

[26] Dujic, et al. (2007). Influence of Openings on Shear Capacity of Wooden Walls. NZ Timber Design Journal, 16(1), Ljubljana.

[27] Pai, S. G. S., Lam, F., & Haukaas, T. (2017). Force transfer around openings in Cross-Laminated Timber Shear Walls. Journal of Structural Engineering, American Society of Civil Engineers.

### 10.5 Sources chapter 5

[Program] SCIA Engineer version 19.1 & 20.0 64bit

### 10.6 Sources chapter 6

[28] Chiewanichakorn, P., Srisuwan, S., & Praserthdam, P. (2004). Effective Flange Width Definition for Steel–Concrete Composite Bridge Girder. Journal of Bridge Engineering, 9(4), 367-373.